What are the Mechanisms Responsible for the Wet Season Onset over Tropical South America?

A Dissertation
Presented to
The Academic Faculty

By

Wenhong Li

In Partial Fulfillment
of the Requirements for the Degree of
Doctor of Philosophy in Earth and Atmospheric Sciences

Georgia Institute of Technology
August 2003

What are the Mechanisms Responsible for the Wet Season Onset over Tropical South America?

Approved by:

Dr. Rong Fu, Chairman

Dr. Robert E. Dickinson

Dr. Peter J. Webster

Dr. Robert X. Black

Dr. E. Michael Perdue

Date Approved 08/13/03

Dedication

To my family for their love and support

Acknowledgments

It is my pleasure to acknowledge the keen guidance and support provided by my advisor, Dr. Rong Fu. Her guidance and encouragement have been of immense help in my research and have influenced my professional career greatly.

I also wish to thank Dr. Robert Dickinson, Dr. Peter Webster, Dr. Robert Black and Dr. Michael Perdue for serving my thesis committee and providing me many advices, comments and suggestions of this Dissertation. Without these, the thesis should not be the same.

Special thanks go to Dr. Hui Wang for many helpful discussions during my study. I would also like to thank Dr. Shaikh Mohammad, Jonathan Wright, Mingxuan Chen, Margaret Rae, Amy Sullivan, and Meg Grantham for their assistance with ERA data and editorial help.

Personally, I would like to thank my parents, my husband, my daughter and my friends for their constant support, and encouragements.

CONTENTS

LIST OF TABLE

LIST OF FIGURES

Summary

This dissertation examines the large-scale atmospheric conditions, land-surface processes, and triggering mechanisms for the wet season onset over tropical South America (5–15°S, 45–75°W). Our results suggest that the transition from the dry to the wet season can be divided into three phases. The initiating phase begins about 90 days prior to the onset of the wet season. This phase is characterized by the increase of local land surface fluxes, especially latent heat flux, which increases the available potential energy of the lower troposphere. The large-scale, cross-equatorial flow and upper tropospheric circulation remain unchanged from those of the dry season. The second phase or developing phase is dominated by the seasonal transition of the large-scale circulation, which accelerates by dynamic feedbacks to an increase of local thermal-driven rainfall, starting from about 45 days before the onset of the wet season. During this stage, the reversal of the low-level, cross-equatorial flow in the western Amazon increases moisture transport from the tropical Atlantic Ocean and leads to net moisture convergence to the Southern Amazon region. In the upper troposphere, the divergent kinetic energy begins to convert into rotational kinetic energy, and geopotential height increases rapidly. These processes lead to the onset of the wet season and an increase of anticyclonic vorticity at the upper troposphere. The third stage is after the onset. The lower tropospheric potential energy reaches equilibrium, but the conversion from divergent to rotational kinetic

energy continues to spin up the upper troposphere anticyclonic circulation associated with the Bolivian High to its full strength.

An analysis of wet season onset on an interannual scale shows that land surface conditions during dry and early transition seasons can contribute significantly to the interannual changes of the wet season onset. A longer dry season with lower rainfall reduces surface latent heat flux and results in a higher Convective Inhibition Energy (CINE) and a lower Convective Available Potential Energy (CAPE), hence a delay in the increase of local rainfall in the initiating phase of the transition and consequently in the onset of the wet season. Conversely, a wetter dry season leads to a higher surface latent flux and a weaker CINE, thus providing a necessary condition for an earlier increase of local rainfall and an earlier onset of the wet season.

In the literature, there is virtually no investigation into what triggers the onset of the wet season over the Amazon. For the first time, our results suggest that cold fronts from midlatitude can serve as an important trigger of the wet season onset. These cold front incursions produce rapid enhanced precipitation from the western Amazon to the southeastern Brazil. Such pattern is one of the distinctive features of the onset of the wet season over Amazon. On the other hand, lack of frequent and strong enough cold air triggering, the onset of the wet season in 1982 was delayed, even though the land surface and large-scale thermodynamic structure appear to be unstable enough for the onset of the wet season.

CHAPTER 1

INTRODUCTION

1.1 Background

One of the main centers of convective activity in the global tropics is the Amazon Basin of South America. It is the world's largest rain forest, with an area over 5×10^6 km^2 (Keller et al. 2001). The basin contains approximately 30% of the biospecies on Earth and 20% of the world's fresh water (WWF Profiles). It is a main contributor to the variations of global atmospheric carbon dioxide (Tian et al. 1998). A better understanding of Amazonia's rainfall and its change is important not only for local climate prediction, but also for determining changes in the ecosystem of Amazonia and their contribution to the global carbon cycle and to global climate (Cox et al. 2000).

Annual rainfall over the Amazon varies by as much as 40% interannually (Kousky 1988; Marengo et al. 2001). Amazon convection releases about 20% of the latent heat in the global atmosphere, therefore, variations of Amazon precipitation due to either natural forcing or land use would significantly regulate the water and energy budgets of the atmosphere (Grimm et al. 1995; Gandu and Silva Dias 1998; Keller et al. 2001). Model simulations showed that Amazonia acted as a net source of carbon in the range 0.2–1.2 Pg y^{-1} from 1992 to 1993 (Stroppiana et al. 2000). However, the net emissions are strongly dependent on the annual rainfall patterns. The forest appears to be absorbing carbon in the wet season and emitting carbon during the dry season (Vourlitis et al,

2001). Recent studies have suggested that changes in precipitation over Amazonia dominate the interannual variation of the global atmosphere – terrestrial carbon exchange (Tian et al. 1998) and the terrestrial carbon feedback to the increase of anthropogenic emission of carbon dioxide (Cox et al. 2000).

Namias (1972) and Paegle et al. (2000) have shown the correlation between the precipitation change over tropical South America and the climate over Greenland in North America during boreal winter. Interannual variations in the winter North Atlantic Oscillation (NAO) index during boreal winter are suggested to be attributed to the variations in tropical heating associated with the South American summer monsoon (Watanabe and Kimoto 1999; Robertson et al. 2000; Cassou and Terray 2000). Grimm and Silva Dias (1995) found a connection among the South Pacific convergence zone (SPCZ), the South Atlantic convergence zone (SACZ) and Eurasian pattern systems. Therefore, teleconnection from tropical South America influences atmospheric patterns over the surrounding oceans, extending into the Atlantic and South Pacific subtropical highs (Gandu and Silva Dias 1998; Paegle et al. 2002).

1.2 Motivation

Onset of Amazon rainfall is distinctively different from wet season onsets in other monsoon regions in at least two aspects: areas of high rain rate (about 4–6 mm day^{-1}) spread southeastward from the tropical western Amazon to subtropical southeastern Brazil across 15–20 degrees of latitude within a week or two (Horel et al. 1989); also, the

onset dates can vary by as much as three months, and the annual rainfall can vary by 40% on an interannual scale (Kousky 1988). In the past five years, significant progress has been made in terms of identifying the components of the mechanism that controls precipitation variability over South America. For example, Zhou and Lau (1998) demonstrated that the seasonal changes in the atmospheric circulation over South America are similar to those of a monsoon system when annual means are removed. Summer precipitation is mainly controlled by the summer monsoon circulation. The precipitation is also influenced by the subtropical Low Level Jet (LLJ, Paegle et al. 2002) and cold air incursions (Marengo et al. 1997; Garreaud and Wallace 1998). Liebmann and Marengo (2001) further suggested that the timing of the onset and end of the rainy season contributes more to the interannual variation of precipitation than do changes in precipitation intensity during the rainy season. Hence, understanding what causes the wet season onset is a necessary prerequisite for improving climate prediction of precipitation.

Whether the local land surface fluxes or remote influences from adjacent oceans control the rainfall and circulation of the wet season has been debated for years. For example, many previous studies have suggested that Sea Surface Temperatures (SSTs) in the tropical Atlantic and Pacific Oceans have a strong impact on wet season precipitation over Amazonia (Namias 1972; Rowntree 1976; Hastenrath and Heller 1977; Markham and McLain 1977; Moura and Shukla 1981; Serra 1973; Covey and Hastenrath 1978; Aceituno 1988; Ropelewski and Halpert 1989; Fu et al. 2001). The main source of moisture during the wet season is the transport from the Atlantic (e.g., Gibbs 1979; Rao et al.

1996). However, these SST influences alone cannot explain all interannual variabilities. Using water balance calculation and isotopic analysis, Salati et al. (1979) found that 50-60% of rainfall originates from the recycling of water vapor through evapotranspiration. This implies that local surface fluxes are also important for the rainfall (Gutman and Schwerdtfeger 1965; Rao and Erdogan 1989; Salati 1991). How the changes of large-scale atmospheric circulation and local land surface conditions together determine the interannual variations of Amazon rainfall is still an open question.

The onset of the wet season usually features rapid southeastward expansion of the rainy area from the western Amazon to subtropical southeast Brazil. What triggers such rapid spread of rainfall remains a mystery. The cold surges from mid-latitude South America have been shown to frequently cause rainfall in the western Amazon in austral summer and winter (Garreaud and Wallace 1998, Marengo et al. 1998, Vera et al. 2000). However, we do not know how these cold air intrusions impact the wet season onsets. This thesis aims to seek answers to these open questions.

1.3 Objectives And Outlines Of This Dissertation

In this Dissertation, the mechanisms responsible for the wet season onset over tropical South America are examined. Our purpose is twofold. First, our studies will analyze the evolution of land surface processes and large-scale circulation during the transition from the dry to the wet season over tropical South America. This effort focuses on the controlling mechanism of a climatological onset of the wet season over that

region. Then, we will apply the mechanism to determine the causes of abnormal wet season onset. This application also serves as a test of the validity of the mechanism developed, based on the climatology. We will focus on the influence of the land surface conditions and the triggering mechanisms for the wet season onset because they are less understood than the influence of SSTs on Amazon rainfall. We will also compare the South American Summer Monsoon system (SASM) with a classical Asian monsoon system to determine the similarities and differences between them. This is the first step of my approach to place the SASM in the framework of global monsoon research.

There are five chapters in this Dissertation following the Introduction. The driving factors and the onset mechanisms responsible for the summer monsoon systems in global perspective are reviewed in Chapter 2.

In Chapters 3 and 4, we investigate the evolution of large-scale atmospheric and land surface conditions critical to the wet season onset. The effort is to examine the large-scale environment necessary for the transition from the dry to the wet season.

Chapter 3 focuses on the climatological transition obtained from the composites of fifteen-year instantaneous European Center for Medium-range Weather Forecasts Reanalysis data (ERA), along with rain-gauge data and Global Precipitation Climatology Project (GPCP) data.

The causes of early and late onsets are examined in Chapter 4, with focus on the relative importance between land surface conditions and large-scale atmospheric

circulation changes on an interannual scale. The implications of the land use change over Amazonia are also discussed.

In Chapter 5, we examine what triggers wet season onset over Amazonia, especially the role of cold surges that dominate the synoptic influence over South America (Marengo et al. 1998). It also discusses how, when the necessary large-scale environment as discussed in Chapters 3 and 4 is ready, these synoptic systems impact the wet season onset in general and on an interannual scale.

Chapter 6 discusses the implications of the results to the general understanding of the wet season onset over tropical South America. The similarities and differences between the South American summer monsoon system and the classic Asian monsoon are presented. Outstanding questions and proposed future work in this research area are also discussed.

CHAPTER 2

SUMMER MONSOON: A GLOBAL SURVEY AND ONSET MECHANISMS

The word "monsoon" originates from the Arabic word "mausim", meaning "season" (Ramage 1971; Das, 1972). It was used by seamen about seven centuries ago to describe a system of alternating winds in the Arabian Sea. These winds appear to blow from the northeast for about six months and from the southwest for another six months. Now the usage of "monsoon" has broadened to include almost all of the phenomena associated with the annual weather cycle within the tropical and subtropical continents of Asia, Australia, Africa, the Americas, and their adjacent seas and oceans (Webster et al. 1998). There is no agreement on the precise definition of "monsoon". In a broad sense, the term "monsoon" usually indicates a seasonal reversal in the large-scale circulation system driven by differential heating between the continents and the oceans, associated with precipitation in the tropics and subtropics (Ramage 1971; Das 1972; Lau and Li 1984; Zhou and Lau 1998; Trenberth et al. 2000). The annual cycle of monsoon systems can be divided into two distinct phases (Webster et al. 1998):

- Wet-warm phase: the summer rainy season, during which warm, moist, and very disturbed winds blow inland from the warm tropical oceans;
- Dry-cool phase: the other half of the year, during which winds bring cool and dry air across the monsoon regions from the winter continents.

Based on the climatological monsoon features, the Asian, Australian, and African monsoons have been clearly identified as monsoon systems for years and have been studied extensively. Traditionally, North America and South America were not considered monsoon regions, due to the lack of a strong thermal low and clear meridional temperature and wind reversals (Ramage 1971; Webster et al. 1998). In recent years, however, studies have revealed monsoon-like features in the seasonal changes of atmospheric circulation and rainfall in these two regions. For example, the elevated heating provided by the Rockies and Andes and the seasonal cycles of temperature and precipitation over portions of North and South America are similar to the classic Asian monsoon (e.g., Tang and Reiter 1994; Douglas et al. 1993; Adams and Comrie 1997; Zhou and Lau 1998). Although many researchers have accepted the concepts of North and South American monsoon systems, the extent to which they are controlled by similar mechanisms and the ways in which their differences are explained relative to the classic monsoon still remain unclear. We begin this Chapter by discussing the basic driving factors involved in the summer monsoon systems, and then we review the monsoon systems based on their onset mechanisms.

2. 1 Basic Driving Factors Of Summer Monsoon Systems

Monsoons may be thought of as the circulation responding to the annual cycle of solar heating in an interactive ocean-atmosphere-land system. Generally, four basic elements are recognized as controls on the dynamics of monsoon system onset:

- *The differential heating of the land and the ocean and the resulting pressure gradient force between the summer and winter hemispheres:*

In summer, the air over the continents is much warmer and less dense than the air over the oceans. Consequently, the pressure decreases more slowly with height over the lands than it does over the oceans. If the sea-level pressure were the same over the lands and the oceans, the pressure in the upper troposphere over the continents would be greater than over the oceans. The winds tend to blow from higher pressure to lower pressure (i.e., from land to ocean in the upper troposphere). To compensate for this upper flow of winds, there would be a reverse flow at lower levels from the oceans to the lands (Das 1972; Ding et al. 1996). The strength of the differential heating is controlled by the latitudinal location of the continental land mass due to geostrophic adjustment processes, land surface features, and topography. Strong latitudinal temperature gradients and heating over elevated surfaces produce stronger differential heating, as is the case with the Indian monsoon. Conversely, the differential heating is weak for the South American monsoon because of a weak latitudinal temperature gradient and less extensive surface heating.

- *The impact of the rotation of the planet, relative to the geographic form of the lower boundary and the distribution of differential heating:*

The equilibrium geopotential height in the upper troposphere over a monsoon region is dependent on the Rossby Radius of deformation ($\lambda_R = f^{-1}\sqrt{gH}$). For a similar initial perturbation of geopotential height caused by latent heating of rainfall, the increase of the equilibrium geopotential height over the tropical Amazon (with small *f*, for example) would be less compared to that over the subtropical Indian monsoon region (with large *f*).

- *Land surface properties and processes:*

Land surface properties affect the atmosphere via the surface-atmosphere fluxes of water, energy, and momentum (Shukla and Mintz 1982; Shuttleworth 1991). These land surface properties and fluxes, therefore, significantly influence the onset and structure of the monsoon. For example, over the Sahara, with little evaporation or cloud cover, the desert/semiarid area is heated by a strong diurnal component of sensible heating and causes a higher planetary boundary layer up to 500-hPa. The result of the boundary layer heating is a reduction of the mass in the column developing the heat low (Figure 27 in Webster et al. 1998), the first step of the West African monsoon onset. Charney (1975) suggested that the large albedo over a continental surface such as West Africa might cause precipitation decrease. Xue and Shukla (1993) and Fennessy et al. (1994) demonstrated the influences of surface characteristics on the structure of monsoon systems by

modifying the soil moisture and vegetation. Soil moisture strongly controls the nature of atmospheric fluxes, including the partitioning of available energy between latent and sensible heating (Entekhabi and Rodriquez-Iturbe 1994) and the magnitude of the net radiation absorbed by the surface (Eltahir 1998), thus causing differences in the structure of monsoon systems. For example, over tropical South America, rainforest occupies 65% of the area. The more moist soil over tropical South America leads to a smaller sensible heat flux and a larger latent heat flux, resulting in a smaller Bowen ratio than for dry lands such as the Sahel or the Indian subcontinent. This contributes to a weaker continental-ocean surface temperature difference for the South American monsoon (Li and Fu 2003).

More (less) Eurasian snow amount during the previous cold season has been found to correlate to a weak (strong) Asian monsoon during the following summer (e.g. Kripalani et al., 1996). Modeling studies demonstrated that albedo and the hydrological effects of snow cover may be responsible for anomalous seasonal heating of the atmosphere (Barnett et al. 1989; Yasunari et al. 1991)

Mountainous regions, such as the Himalayas, the Burma Highlands, and the East African Highlands, strengthen the atmospheric response to the solar heating gradient by either elevating the land heating of the atmosphere to the middle troposphere or by creating barriers to the atmospheric flow as shown by Webster et al. (1998).

- *The variation of SST of the major tropical oceans resulting from the annual cycle of the solar heating and the oceanic heat transports induced by the atmospheric winds:*

The response of the oceans to both the annual cycle of solar radiation and to the winds induced by differential heating between the land and the ocean is a critical element of the monsoon systems. Shukla and Fennessy (1994) showed that a dramatic reduction in the monsoon rainfall over the Arabian Sea, India, the Bay of Bengal, and southeast Asia could not be explained without considering the annual cycle of SST. Temporal variations of the heating gradients are induced by the large heat capacity of the water and by the ability of the ocean to store heat below the surface of the ocean. Furthermore, heat is transported by ocean currents that are driven by the atmospheric monsoon flow. El Niño-Southern Oscillation (ENSO) has been shown to influence the interannual variability of monsoon precipitation (Shukla and Paolina 1983; Torrence and Webster 1998). Statistical studies demonstrated that all El Niño years in the Pacific Ocean were followed by drought years in the Indian region, whereas La Niña years were associated with abundant rainy seasons. The specific mechanisms on each monsoon systems are still a subject of active research.

2.2 Regional Aspects Of Summer Monsoons—The Onset Mechanism

a. The Asian Monsoon

The Asian Monsoon includes the Indian monsoon and the East Asian monsoon, both of which have been investigated extensively. The Indian and the East Asian monsoon systems are not independent systems because of the shared large heat source over Tibet and similar heat sink over the tropical Pacific and Indian Oceans during boreal summer.

Observations have shown that seasonal heating of the elevated surface of the Tibetan Plateau and the consequent reversal of the meridional temperature and pressure gradients south of 35°S are essential to the establishment and maintenance of the large-scale general circulation change over Asia and therefore to moisture transport into the region (Flohn 1957; Ye et al. 1979, Gao et al. 1981; Fu and Fletcher 1985; He et al. 1987; Murakami 1987; Yanai et al. 1992). Li and Yanai (1996) have demonstrated that the surface sensible heat flux over the Tibetan Plateau in spring leads to a reversal of the temperature and pressure gradients over Asia. Krishnamurti and Ramanathan (1982), Kuo and Qian (1982) and Krishnamurti et al. (1998) have suggested that summer monsoon onset is closely related to the irregular distribution of large-scale diabatic heating over Asia. Surface sensible heat flux dominates the increase of potential energy. During the development of the monsoon system, potential energy, divergent kinetic energy and rotational kinetic energy all increase with time. The potential energy increases first, due to uneven diabatic heating, it converts to divergence kinetic energy, and finally the divergence kinetic heating turns into rotational kinetic energy. The rotational kinetic energy helps to sustain the monsoon circulation.

b. Australian Monsoon

Based on Ramage's definition of monsoon (i.e., atmospheric circulation differences between January and July), the area north of 25°S over Australia could be considered monsoonal. Australian monsoons are weaker and more variable than the Asian ones. The onset of the summer monsoon is also caused by differential heating between the continents and the surrounding oceans; however, the major heating due to the temperature gradients remains close to the north coast of the continent and the equator because the Australian continent is rather flat, resulting in a faster geostrophic adjustment than the Tibetan Plateau.

During the pre-monsoon season between October and December, an increase of insolation increases surface temperature and surface sensible heat flux in the north-western part of Western Australia, which results in a deep mixed layer. This process initiates a low-pressure area with cyclonic circulation below the 800-hPa level. The steady development of the heat low has been shown to be important to the formation of the Australian summer monsoon circulation (Falls 1970a, 1970b; Leighton 1979; McBride 1975; Lesleie 1980; Suppiah, 1992; Kawamura et al. 2002). The low pressure system usually couples with a thermal high around 600–700 hPa (Kawamura et al. 2002). Intensified low-level westerly anomalies and increased solar radiation in less cloudy air induced by the subsidence in the periphery of the Australian thermal low result in increasing SSTs along the northern coast of Australia. The thermal high concurrent with the shallow vertical circulation leads to a dry intrusion into the layer at about 700 hPa

over the Arafura Sea and Coral Sea through the horizontal and vertical advective processes. The combination of the increase in SST and the dry intrusion creates a more convectively unstable condition. When convective instability is intensified through large-scales disturbances with ascending motion, such as by the Madden-Julian Oscillation (Hendon and Liebmann 1990), deep cumulus convection becomes dominant, and the summer monsoon onset occurs.

c. African Monsoon

Although almost all of the African continent and adjacent east Atlantic and West Indian Oceans can be delineated as monsoonal (Ramage 1971), the most remarkable area is confined to equatorial Africa and the northern part of the continent (Klevin 1957; Flohn and Struning 1969). Here we focus on reviewing the onset mechanism of the summer monsoon over western Africa (west of 30°E). The major difference between the African monsoon system and the Asian summer monsoon is the lack of elevated heating associated with terrain as large and extensive as the Tibetan Plateau (Webster et al. 1998). The seasonal reversal of the trade wind direction over western Africa begins near the equator in April (Grodsky and Carton 2001). The northeast trades and southeast trades then converge in the Inter-Tropical Convergence Zone (ITCZ). In May and June the disturbances are evident between 4°N and 6°N, while by July or August they extend as far as about 10°N.

When the seasonal radiative forcing increases over western Africa, a heat low develops over the Sahara desert (Ramage, 1971; Sultan and Janicot, 2002). Lower

tropospheric air generally converges into the heat low from the continent and ocean, and thus a considerable discontinuity exists along the axis of the heat trough between the dry desert air and relatively moist, originally maritime air (Ramage 1971). Over northern Africa, this discontinuity is termed the "intertropical front" (ITF). When the ITF moves northward gradually from 15°N, the ITCZ is centered at 5°N. The onset stage of the summer monsoon over western Africa is linked to an abrupt latitudinal shift of the ITCZ from a quasi-stationary location near 5°N in May-June to another quasi-stationary location near 10°N in July–August. This leads to an increase of rainfall over the Sudano-Sahelian zone marking the northernmost location of the ITCZ and the beginning of the monsoon season. The shift occurs mostly between 10°W and 5°E, where a meridional land-sea contrast exists, and it is characterized by a temporary rainfall and convection decrease over western Africa. The meridional circulation intensity of the heat low is highest at the beginning of the monsoon onset. This can lead to increased convective inhibition in the ITCZ through intrusion of dry and subsiding air from the north. It can also lead to the increase of potential instability through greater inland moisture advection in the low levels, through higher vertical wind shear due to westerly monsoon wind and acceleration of the mid-level African Easterly Jet (AEJ), through enhancement of the instability character of the AEJ, and through increased short-wave radiation received at the surface (Sultan and Janicot, 2002). The accumulated potential instability breaks the convective inhibition, leading to an abrupt northward shift of the ITCZ to about 10°N.

The surface temperature difference between the land and surrounding oceans initiates the heat low and the ITF, which cause the summer monsoon onsets.

d. North American Monsoon

Although the North American monsoon is less impressive than its cousins in Asia, Australia, and Africa, the summertime circulation centered on northwestern Mexico has been identified as monsoonal (Adams and Comrie, 1997; Barlow et al. 1998; Higgins et al., 2003). The North American monsoon displays many similarities, as well as differences, when compared with other regional monsoons. Notable features of the North American summer monsoon system include major low-level inflow of moisture to the continent (Tang and Reiter 1984; Badan-Dangon et al. 1991), a seasonal increase in continental precipitation (Masino and Garcia 1974; Douglas et al. 1993), and a relatively warm troposphere over the monsoon region, resulting in a "monsoon high" in the upper troposphere (Bryson and Hare 1974). In contrast with classic monsoon patterns, the low-level flow is not cross- equatorial (Webster et al., 1998).

Although the onset mechanism is still not fully understood, the onset of the North American summer monsoon can be thought of as the result of two meteorological changes: the movement westward and northward from winter to summer of the huge upper-level subtropical high-pressure system known as the Bermuda High, and the creation of a thermal low due to intense heating in the Mohave desert, creating rising air and surface low pressure (NOAA Sciences Report 2002). The two features combine to create strong southerly flow over western North America. The southerly low-level winds

help to bring in moisture from the Gulf of Mexico, the Gulf of California, and the Pacific Ocean. From June to July, when humidity reaches its peak values in the region, warm SSTs spread up along the western coast of Mexico, the sea-level pressure (SLP) increases over the southwestern United States (Okabe 1994), and geopotential height increases in mid-latitudes associated with the seasonal heating of the troposphere, due to the elevated terrain of the western United States and Mexico. The resulting middle and upper tropospheric "monsoon high", analogous to the Tibetan High over Asia (e.g., Tang and Reiter 1984), is also associated with enhanced easterlies or weaker westerlies and enhanced Mexico Monsoon rainfall (Douglas et al. 1993) in July-August, when the North American summer monsoon matures.

Overall, the Asian, Australian, African, and North American monsoon systems are all driven by a rapid intensification of land-ocean thermal contrast. The strong sensible heat fluxes over continents result in either an anticyclonic system in the middle to upper troposphere, such as for the Asian monsoon, or thermal low systems at the lower troposphere, such as for the Australian, West African, and North American summer monsoon systems. The heat low helps to form the monsoon trough (McBride and Keenan 1982) over Australia, influence the abrupt shift of the ITCZ through ITF over western Africa (Sultan and Janicot 2002), and cause the low-level southerly flow into southwest North America (NOAA Sciences Report 2002). These processes increase the summer monsoon precipitation and drive the wet season onset. Energy analysis for the classic Asian monsoon further suggests that surface sensible heat flux dominates the

increase of the available potential energy (Li and Yanai 1996; Krishnamurti et al. 1998) and is a main contributor to the maintenance of the summer monsoon systems.

e. South American Monsoon

The climate of tropical South America is characterized by a regular and pronounced cycle in rainfall (Figures 2.1 and 2.2). The climatological seasonal march is illustrated in Figure 2.2 by using 15 years mean precipitation and atmospheric circulation of European Centre for Medium Range Weather Forecasts reanalysis data (ERA). During the austral winter (June, July, and August, JJA), the heaviest precipitation is found over Southern Central America and northern South America, and in ITCZs in the eastern Pacific and tropical Atlantic. It is at these times that the central part of the continent experiences its dry season, occasionally interrupted by the passage of modified cold fronts from midlatitudes. The onset of wet season occurs around the end of October as a rapid shift of the area of maximum convection from the northern extreme of the continent into the central Amazon basin (Horel et al. 1989). Following the annual march of the solar radiation, the precipitation maximum reaches its southernmost position during the austral summer (December, January and February, DJF), encompassing the southern Amazon basin, the central Andes and a portion of the subtropical plains of the continent, and extending southeastward into the South Atlantic convergence zone. The end of the west season tends to occur around May.

South America has not been treated as monsoon region according to Khromov and Ramage definitions (Ramage 1971) because of the lack of a seasonal reversal of wind

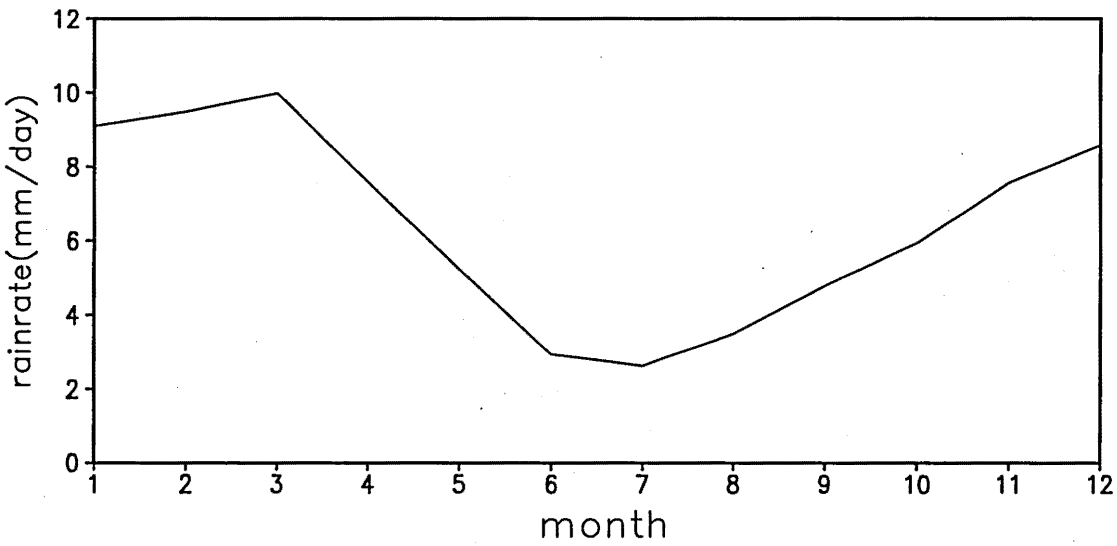

Figure 2.1 Climatological monthly mean precipitation over Southern Amazon region (5°–15°S and 45°–75°W).

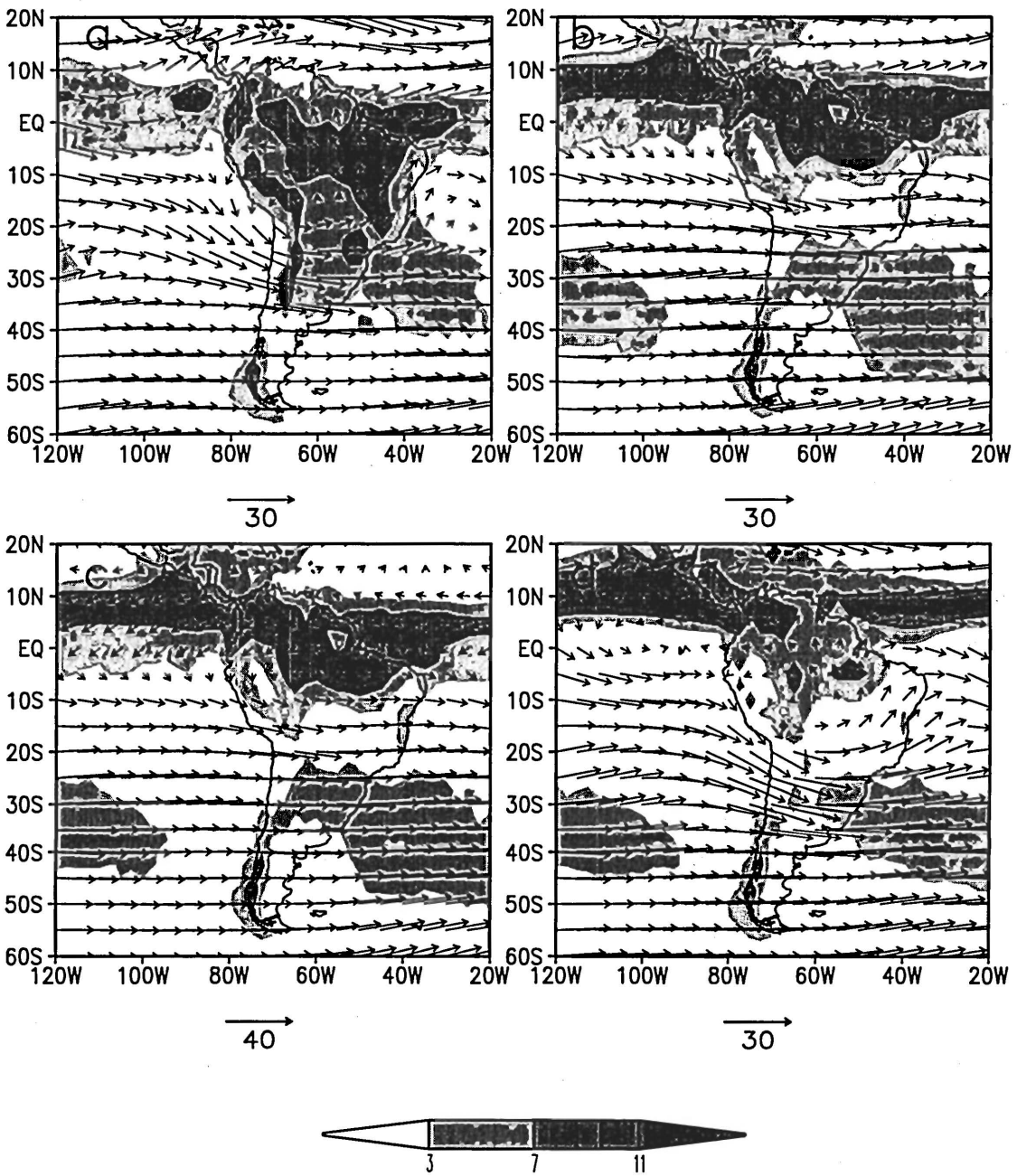

Figure 2.2 Quarterly map of the 15-year mean precipitation (shaded) and 200-hPa winds in austral (a) summer (DJF), (b) autumn (MAM), (c) winter (JJA), and (d) spring(SON) using ERA (1979-1993). The reference vectors for wind are indicated at the bottom of the panels.

direction in the lower troposphere (Fig. 2.3) and no apparent meridional temperature gradient reversal in the upper troposphere (Webster et al. 1998). Zhou and Lau (1998) described the apparent seasonal reversal of the low-level wind over South America after removing the annual mean of the wind. They further showed features of the South American monsoon system similar to those of the Asian monsoon, such as low-level cross-equatorial flow, the Bolivian High vs. the Tibetan High, and the SACZ vs. the Meiyu front of the Asian monsoon. However, the mechanisms controlling wet season onset remained unknown.

Most of the land mass of South America is located in the tropical region, and about 65% of this area is covered by rain forest (Neptad et al. 1999). The daily mean surface temperature gradient between the land and the Atlantic Ocean is only about 2—3°C during austral summer (Satyamurty et al. 1998). The small temperature difference between the land and oceans seems unfavorable to classic monsoon systems. Amazon precipitation systems have been shown to exhibit characteristics that resemble those of maritime precipitation found over the Indian Ocean and the South China Sea, based on cloud reflectivity structure (Petersen and Rutledge 2001). This precipitation type is quite different from the continental convective precipitation observed over other monsoon regions. The causes of the South American summer monsoon onset and its unique precipitation features have just begun to be addressed by the climate research community.

Unlike other summer monsoon systems, the onset date of the tropical South American rainy season may vary by about three months interannually, based on rain

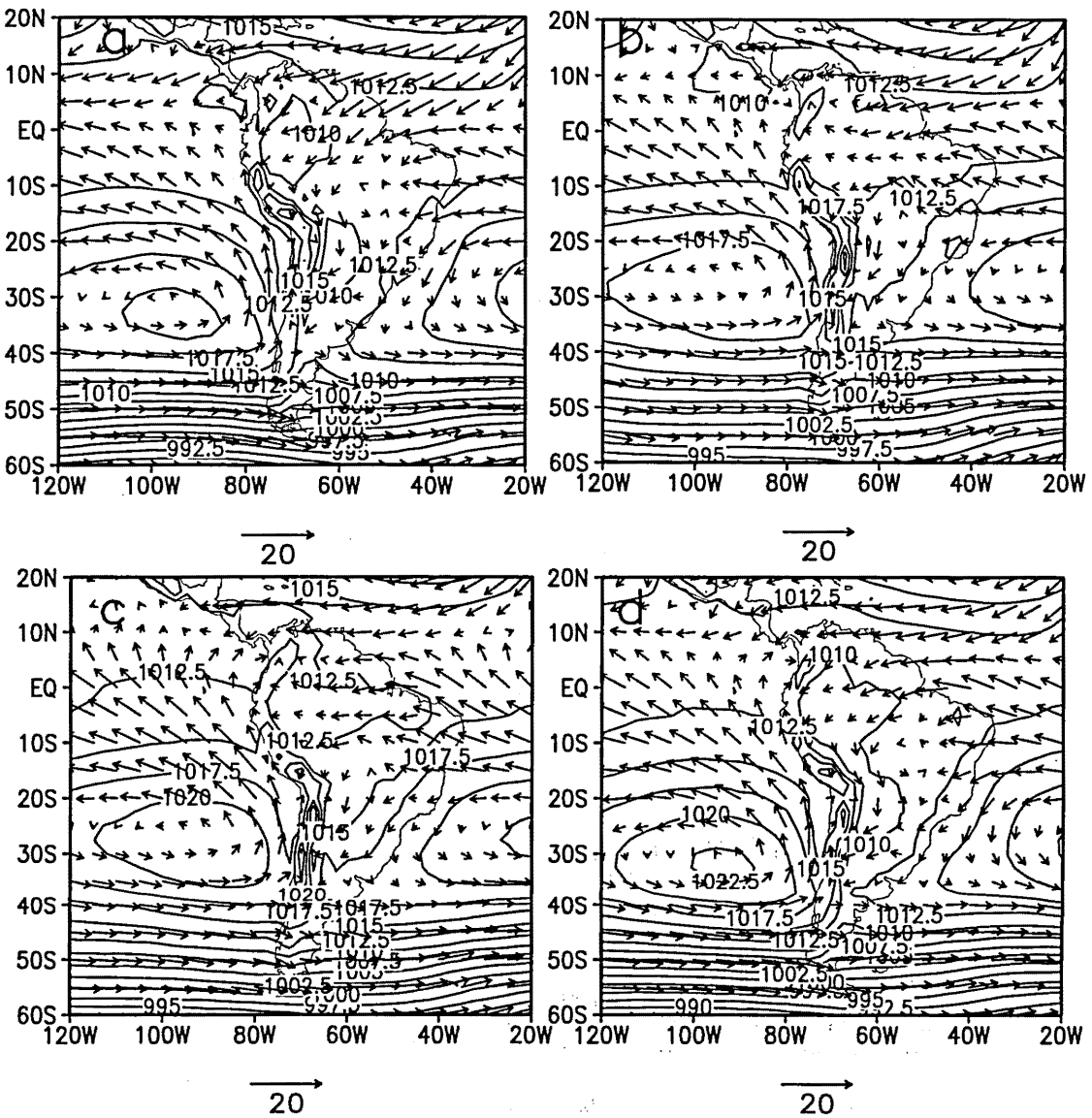

Figure 2.3 Quarterly maps of the 15-year mean sea level pressure (contoured every 2.5hPa) and 925-hPa winds in austral (a) summer (DJF), (b) autumn (MAM), (c) winter (JJA), and (d) spring (SON) using ERA (1979-1993).

gauge data (Marengo et al. 2001). Li and Fu (2003) suggested that the onset of the wet season may start as early as late August in one year and as late as the end of December in another year. Since increased precipitation over tropical South America is needed to form the South American summer monsoon (e.g., Lenters and Cook 1997), an understanding of the causes of the large interannual variation in wet season onset over the Amazon is important to determine the mechanism of the South American summer monsoon.

The summer monsoon onset usually proceeds from the northwestern part of South America. The deep convection band then expands rapidly southward to southeastward from the western Amazon to southeastern Brazil in late austral spring, and finally progresses eastward to northeastern Brazil, covering the entire basin (e.g., Kousky 1988; Sugahara 1991). The monsoon retreats gradually from the south to the north following the sun migration (Liebmann and Marengo 2001), which is not symmetric to the path of wet season onset over the region. This unique onset process is also different from the other monsoon systems. Understanding the causes of this process will help us to determine the processes and factors that control monsoon onset over South America.

CHAPTER 3

MECHANISM OF WET SEASON ONSET OVER TROPICAL SOUTH AMERICA—CLIMATOLOGY

The wet season onset date and the amount of rainfall are critical for agriculture, hydroelectric power generation, and local ecosystems for the Amazon region. Liebmann and Marengo (2001) have shown that change of the timing of onset and end of the rainy season contributes more to the interannual variation of precipitation than change of the intensity of precipitation during the rainy season. The transition from dry to wet seasons is ultimately driven by the seasonal migration of the sun, however, what controls the timing of the onset and its variability over South America is still unclear. In particular, it is not known how land surface fluxes increase and change of land-ocean surface temperature gradient affect the destabilization of the atmosphere and the supply of the water vapor needed for wet season rainfall. The answer to this question is key for understanding interannual variability of the precipitation and for determining the climatic impact of land use in the region. For example, if the land surface latent heat flux is a critical source of moisture for the transition, a preseasonal decrease in the surface latent heat flux would effectively slow the transition and delay the onset of the wet season. On the other hand, if the primary source of moisture is the transport from the Atlantic, a preseasonal dry condition would enhance the moisture transport from the Atlantic Ocean,

as a result of a stronger surface sensible heat flux and consequently a stronger land-ocean temperature gradient. This preseasonal dry condition would accelerate, instead of decelerate, the transition from dry to wet seasons.

Whether the local land surface fluxes or remote influences from adjacent oceans control the rainfall and circulation of the wet season has been debated for years. For example, Gutman and Schwerdtfeger (1965), Salati et al. (1979), and Rao and Erdogan (1989) suggested that the land surface fluxes control the wet season circulation pattern over South America and water flux is the main contributor of moisture in the wet season. On the other hand, many other studies (e.g., Namias 1972; Serra 1973; Rowntree 1976; Hastenrath and Heller 1977; Markham and McLain 1977; Covey and Hastenrath 1978; Moura and Shukla 1981; Aceituno 1988; Ropelewski and Halpert 1989; Fu et al. 2001) have suggested that SSTs in the tropical Atlantic and Pacific Oceans strongly control the precipitation over the Amazon through the direct thermal circulation of the Atlantic ITCZ as well as by Rossby waves propagating from the extratropical South Pacific to subtropical South America. The main source of moisture during the wet season is the transport from the Atlantic (e.g., Gibbs 1979; Rao et al. 1996). Reconciliation of these apparent differences among the previous works and their implications for the main driver from dry to wet seasons must be undertaken in order to adequately understand the seasonal transition.

How the atmosphere is destabilized during the transition from dry to wet seasons has been examined by Fu et al. (1999). They observed that a moistening planetary

boundary layer (PBL) and a weakened inversion due to declining temperatures at the top of the PBL appear to be the main contributors to the destabilization. Their results suggest that half of the extra moisture in the PBL during the wet season is obtained from the entrainment of more humid air during diurnal growth of the PBL. This phenomenon implies that the moisture transport which increases the humidity above the PBL is an important contributor to the moisture increase in the PBL. These results were obtained by comparing a dry season with a peak wet season, although whether they are applicable to the transition period is unclear.

The importance of the large-scale dynamical processes to the onset of the rainy season has been suggested by many previous studies. However, most such earlier studies have focused on the relationships among Amazon convection, the Bolivian High, and large-scale, lower-level flow during the peak phase of the Amazon rainy season (e.g., Virji 1981; Nishizawa and Tanaka 1983; Chu 1985; Hastenrath 1990). Whether such relationships characterize the expected dynamic responses to tropical convection (Gill 1980) or the causes of the convection is unclear. Horel et al. (1989) have suggested that deep convection in the Amazon basin appeared prior to the establishment of the Bolivian High in the case of 1985–1986. This implies that the Bolivian High may be a result, instead of the cause, of the Amazon precipitation. This result is consistent with the numerical simulations of Silva Dias et al. (1983), Gandu and Geisler (1991), and Lenters and Cook (1997), which indicate that the latent heat released by Amazon convection is needed for building up the Bolivian High to its observed strength. Hence, the onset of the

rainy season in the Amazon could be an early step in the transition to the South American summer monsoon circulation. Therefore, the processes controlling the convection prior to the establishment of the Bolivian High is probably also crucial to the onset of the South American summer monsoon.

Examining how the increased solar energy is transformed into kinetic energy to support the development of the wet season circulation can also shed light on the dynamic processes that drive the transition. Krishnamurti et al. (1998) have examined the mature South Asian monsoon system and have found that the increased available potential energy (APE) provided by differential heating between land and ocean is sufficient to support the summer South Asian monsoon circulation. Such APE is first converted into divergent kinetic energy, and then transformed into rotational kinetic energy[1]. The latter spins up the upper tropospheric, anticyclonic flow similar to that observed in South Asia. Moscati and Rao (2001) have applied a similar analysis of energy conversion in the mature South American monsoon system. They found that the APE is converted into divergent kinetic energy through a direct circulation response to the atmospheric heating. The conversion from divergent to rotational kinetic energy is similar to that of the South Asian monsoon. In this study, instead of examining a mature monsoon system, we will examine the energy conversions during the transition from dry to wet seasons by using instantaneous ERA data and the formulas of Krishnamurti and Ramanathan (1982) and

[1]The divergent and rotational kinetic energy are defined as $\frac{1}{2}((-\frac{\partial \chi}{\partial x})^2 + (-\frac{\partial \chi}{\partial y})^2)$ and $\frac{1}{2}((-\frac{\partial \psi}{\partial y})^2 + (\frac{\partial \psi}{\partial x})^2)$, respectively, where χ and ψ are velocity potential and streamfunction.

Krishnamurti et al. (1998). This Chapter pursues these goals and provides a systematic assessment of the processes that initiate and accelerate transition to the wet season onset over the Southern Amazon region.

3. 1 Data And Method Description

3.1.1 Data Sets

We use ERA, rain gauges data (Liebmann and Marengo 2001; Marengo et al. 2001) and the GPCP blended precipitation data in this study. The rain gauges are located within the Brazilian Amazon basin, the gauge data were originally from the National Water and Electric Energy Agency of Brazil (ANEEL). ERA has produced global reanalysis 4 times daily from 1979 to 1993. To determine how well ERA precipitation data represent the rainfall pattern in the Amazon Basin, these data on 2.5° latitude and 2.5° longitude resolution were compared to the rain gauge data and GPCP data in the domain of 5°–15°S, 45°–75°W (Fig. 3.1, domain DEFG, referred to hereinafter as the Southern Amazon region) at the same period. The most significant discrepancy between the data sets is that the ERA overestimates dry season rainfall by as much as 3 mm day^{-1} compared to rain gauge measurements (Fig. 3.2a), although ERA is comparable to that of GPCP. During wet season, the ERA rainfall is about 2–3 mm day^{-1} lower than that of the rain gauge data. The assimilated seasonal cycle of rainfall is evaluated by removing the

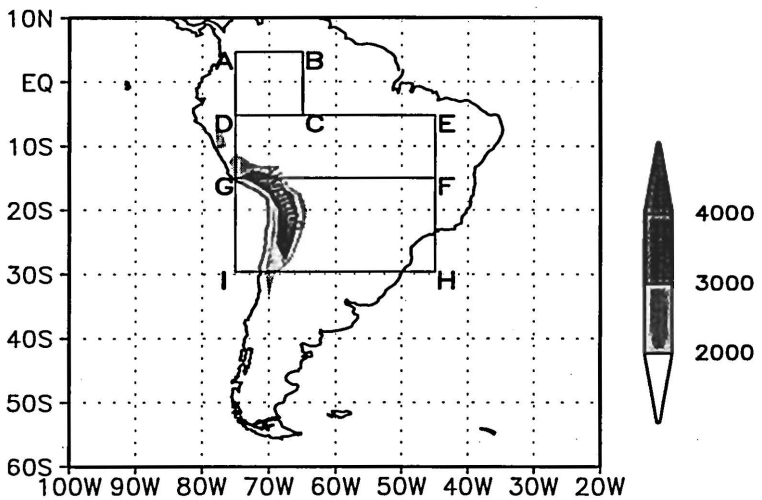

Figure 3.1. The domains for V-index (5°S–5°N and 65°–75°W, ABCD), Southern Amazon region (5°–15°S and 45°–75°W, DEFG), and the extension for geopotential height at 200 hPa Z_{200hPa} (5°–30°S and 45°–75°W, DEHI), respectively. The darkest shaded region indicates terrain elevation in excess of 4000 m.

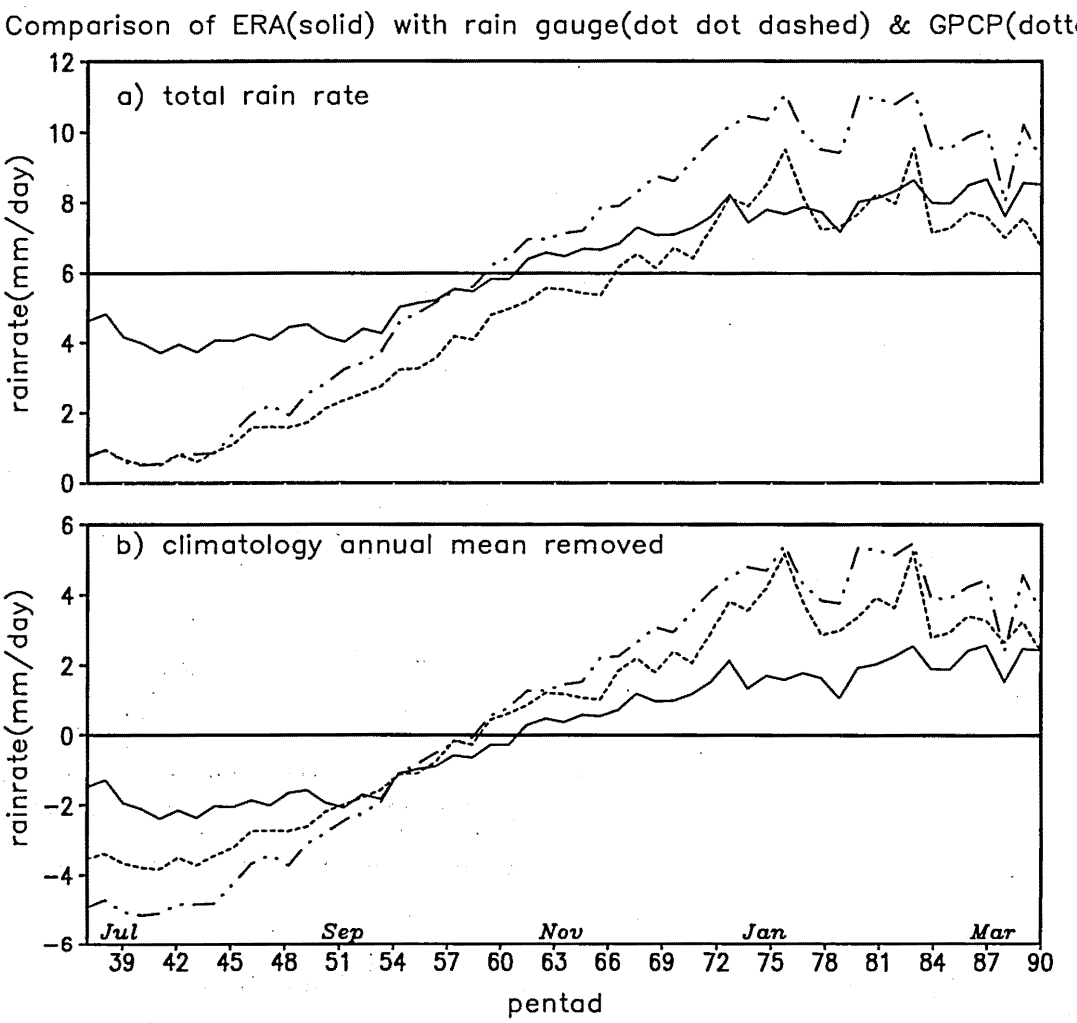

Figure 3.2. (a) The 15-year (1979–1993) mean seasonal variations of pentad rain rate (mm day^{-1}) for ERA (solid line), GPCP (dotted line), and rain gauge data from ANEEL (dot-dot-dashed line) averaged over Southern Amazon region; (b) same as (a) but the climatology annual mean has been removed.

climatological annual mean, calculated for the period of 1979–1993 (Fig. 3.2b). The timing and general trends of the transition from the dry to the wet seasons derived from ERA are similar to those of rain gauge and GPCP data, although the rate of increase is only about half that of observations. The calendar date of rain-rate increase during the early stage of the transition obtained from ERA is delayed by nearly 45 days, compared to that of the rain gauge data. To address the impact of the error in the ERA rain rate, we will use observed rain rates as well as that of ERA in our composite analysis. Other observations of atmospheric and surface conditions related to rainfall are very limited over the Amazon. Fu et al. (2001) compared the climatological monthly mean vertical profiles of temperature, humidity, and zonal and meridional winds assimilated by the ERA with those derived from radiosondes at Manaus (3°S, 60°W) for each calendar month during the period of 1987–1993. Their comparison (their Figs. 5 and 6) suggests a less than 1K difference in temperature profiles, a good agreement of humidity between 925 hPa and 100 hPa, and about 10% systematically overestimated humidity between the surface and 925 hPa. The differences of zonal and meridional wind profiles were less than 2 m s^{-1} below 200 hPa. The surface fluxes and structure of the PBL of the European Center for Medium-range Weather Forecasts (ECMWF) short-term forecast for a wet season have been carefully compared by Betts and Jakob (2002) using observations from the Wet Season Atmospheric Mesoscale Campaign (WETAMC) of the Large-scale Biosphere-Atmosphere Experiment in Amazonia (LBA). They found the model biases were rather small for the mean diurnal cycles of potential temperature, mixing ratio,

equivalent potential temperature, and the pressure height to the lifting condensation level. ECMWF was also able to qualitatively capture the patterns and relative importance of each type of flux in the surface energy budget equation for wet season condition. Quantitatively, ECMWF tended to overestimate the net radiative flux by as much as 10%. This extra incoming energy was largely balanced by greater latent heat flux than the tower observations.

How well ERA can assimilate the changes of surface sensible and latent fluxes during the transition from the dry to the wet season is examined by comparing to the data from the Anglo-Brazilian Climate Observation Study (ABRACOS) sites in Reserva Jaru (RJ, 10°05'S 61°55'W), near Ji-Parana, Rondonia, during the transition period from the dry to the wet seasons in 1992 and 1993, the observations of ABROCOS are chosen for their overlap with the period of the ERA. Notice the spatial scale difference between the ERA and the *in situ* measurements from the ABRACOS flux tower, a complete agreement between the ERA and ABRACOS should not be expected. Figure 3.3 shows the comparisons of surface latent fluxes between ERA and observations. The differences of latent and sensible heat fluxes between ERA and the observations are larger than the random noises for the observational fluxes during the dry season, but the general trends of latent heat fluxes assimilated by ERA agree well with the observations prior to early September. This agreement during the early stage of the transition is likely to support an adequate initiation of the transition in ERA because the increase of latent surface flux dominates the increase of the local moist static energy (Li and Fu 2003). ERA

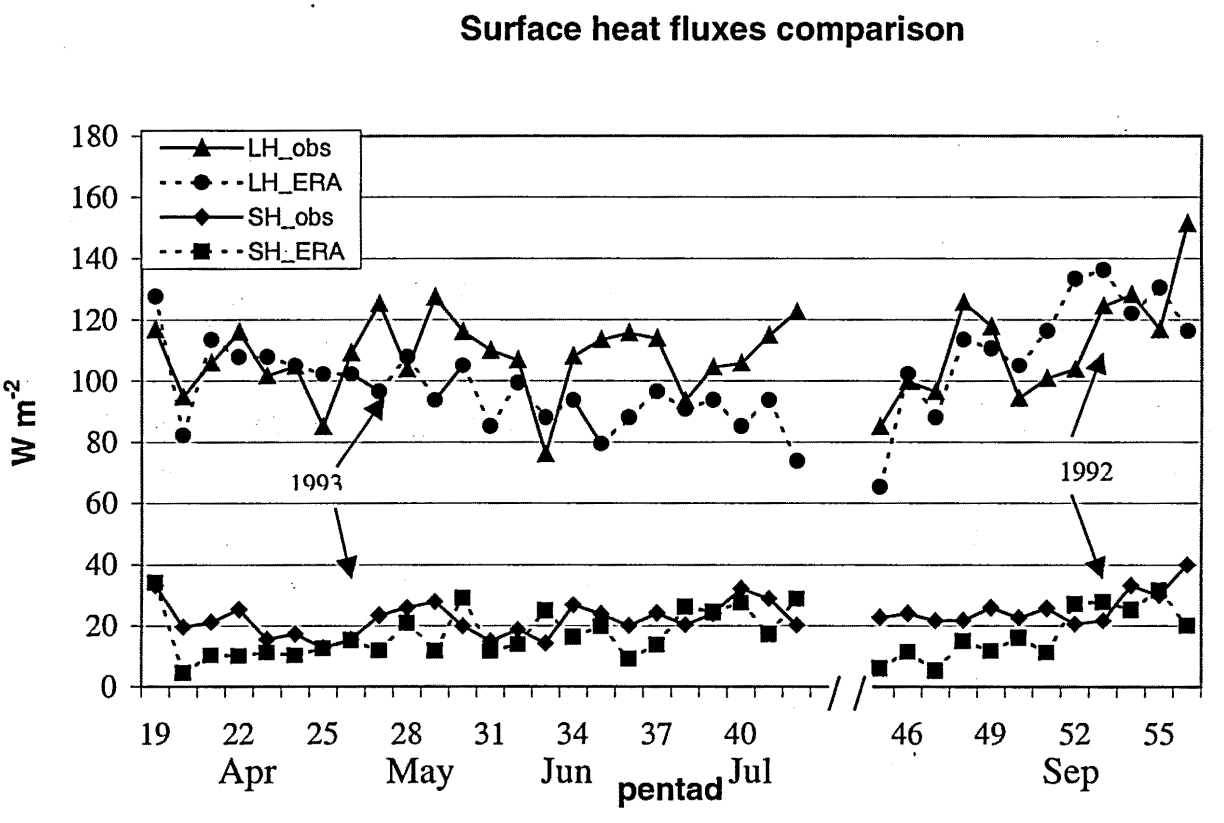

Figure 3.3. Time series of the surface sensible (SH) and latent (LH) fluxes averaged over the 1992 and 1993. The surface fluxes obtained from ERA are plotted in curves with squares (SH) and dots (LH), respectively. The surface fluxes obtained from *in situ* ABRACOS observations are plotted in curves with diamonds (SH) and triangles (LH), respectively. The numbers of pentads in the abscissa are determined by their calendar dates. The ABRACOS observations of SH and LH are obtained from the tower measurements at the forest site in Reserva Jaru, Rondonia (10.08°S, 61.93°W) near Ji-Parana. The ERA SH and LH are obtained from the 2.5° grid box overlap with this ABRACOS site. The unit is Wm^{-2}.

significantly underestimates the surface latent flux between middle September and middle October (from pentad 50 to pentad 57). However, these discrepancies on this stage of the transition should have a limited influence because the transition is now increasingly dominated by changes of the large-scale circulation. ERA underestimates the surface sensible heat flux by as much as 50% prior to late September (pentad 52), but overestimates the increase of the sensible heat flux during the transition. Culf et al. (1998) have shown that ERA underestimates the surface solar flux at Reserva Jaru, especially during May to August due to the errors of cloud cover in the ERA. This underestimation of surface solar flux may contribute to the underestimation of surface latent and sensible flux as shown in Fig. 3.3. In short, ERA appears to reasonably capture the evolution of atmospheric circulation key to the transition from the dry to the wet season over the Amazon. The land surface conditions may be not statistically significant in the dry season, but reasonably represent the variations of the real atmosphere during the early stage of the transition and the wet season (Betts and Jacob 2002).

We use horizontal wind, vertical velocity, geopotential height, temperature, relative humidity, and specific humidity from ERA data at 13 levels (1000, 925, 850, 775, 700, 600, 500, 400, 300, 250, 200, 150, and 100 hPa, respectively) to derive the atmospheric thermal and dynamic fields related to the change of rainfall for the Southern Amazon region. All variables in the study, especially those nonlinear terms related to the input fields, are first computed from instantaneous input values at six-hour intervals. They are then averaged over a period of five days (a pentad). The pentad resolution has been

shown to minimize daily variations and noise but still to be fine enough to resolve the changes during the transition from dry to wet season over the Amazon (e.g., Kousky 1988; Horel et al. 1989).

3.1.2 Domain Of The Analysis

Because the peak of the rainy season varies from July to January from the northern to southern Amazon, we choose the Southern Amazon region (5°–15°S, 45°–75°W) as the domain of our interest (domain DEFG in Fig. 3.1), to clearly capture the seasonal cycle of the rainfall over Southern Hemisphere Amazon. As shown in Kousky (1988) and Marengo et al. (2001), the wet season onset in this domain generally occurs in austral fall (October to November). This domain is mostly within the Amazon basin except for an inclusion of a small segment of Andes in the southwestern corner of the domain. The wet season in this domain starts before the establishment of the South American summer monsoon and presumably provides the needed latent heat for the development of the Bolivian High (Silva Dias et al. 1983; Gandu and Geisler 1991; Lenters and Cook 1997). Because the upper troposphere high is expected to occur to the southwest of the latent heating in the Amazon (e.g., Gill 1980; Lenters and Cook 1995), we expand the southern boundary of our domain southward to 30°S when we diagnose the changes of 200-hPa geopotential height (domain DEHI in Fig. 3.1). This expansion allows a more complete inclusion of the upper tropospheric response to the Amazon heating and the Bolivian High.

3.1.3 Computation of The Key Variables

One effective way to understand what drives the transition from the dry to the wet seasons over South America is to clarify the similarities and differences between the South American and a more thoroughly studied classical monsoon system. Specifically, we aim to clarify whether the formation of the wet season circulation over the Southern Amazon region is driven by atmospheric dynamic processes similar to those of the Asian monsoon. We also hope to determine whether the onset of wet season over the Amazon is initiated mainly by an increase of the land sensible heat flux, as occurs in the South Asian monsoon, or by an increase of surface latent heat flux. The former leads to the reversal of the land-ocean surface temperature gradient, consequently the reversal of the low-level cross-equatorial flow and moisture transport. The area remains very dry until the reversal of the cross-equatorial flow. If the latter is the case, an increase of surface latent flux could destabilize the local atmosphere and increase convection even before the reversal of the large-scale wind and moisture transport. The sensitivity of the monsoon onset to the surface fluxes would be very different in these two cases. To clarify how the onset of the wet season over the Amazon is initiated, we will examine the evolution of the lower tropospheric moist static energy, the cross-equatorial flow that transports moisture into the domain, energy conversion, and the circulation at the upper troposphere. These conditions are represented by the equivalent potential temperature (θ_e) at 850-hPa, the V-index (Wang and Fu 2002), net moisture convergence, the

conversion function between the atmospheric divergent and rotational kinetic energy (C), and 200-hPa geopotential height ($Z_{200\,hPa}$).

Equivalent potential temperature is computed from instantaneous temperature and specific humidity from ERA. The tendency of θ_e ($\frac{\partial \theta_e}{\partial t}$) is computed from the difference between subsequent daily mean θ_e and previous daily mean θ_e divided by the two-day interval in the unit of K day^{-1}. Five daily values are then averaged to obtain a pentad averaged value $\frac{\partial \theta_e}{\partial t}$. To diagnose the causes of increasing $\frac{\partial \theta_e}{\partial t}$ at 850-hPa, we also compute the contributions of the tendencies of temperature ($\frac{\partial T}{\partial t}$) and specific humidity ($\frac{\partial q}{\partial t}$) to $\frac{\partial \theta_e}{\partial t}$ at 850-hPa expressed as the following:

$$\frac{\partial \theta_e}{\partial t} \cong \underbrace{\frac{\theta_e}{T_l}\frac{\partial T}{\partial t}(1+F)}_{A} + \underbrace{\frac{\theta_e}{T_l}\frac{L_c}{C_p}\frac{\partial q}{\partial t}(1-G)}_{B} \qquad (1)$$

where L_c is the latent heat of vaporization, C_p is the specific heat for constant pressure, and T_l is the temperature at the lifting condensation level. F and G are defined as in (2) and (3), where e is the vapor pressure, q is the specific humidity and p is pressure:

$$F = \frac{L_c}{C_p}\frac{2840 \times 3.5q}{T_l^2 (3.5\ln T - \ln e - 4.805)^2} \qquad (2)$$

$$G = \frac{2840 \times 0.622 pq}{eT_l (3.5 \ln T - \ln e - 4.805)^2 (0.622q)^2} \quad (3)$$

Term A of (1) represents the contribution of $\frac{\partial T}{\partial t}$ to $\frac{\partial \theta_e}{\partial t}$ at 850-hPa, and term B represents the contribution of $\frac{\partial q}{\partial t}$.

The V-index is defined as the averaged meridional wind at 925-hPa for the area of 5°N–5°S, 65°–75°W by Wang and Fu (2002) (Fig. 3.1, domain ABCD) to represent low-level cross-equatorial flow. The net moisture convergence is calculated from the net zonal and meridional moisture transport (Δ(uq) and Δ(vq)), respectively, to the Southern Amazon region. Zonal moisture fluxes are first integrated from 1000-hPa to 100-hPa and from 5°S to 15°S along 75° W ($(uq)_{75°W,5°-15°S}$) and 45°W ($(uq)_{45°W,5°-15°S}$) respectively. The net zonal moisture convergence Δ(uq) is calculated by the difference between these terms. A positive value of $\Delta(uq)$ represents a net zonal moisture convergence to the region. Similarly, $(vq)_{5°S,45°-75°W}$ and $(vq)_{15°S,45°-75°W}$ are meridional moisture fluxes integrated from 1000-hPa to 100-hPa and from 45°W to 75°W along 5°S and 15°S respectively. The net meridional moisture transport $\Delta(vq)$ is computed from the difference between these two meridional moisture transport terms. The total moisture convergence to the Southern Amazon region, i.e., the sum of $\Delta(uq)$ and $\Delta(vq)$, is then converted into precipitable water per day per square meter, in order to compare with the rain rate.

The energy conversion from divergent to rotational kinetic energy, C, is calculated using the formulas of Krishnamurti et al. (1998).

$$C = \langle f\nabla\psi \bullet \nabla\chi \rangle + \left\langle \nabla^2\psi\nabla\psi \bullet \nabla\chi \right\rangle + \left\langle \nabla^2\chi\frac{(\nabla\psi)^2}{2} \right\rangle + \left\langle \omega J(\psi, \frac{\partial\chi}{\partial p}) \right\rangle \qquad (4)$$

where f is the Coriolis parameter. ψ and χ are stream function and velocity potential respectively. $\langle\ \rangle$ denotes the integrations in the horizontal and vertical domain (5°–15°S, 45°–75°W, and from 1000 hPa to 100 hPa). The integration is then averaged over the area. We calculated all the terms in formula (4), and our calculation shows that the first term $f\nabla\psi \bullet \nabla\chi$ dominates the total conversion, which agrees with the results of Krishnamurti et al. (1998) for the South Asian monsoon and of Moscati and Rao (2001) for the tropical Amazon region. This term is proportional to the projection of the divergent wind on the rotational wind. When $\nabla\psi \bullet \nabla\chi$ is negative, divergent kinetic energy transforms to rotational kinetic energy. This leads to a positive C for negative Coriolis parameter in the Southern Hemisphere.

3.1.4 Composite Analysis

We use the composite method to highlight the common features for the 15 transitions. Because the year-to-year variation of the onset date over Amazon can vary as much as three calendar months (cf. Marengo et al. 2001), our composite is centered at the pentad of the onset (defined as pentad 0, the threshold for defining the onset date is listed in the following subsection) of each year, rather than by calendar dates. The n^{th} pentad

before the onset at each year is defined as pentad $-n$, and the n^{th} pentad after the onset is defined as pentad n. Each of the composite variables for a given pentad, i, is calculated from the 15 values of that variable for the pentad i of each year during the period of 1979–1993. This approach of using relative pentads enables us to more clearly focus on the large-scale circulation change associated with the evolution of the onset process, instead of calendar dates, over the Southern Amazon region.

Figure 3.4 shows 95% confidence level of each composite variable using student-t distribution. The narrow confidence intervals of rain rate, V-index and moisture convergence suggest close agreements between the estimated composite values and statistically "true" composite values. The changes of these variables through the transition are larger than the uncertainties of the estimated values. The confidence intervals of C and $\frac{\partial \theta_e}{\partial t}$ are not as narrow as those of V-index, rainrate and moisture convergence. However, C still shows statistically significant change from negative to positive from the initial phase to the onset during the transition. Comparing to the confidence interval, the increase of $\frac{\partial \theta_e}{\partial t}$ at 850 hPa is also significant for the period of pentad –18 to pentad –4. For the rest of the transition period, especially after pentad –4, the fluctuations of $\frac{\partial \theta_e}{\partial t}$ at 850 hPa around zero become too small to be statistically significant. Hence, we will focus our discussion of the $\frac{\partial \theta_e}{\partial t}$ at 850 hPa on the early stage

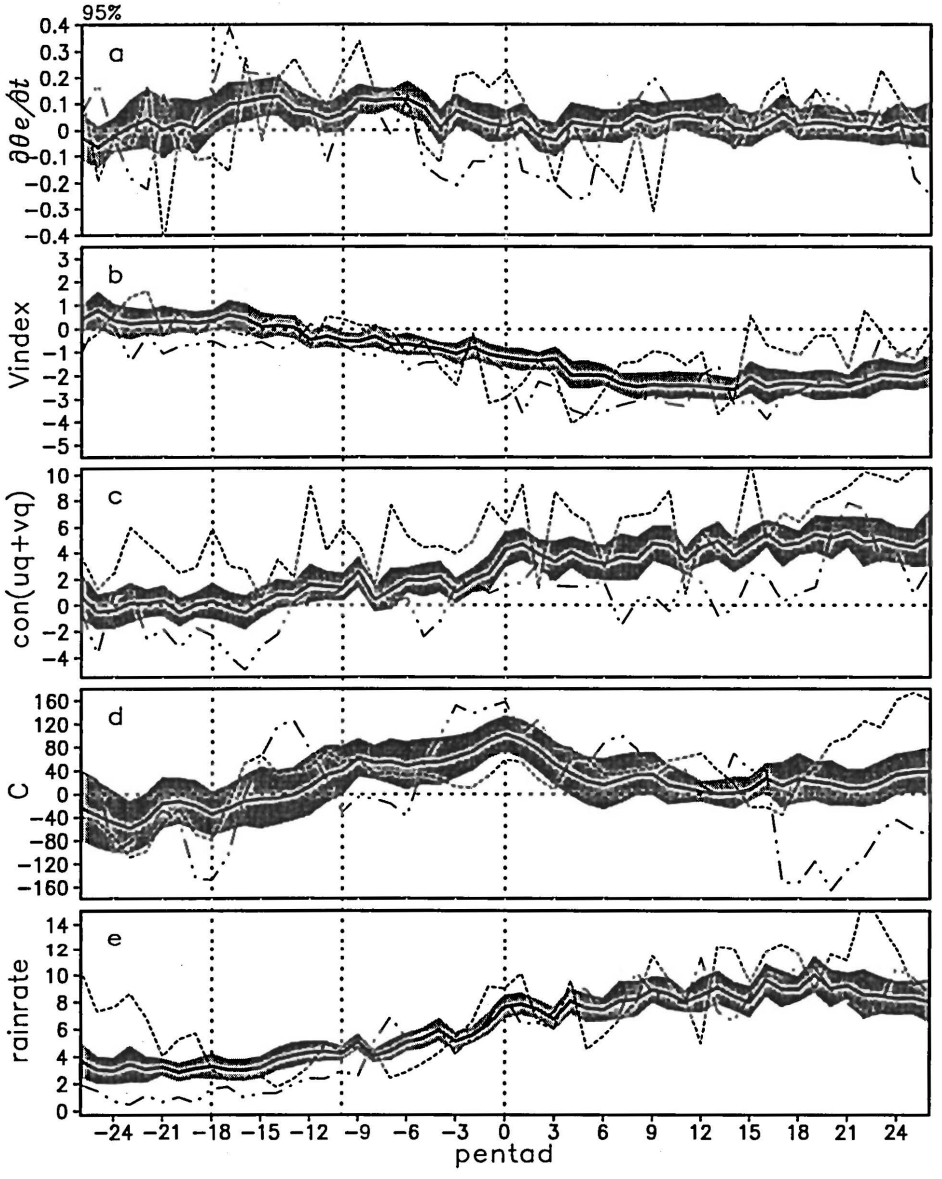

Figure 3.4. Seasonal changes of: (a) $\partial\theta_e/\partial t$ at 850 hPa (K day^{-1}); (b) V-index (m s^{-1}); (c) net moisture convergence (mm day^{-1}); (d) kinetic energy conversion function C (10^{-6} m^2 s^{-3}); (e) rain rate (mm day^{-1}). Solid lines in each panel are the composite results for each variable. Shaded areas represent the confidence intervals at 95% significance. Dotted lines and dot-dot-dashed lines show the years with maximum positive and maximum negative departures from the composite results integrated through the entire transition periods. The three vertical dotted lines divide times between the initiating, developing and maturing phase respectively, of the transition.

of the transition (from pentad –18 to –4), during which its increases are statistically significant. As we will show later, this is also the period during which the accumulation of lower troposphere potential energy is the most critical to the transition.

The composite results are compared to extreme cases in 15 years of the analysis. Figure 3.4 shows that the variables change in the years of maximum positive (dotted lines) and maximum negative (dashed lines) departures, respectively, from the composite results (solid lines) integrated through the entire transition period. Notice that the years of the extreme cases for each variable are determined independently, based on the maximum accumulated departure from its composite time series. Hence, the years of extreme cases can vary from one field to another. This approach presents a maximum possible departure of each field from its composite. As seen from Fig. 3.4, despite expected higher frequency variations and systematic higher or lower shift of the curves for the extreme cases, the general trends of V-index, net moisture convergence, the energy conversion function, and rain rate for the composite and extreme cases are similar. The large deviations from the composite values for $\frac{\partial \theta_e}{\partial t}$ at 850 hPa from the pentad –5 to pentad 8, and for the energy conversion function after pentad 15 suggest that the composites do not adequately represent extreme cases during these periods for these variables. Fig. 3.5 compares the composite evolutions of rainfall obtained from ERA with those obtained from the rain gauges and GPCP blend rainfall data, respectively. The composite results of the rain gauges and GPCP data are calculated using the same method

described above except the onset criteria are based on their own climatological means. Fig. 3.5 shows that the rainfall changes associated with the onset processes in ERA are more realistically assimilated than the seasonal cycle based on the calendar date, as shown in Fig. 3.2. This is due to the fact that our composite method allows us to remove the bias of ERA in terms of calendar onset dates and to focus on the thermal and dynamic consistency of ERA with real transition process. Overall, Figures 3.4 and 3.5 suggest that our composite changes are mostly statistically significant, and reasonably represent the climatology of the transition.

3.1.5 Defining The Onset of The Wet Season

How to best define the wet season onset over the Amazon is still a subject of ongoing discussion (Liebmann and Marengo 2001). Kousky (1988) defined the climatological onset date by choosing a threshold of 240 W m^{-2} for the pentad outgoing longwave radiation (OLR). The onset date is identified as when OLR in 10 out of 12 subsequent pentads is below 240 W m^{-2} and OLR in 10 out of 12 previous pentads is above 240 W m^{-2}. His approach captures the large increase, both in frequency and intensity, of the precipitation associated with the onset of the wet season. His results show that the onset of the convection expands rapidly from northwest of the Amazon basin to the south and the southeast, then migrates eastward at a slower pace. Following a similar approach, Marengo et al. (2001) defined the onset of the wet season using rain

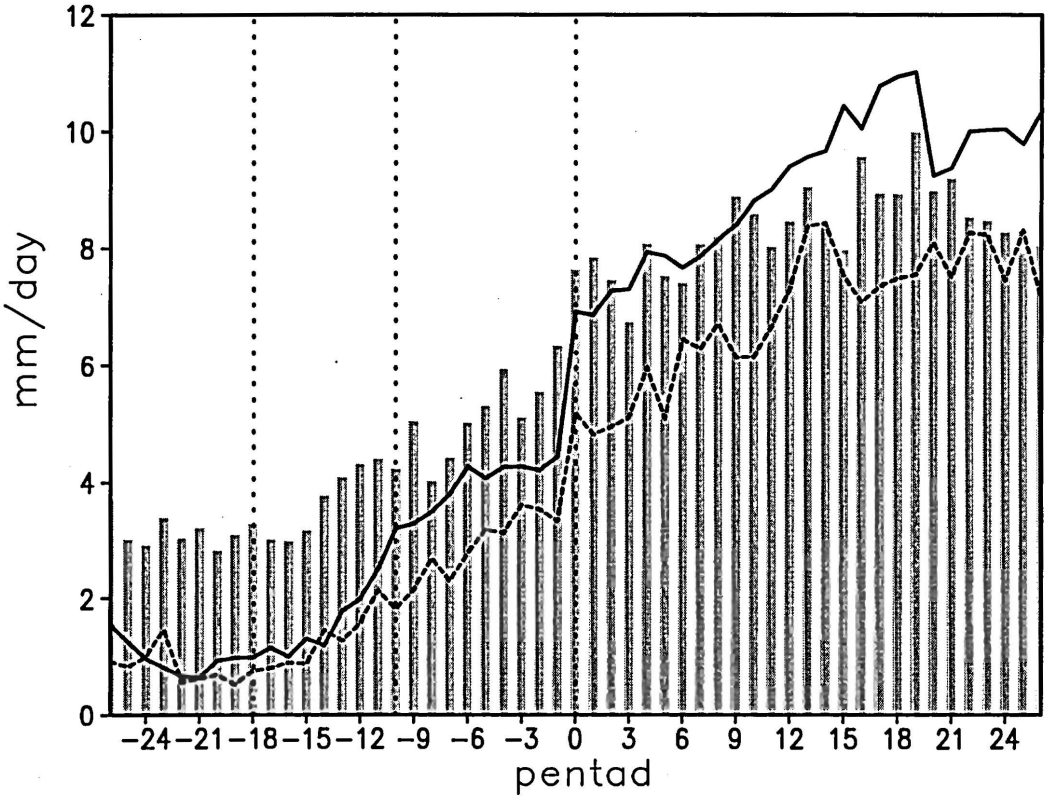

Figure 3.5. Composite time series of precipitation (mm day^{-1}) for ERA (bar), GPCP (dashed line), and rain gauge data (solid line) averaged over the Southern Amazon region. The three vertical dotted lines represent the beginning of the initiating, developing and maturing phase respectively during the transition.

gauge data in the Brazilian Amazon. They defined the onset as the time after which the rainfall exceeds4.5 mm day^{-1} in six out of eight subsequent pentads and before which the rainfall is well below 3.5 mm day^{-1} in six out of eight preceding pentads. Their definition produces an onset pattern similar to that of Kousky (1988). However, they have also shown that the onset dates vary with the somewhat arbitrary rain-rate threshold. How to objectively choose the rain-rate threshold for the onset is unclear. To address this issue, Liebmann and Marengo (2001) used the annual averaged daily rainfall of each year for each location as the threshold for the onset of that year. While this definition objectively determines the rain-rate threshold, it leads to a very different onset pattern from those of Kousky (1988) and Marengo et al. (2001).

Our purpose is to investigate how large-scale circulation changes during the transition, rather than determining the precise date of the onset. Nevertheless, we still need to specify a reasonable rain-rate threshold and show that our results are qualitatively insensitive to the rain-rate threshold, as long as it is within the range of observed annual mean rain rate over that region for the period of our analysis.

The influence of the uncertainty involved defining the onset on our results is examined, for example, in Fig. 3.6. This figure shows the changes of rainfall, moisture convergence and the evaporation through the transition derived from rain-rate thresholds varying from 5 to 8 mm day^{-1} of ERA, within the range of the year-to-year variation of the annual mean rain rate during the 15-year period for the Southern Amazon region. We use evaporation with the unit of mm day^{-1} instead of surface latent heat flux, to compare

with moisture transport and rain rate. The persistent increase of rainfall and moisture convergence during the transition, the peak values, and the large increase of these two fields associated with onset are consistent among all four rain-rate thresholds tested here. The relative contributions of the evaporation and moisture convergence as sources of the moisture for rainfall during the periods are also consistent among all cases. The timing of the peak rainfall and moisture convergence after the onset shifts forward relative to the onset pentad as the rainfall threshold exceeds 7 mm day^{-1}. This shift is due to the postponement of the onset date toward the peak rainy season as the onset threshold approaches the climatological seasonal peak rain rate for the Southern Amazon region (8 to 9 mm day^{-1}).

One way to objectively specify the rain-rate threshold is to use the climatological annual mean rain rate. For the Southern Amazon region, the 15-year climatology mean rain rate derived from the ERA is about 6.1 mm day^{-1}. Therefore, we define the onset as the pentad before which rain rate is less than 6.1 mm day^{-1} for 6 out of 8 preceding pentads and after which rain rate is greater than 6.1 mm day^{-1} for 6 out of 8 subsequent pentads. This definition adopts the approach of Kousky (1988) and Marengo et al. (2001), and also uses an objectively defined rainrate threshold as Liebmann and Marengo (2001). The onset pentad defined by this criterion for the 15 years is listed in Table 1.

Table 1 shows that the onset dates for the Southern Amazon region vary from the end of August to December over the fifteen years. Most of the onsets occurred in October and November (11 out of 15 years), generally consistent with those suggested in

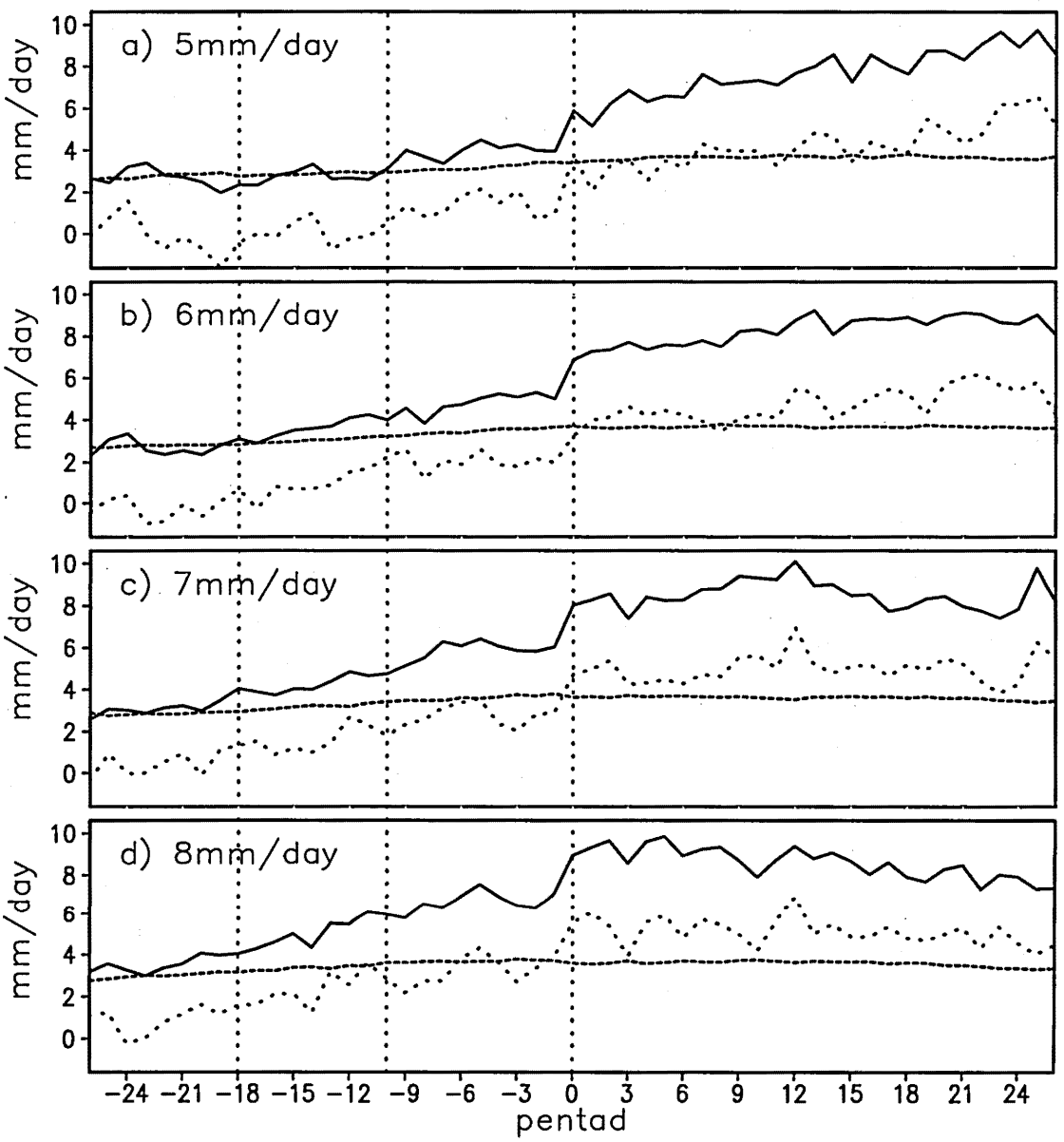

Figure 3.6. Composite time series of the precipitation rate (mm day^{-1}; solid lines), surface evaporation (mm day^{-1}; dashed lines), and net moisture convergence (dotted lines) during the transition based on different onset criteria: (a) 5 mm day^{-1}, (b) 6 mm day^{-1}, (c) 7 mm day^{-1}, and (d) 8 mm day^{-1}. The three vertical dotted lines represent the beginning of the initiating, developing and maturing phase respectively during the transition based on climatological rainrate.

literature. The earliest onset occurred from the end of August to the beginning of September in 1979. The annual mean precipitation of this year was 8.2 mm day^{-1}, the highest in the 15-year period. The onsets occurred at the end of December in 1984 and 1986, about 60 days later than the averaged onset date. The annual rain rates during these two years are lower than the climatology. This is qualitatively consistent with the relationship between the onset dates and interannual changes of the annual precipitation found by Liebmann and Marengo (2001).

3.2 Results

To obtain an overall picture of the evolution of the atmospheric circulation during the transition, we examine Fig. 3.4 again. The time series of $\frac{\partial \theta_e}{\partial t}$ at 850 hPa (Fig. 3.4a) suggests that the increase of lower tropospheric moist static energy starts about 90 days (18 pentads) prior to the onset date of the wet season, and such increase diminishes soon after the onset. During the stage of rapid moist static energy increase, the latent heat flux increases rapidly (Fig. 3.7a) associated with the increases of the net radiation and downward solar radiation at surface (Fig. 3.7b), but land surface sensible heat flux no longer increases (Fig. 3.7a). Large-scale moisture convergence in the Southern Amazon region and a moderate increase of rainfall begin about 60 days prior to the onset (pentad–12). Ten days later, the cross-equatorial flow reverses to northerly, and the conversion from divergent to rotational energy begins (pentad –10). At or shortly after the onset, the

Table 1. Onset pentad for each year based on rain-rate threshold of 6.1 mm day^{-1}

Year	Onset Pentad	Calendar Date	Annual Mean Rainrate (mm day^{-1})
1979	49	Aug 29–Sept 2	8.2
1980	57	Oct 8–Oct 12	6.9
1981	59	Oct 18–Oct 22	7.5
1982	68	Dec 2–Dec 6	6.0
1983	60	Oct 23–Oct 27	6.4
1984	73	Dec 26–Dec 31	4.9
1985	61	Oct 28–Nov 1	6.0
1986	73	Dec 26–Dec 31	5.7
1987	64	Nov 12–Nov 16	5.4
1988	63	Nov 7–Nov 11	5.6
1989	63	Nov 7–Nov 11	6.4
1990	60	Oct 23–Oct 27	5.9
1991	62	Nov 2–Nov 6	6.0
1992	66	Nov 22–Nov 26	4.5
1993	60	Oct 23–Oct 27	6.0

northerly cross equatorial low-level flow, the net moisture convergence to the Southern Amazon region, and rainfall increase rapidly. But the increase of $\frac{\partial \theta_e}{\partial t}$ at 850 hPa and the conversion of kinetic energy quickly diminish.

Figures 3.4 and 3.7 suggest that the transition is mainly driven by increase of land surface latent fluxes at the beginning, by both increases of moisture transport and the surface latent flux during the developing stage, and by the moisture transport during the wet season. Three turning points can be seen during the transition; thus, we divide the transition into three phases and organize our discussion accordingly.

3.2. 1 Initiating Phase (Pentad –18 To Pentad –10)

The initiating phase starts at 90 days and ends about 50 days prior to the wet season onset. It is dominated by an increase of $\frac{\partial \theta_e}{\partial t}$ at 850 hPa (Fig. 3.4a), indicating a local increase of moist static energy of the lower troposphere. In the last 15 days of this phase, rainfall begins to increase, although the rate is small. The low-level cross-equatorial flow is still southerly and moisture diverges for the Southern Amazon domain (Fig. 3.4b). The upper troposphere field remains similar to that of the dry season, as shown by the latitudinal averaged geopotential height at 200 hPa in Fig. 3.8. This suggests that the increase of the local θ_e at 850 hPa cause the increase of thermally driven precipitation. To diagnose the causes of increasing $\frac{\partial \theta_e}{\partial t}$ at 850 hPa, we examine the composite

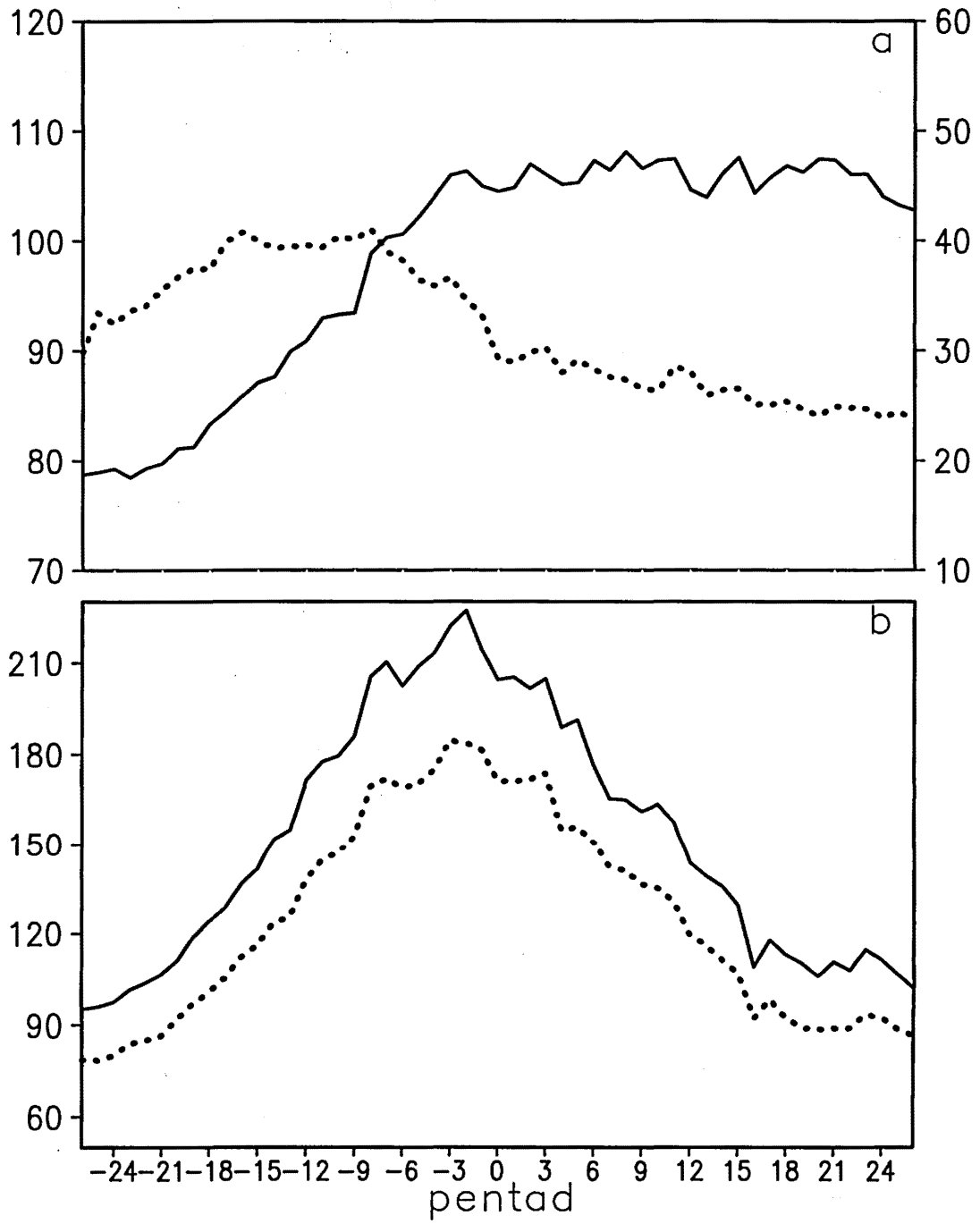

Figure 3.7. Composite time series of (a) the surface latent heat flux (W m^{-2}; solid line,left axis) and sensible heat flux (W m^{-2}; dotted line, right axis), and (b) net radiation (W m^{-2}; dotted line) and downward solar radiation at surface (W m^{-2}; solid line).

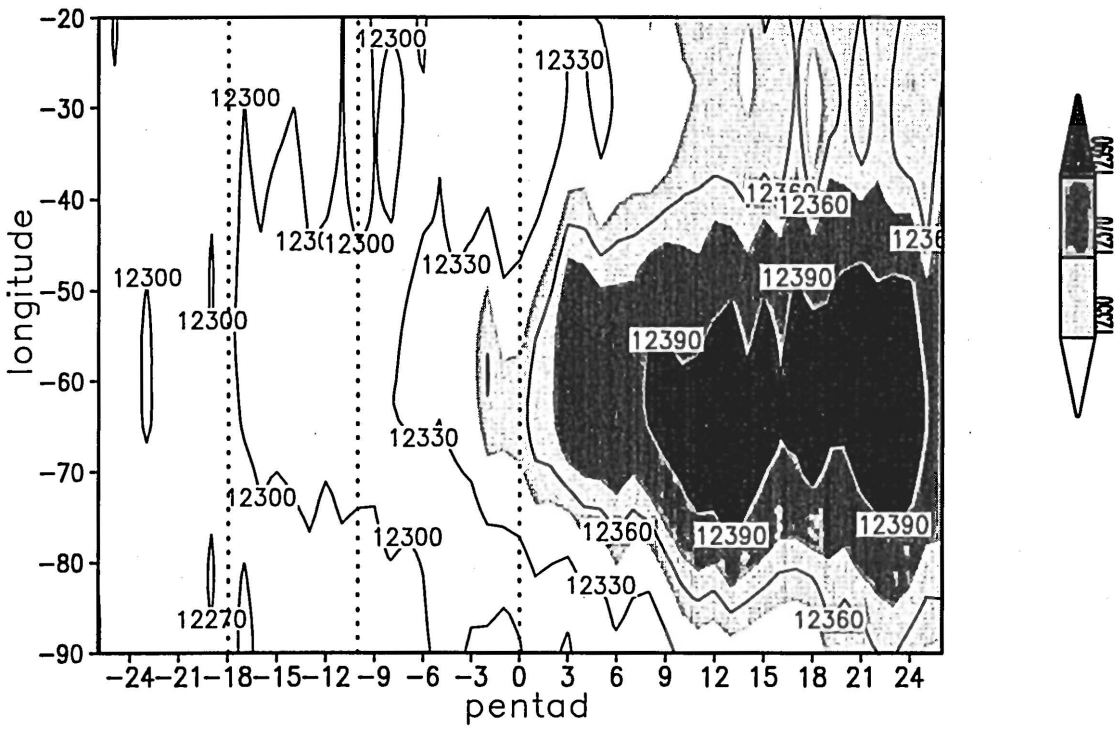

Figure 3.8. Composite temporal and longitudinal distribution of geopotential height at 200 hPa (m) averaged over 5°–30°S through the transition from dry to wet season at pentad resolution. Contour interval is 30 meters.

contributions of temperature and specific humidity changes represented by terms A and B in (1) in Fig. 3.9a during 1979 –1993 to $\frac{\partial \theta_e}{\partial t}$ at 850 hPa. Before the initiating phase begins (pentad –18), the increase of temperature contributes as much as the increase of moisture to the rising $\frac{\partial \theta_e}{\partial t}$ at 850 hPa. During the initiating phase (pentad –18 to –10) and also through the rest of the transition period (after pentad –10), the increase of the moisture becomes more important. The important impact of moisture increase on the lower troposphere moist energy from the dry to the wet season is also suggested by radiosonde observations (Fu et al. 1999; Petersen and Rutledge 2001). Fig. 3.7 shows the variations of surface latent heat flux, sensible heat fluxes, downward solar radiation and net radiation at surface. At the initiating phase, the latent heat flux increases with the increase of net radiation and the downward solar radiation at surface. The increase of the latent heat flux is even earlier than the increase of thermally driven precipitation over the region.

The relative importance between evapotranspiration and large-scale moisture transport during this period is illustrated in Fig. 3.9b, in which the net moisture convergence into the domain is compared with the evaporation within the Southern Amazon region. The changes of both variables are statically significant, although the changes of evapotranspiration appear to be smooth. During the first half initiating stage, moisture is either divergent or near zero convergence. Evaporation is the main

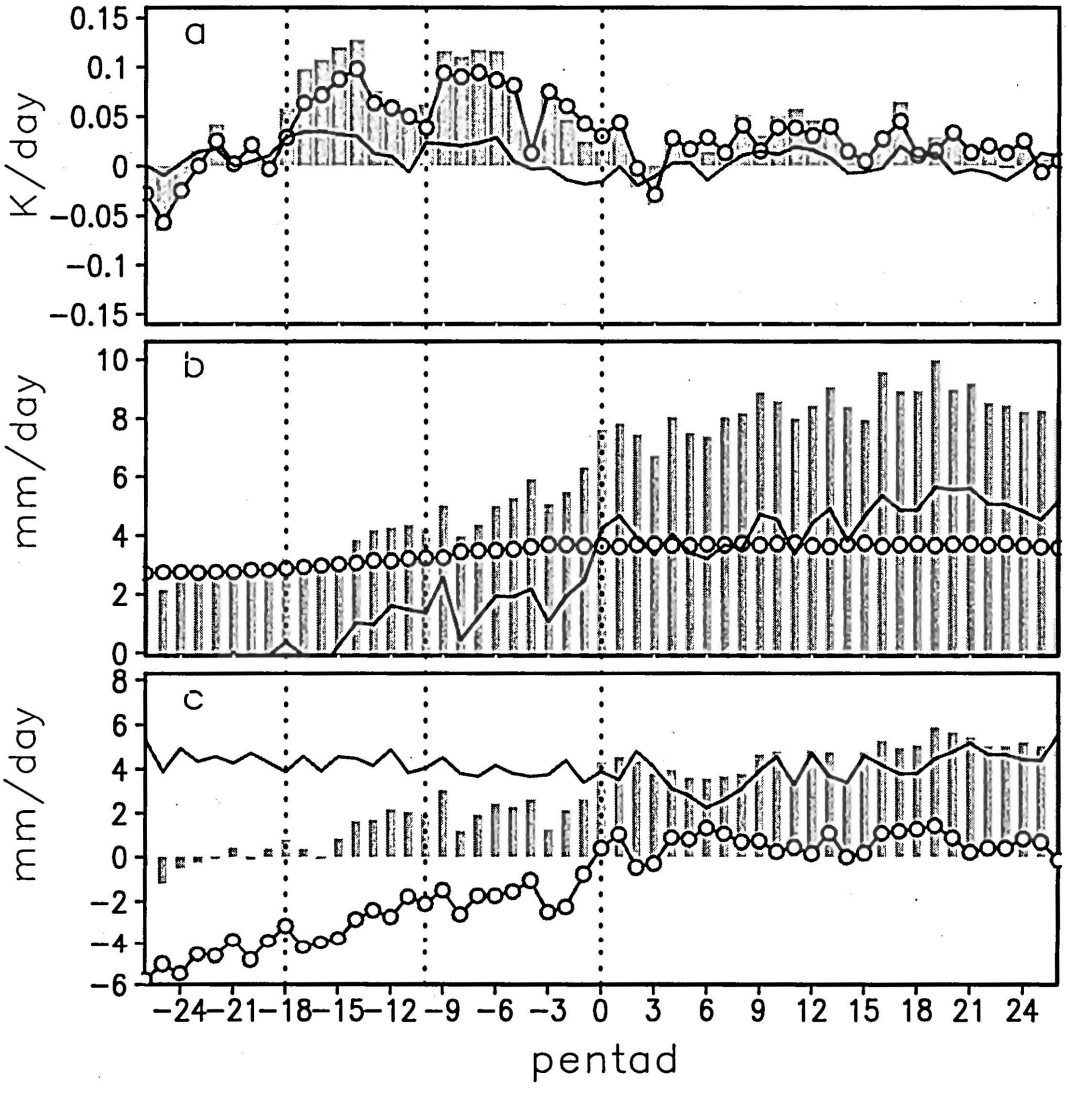

Figure 3.9. Composite time series of (a) contributions of temperature change (K day^{-1}; solid line) and humidity change (K day^{-1}; solid line with circles) to $\frac{\partial \theta_e}{\partial t}$ at 850 hPa (K day^{-1}; bars); (b) surface evaporation (mm day^{-1}; solid line with circles), net moisture convergence (mm day^{-1}; solid line), and precipitation (mm day^{-1}; bar); and (c) total moisture convergence (mm day^{-1}; bar), net zonal moisture convergence (mm day^{-1}; solid line), and net meridional moisture convergence (mm day^{-1}; solid line with circles) for the period of 1979–1993 and averaged within the Southern Amazon region (5°–15°S, 45°–75°W). The three vertical dotted lines represent the beginning of the initiating, developing and maturing phase respectively during the transition.

contributor to the increase of water vapor and remains as the dominant source before the onset. At this stage, the cross-equatorial flow in the western Amazon, as indicated by the V-index, remains the same as that in the dry season. Figure 3.9c shows the contribution of zonal and meridional moisture transport to the net moisture convergence over the domain. The southerly cross-equatorial flow in the western Amazon (Fig. 3.4b) leads to a meridional divergence of moisture flux (Fig. 3.9c) that is strong enough to compensate the zonal moisture convergence and cause net moisture divergence or near-zero convergence over the domain. The evolution of the atmospheric vertical and zonal velocities as well as relative humidity has been plotted along 10°S in Fig. 3.10. During the initiating stage, the vertical structure of the atmosphere remains similar to that of the dry season. The atmosphere above 700 hPa remains dry (relative humidity $\leq$ 50%). Higher relative humidity (RH $\geq$ 70%) is confined to the western part of the Amazon basin. Vertical velocity is either near zero or downward over the Amazon basin. Strong westerly flow dominates at the upper troposphere (Fig. 3.11a). The kinetic energy conversion function is negative (Fig. 3.4d), indicating the absence of the divergent to rotational kinetic energy. The 200-hPa geopotential height is as low as that in the dry season (Fig. 3.8). These dry-season characteristics of the large-scale circulation and the shallowness of the rising motion suggest that the beginning of rainfall increase and the transition from net moisture divergence to convergence shown in Figs. 3.4b and 3.4c must be driven by the increase of surface latent heat flux, instead of by changes of large-scale circulation.

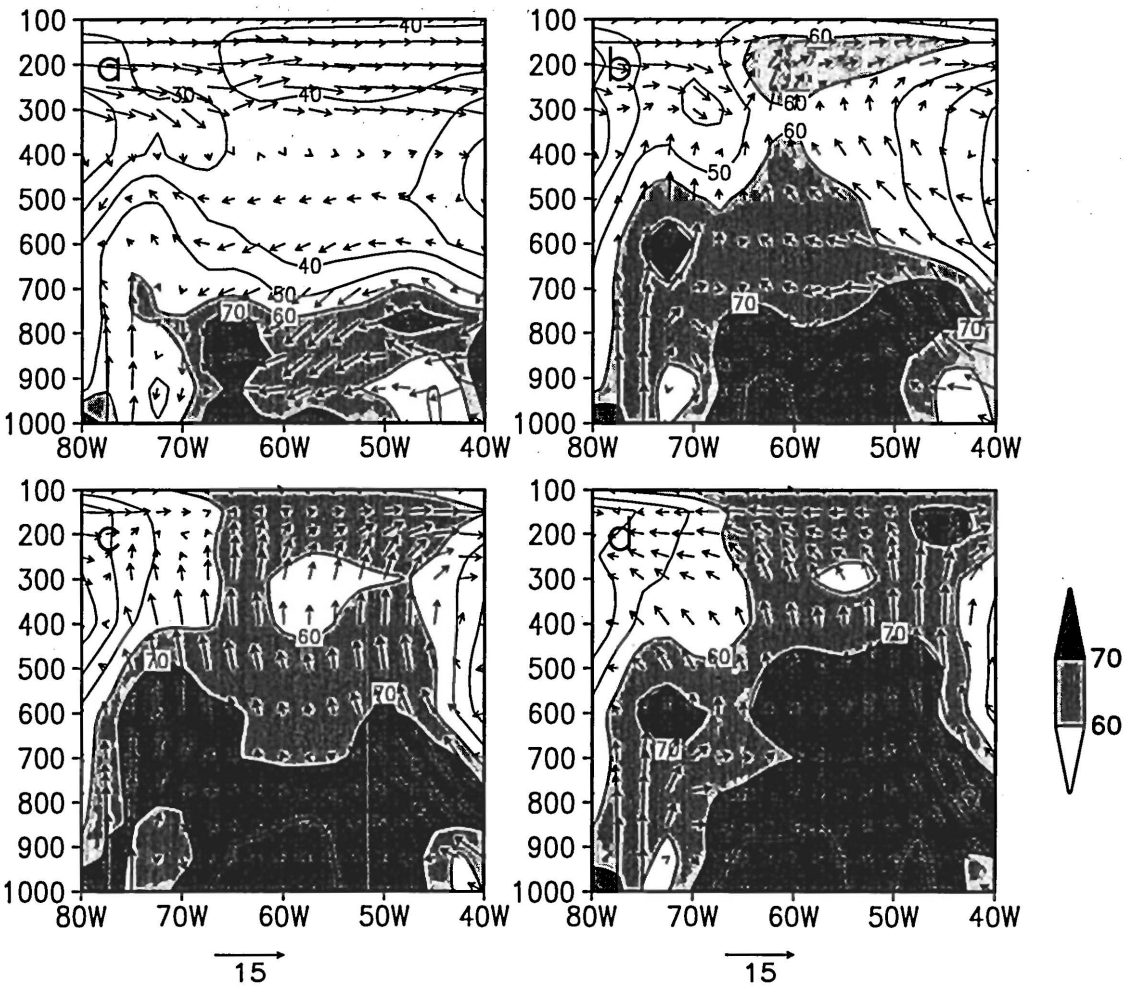

Figure 3.10. Vertical-longitude cross section of the composites of zonal and vertical velocity (m s^{-1}; vectors, here vertical wind is enlarged by 10 times for clarity) and relative humidity (shaded area and contour) along 10°S at: a) pentad −16; b) pentad −6; c) pentad 0; and d) pentad 6, respectively.

3.2.2 Developing Phase (Pentad –9 To Pentad 0)

The developing phase is marked by the increasing importance of the dynamic process and the acceleration of the transition. It begins with reversals of both the V-index and the sign of the energy conversion function, and it ends at the onset of the rainy season with the diminishing of positive $\frac{\partial \theta_e}{\partial t}$ at 850 hPa thereafter. The V-index has changed from southerly to northerly. The northerly cross-equatorial flow brings moist air from the Caribbean Sea to the Amazon Basin (Wang and Fu 2002) and consequently changes the net moisture flux from divergence to convergence (Fig. 3.4c). As expected from the prevailing easterly wind blocked by the Andes, Fig. 3.9c shows that the zonal moisture flux converges to the region through all seasons. However, it is compensated by the meridional moisture divergence before the wet season onset. This constant source of moisture helps to maintain a relatively humid dry season over the Southern Amazon region. The seasonal change of the net large-scale moisture divergence is mainly controlled by the cross-equatorial moisture flux (Fig. 3.9c).

During this stage of the transition, the rate of increase of the evaporation remains about the same as that in the initiating stage (Fig. 3.9b). But the net moisture convergence soon becomes a significant source of water vapor. The total water vapor gain within the domain increases by 50% compared to the initiating phase, and the relative humidity near the surface increases by 80% (Figs 3.10b and 3.10c). Precipitation during the developing phase increases steadily, but is still below the threshold for wet

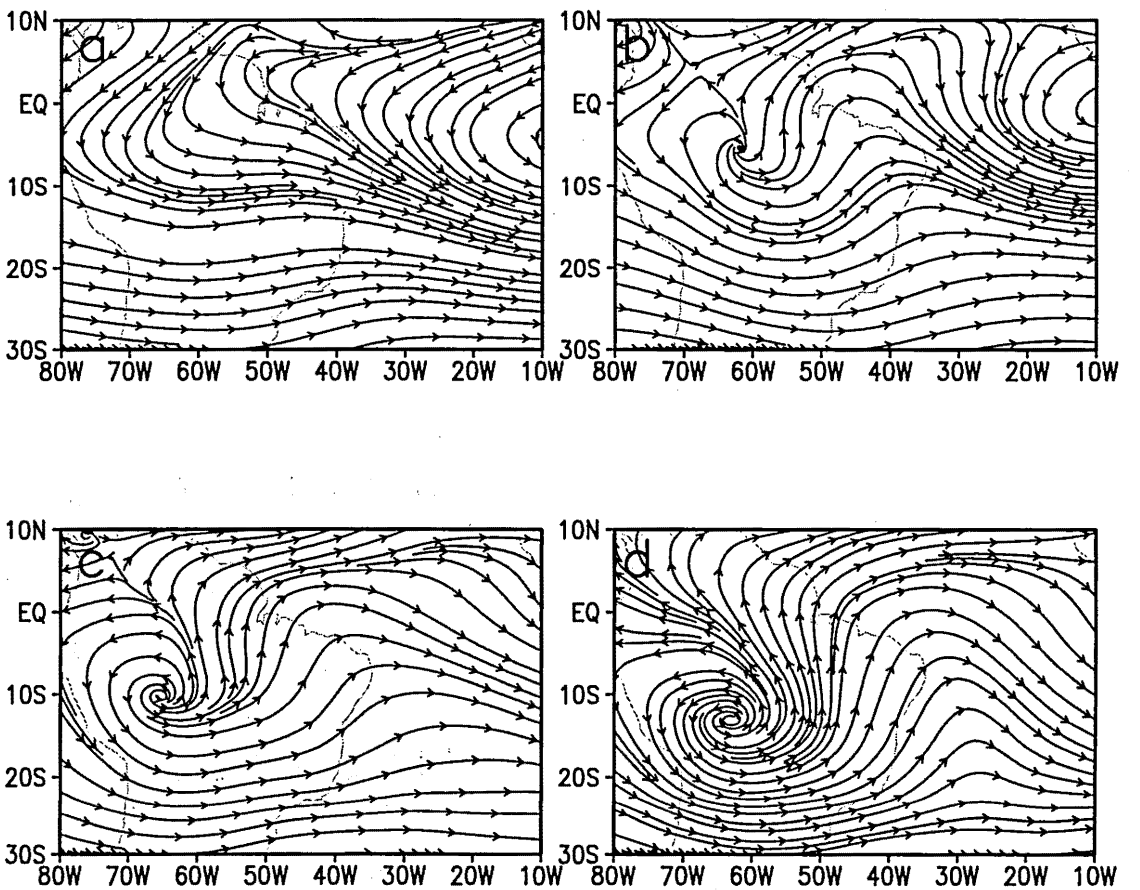

Figure 3.11. Composite 200 hPa streamline at: a) pentad −16; b) pentad −6; c) pentad 0; and d) pentad 6, respectively.

season onset (Fig. 3.4e).

Rising motion appears about 45 days before the onset (pentad –9 to –6) over the Southern Amazon region and becomes stronger with time (Fig. 3.10). The middle troposphere becomes more humid (RH ≥ 50%), presumably due to more frequent occurrence of deep convection. The composite streamline at 200 hPa in Fig. 3.11 shows that anticyclonic circulation in the upper atmosphere begins to form to the southwest of the Amazon basin at pentad –6. It becomes stronger and moves southward with the Amazon convection. These changes are consistent with the expected upper troposphere response to the increasing convection over the Amazon (Lenters and Cook 1997). Geopotential height at 200 hPa also increases about 60 m (about $\frac{2}{3}$ of the total increase from the dry to wet season) within the 30 days prior to the onset of the wet season (Fig. 3.8), suggesting a rapid stretching of the tropospheric column.

The aforementioned developments in $\frac{\partial \theta_e}{\partial t}$ at 850 hPa, vertical motion, rainfall, and the 200-hPa geopotential height are consistent with the energetics of the atmospheric circulation during the transition. The increase of $\frac{\partial \theta_e}{\partial t}$ at 850 hPa during both initiating and developing phases indicates an increase of the moist static energy in the lower troposphere (Fig. 3.4a). The moderate increase of rain rate (about 1 mm day^{-1}) at the beginning of the developing phase suggests a beginning of the stretching of the troposphere column, which transforms moist static energy to divergent kinetic energy

(Moscati and Rao 2001). The conversion function becomes positive (Fig. 3.4d) about 50 days prior to this onset (pentad –10) and increases steadily to its maximum at the onset of the wet season (pentad 0). This suggests the transformation of divergent kinetic energy into rotational kinetic energy. The vertical profiles of the kinetic energy conversion function at different stages of the transition period have been shown in Fig. 3.12. In contrast to the negative conversion function through most of the troposphere prior to the developing phase, the vertically integrated C becomes positive during the developing phase. The peak of the conversion function is initially near 250 hPa, then becomes stronger and rises to 200 hPa towards the onset. Hence the increase of the energy transformation mainly occurs in the upper troposphere centered at 10°–15°S and 55°–70°W, where the anticyclonic circulation is enhanced rapidly during the developing stage (Figs. 3.11b and 3.11c). Evidently, the development of the wet season circulation pattern over South America is supported by energy conversions similar to those of the South Asian monsoon.

3.2.3 Maturing Phase (After Pentad 0)

In the maturing phase, the increase of surface fluxes weakens. The transition appears to be driven by a positive response of moisture convergence to increased rainfall. As shown in Fig. 3.4a, the increase of $\frac{\partial \theta_e}{\partial t}$ at 850 hPa becomes insignificant. The northerly V-index steadily increases to its full strength (Fig. 3.4b), doubling the magnitude of moisture convergence in the developing stage. Consequently, the moisture

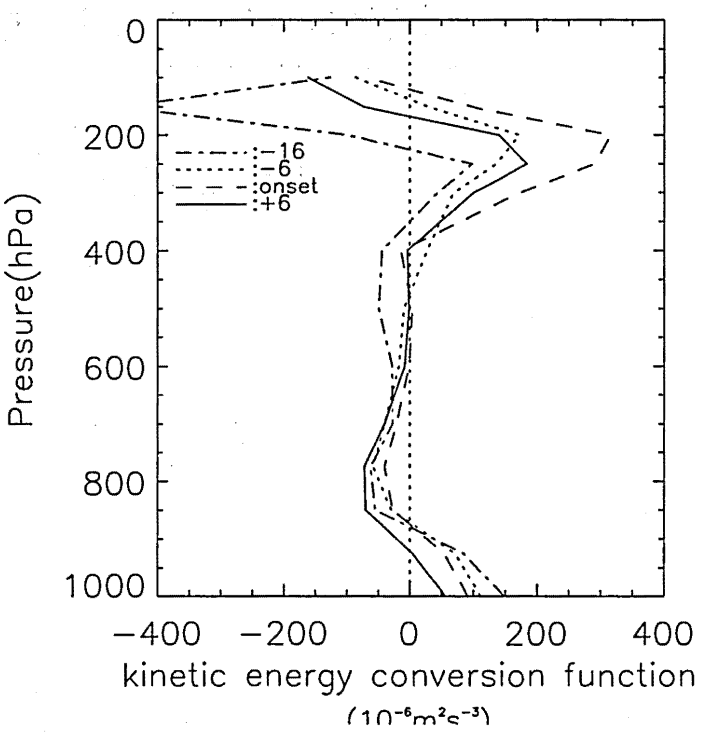

Figure 3.12. Vertical profiles of the composite kinetic energy conversion function (10^{-6} $m^2 s^{-3}$) at pentad −16 (dash-dotted line), pentad −6 (dotted line), pentad 0 (dashed line), and pentad 6 (solid line) averaged over the Southern Amazon region.

convergence becomes a greater source of water vapor than the evaporation (Fig. 3.9b). Precipitation gradually increases to its annual peak of about 8 to 9 mm day^{-1} (Fig. 3.4e).

Figures 3.10c and 3.10d show that the rising motion over the Southern Amazon region is maintained at approximately the same strength since the onset. But high relative humidity (RH≥ 70%) has penetrated further to 400 hPa, presumably due to the accumulated effect of upward convective transport of water vapor. From pentad 0 to 6, the increase of geopotential height suggests a continuous stretching of the atmospheric column within the 30 days after the onset (Fig. 3.8). The positive, but much weaker, conversion function (Fig. 3.4d) indicates a continuous gain of rotational kinetic energy in the upper tropospheric flow at a much decreased rate. A closed center of upper troposphere anticyclonic circulation, associated with the Bolivian High, forms near 18°S about 9–10 pentads (45 days) after the onset of the Amazon wet season (not shown). The results of Figs 3.4 and 3.8 suggest that the convective heating over the Amazon contributes to the development of the Bolivian High, consistent with previous numerical model results of Silva Dias et al. (1983), Gandu and Geisler (1991), and Lenters and Cook (1997).

3.3 Discussion

3.3.1 The Role Of Local Land Surface Processes And Large-Scale Transport

Previous studies have shown that both land surface and large-scale dynamic processes influence the Amazon rainfall. However, their relative importance at different

stages of the transition, and therefore the influences of land surface change and climate variability of oceans on the Amazon rainfall, remain unclear. Our analyses indicate that the increases in surface fluxes, especially latent heat flux, are the dominant contributors to the increase of potential energy and water vapor during the initiating phase of the transition. Our results here are consistent with the radar results of convective structure in the Amazon for the transition season shown in Petersen and Rutledge (2001). Evidently, land surface processes should have the most significant impact during the initiating phase, and become less crucial during the developing and maturing stages. In the Amazon, the surface latent heat flux can increase prior to the increase of rainfall due to its relatively wet condition during the dry season compared to the classic Asian monsoon. This allows an increase of evaporation and, therefore, rainfall at the early stage of transition. This implies a drier land surface during the dry season, caused either by reduced rainfall or by an increase of runoff due to land use, could slow down the build-up of the local moist static energy, consequently delay the transition of the large-scale circulation and wet season onset. The large-scale circulation change associated with SST anomalies in the adjacent oceans could affect the onset at all stages, perhaps being most effective during the developing phase of the onset. During this phase, atmospheric transport becomes an important source of moisture, a deep layer of static instability is needed for convective breakthrough, and favorable upper tropospheric circulations are needed to reinforce the lower tropospheric convergence. The changes of the large-scale

circulation can easily influence these key factors of the transition from the dry to the wet seasons.

3.3.2 Possible Prediction Factors

Our analysis may help to identify the potential precursors for onset of the wet season over tropical South America. For short-term prediction of onset (5–10 days), a 20% or more increase of relative humidity, a persistent increase of northerly pentad V-index to 1 m s^{-1} or higher, and formation of an anticyclonic center at 10°S, together with rain rate, are likely to indicate the onset of the rainy season. For medium term (2–3 months) prediction, a delayed or weak increase of the surface fluxes in later austral winter, a delayed reversal of V-index or a weak northerly V-index (Wang and Fu 2002), and abnormally strong upper troposphere westerlies in early spring probably indicate a delay of the rainy season onset. The latter, in turn, could delay the development of the Bolivian High in the subtropical South American region. The potential use of these variables as quantitative criteria for the onset of the wet season still needs to be further explored. It is important to clarify that these potential prediction factors are applicable only on a large scale. The precise date of the onset varies geographically within the Amazon. The link between the large-scale circulation change and the local onset needs to be further studied.

3.4 Summary

Using 15-year instantaneous ERA data (1979–1993) as well as rain gauge and GPCP data, we have studied the changes of land-surface and atmospheric variables at pentad (5-day) resolution during the transition from the dry to the wet seasons over the Southern Amazon basin. The results suggest that the transition is initiated by an increase of local land surface fluxes and then accelerated by dynamic responses to the increase of moist static energy in the lower troposphere. The transition process can be divided into three stages, according to changes in the main driving process. The initiating stage ranges from 90 days to 50 days before the onset of the rainy season. This stage is dominated by an increase of equivalent potential temperature in the lower troposphere. This is caused by increasing land surface fluxes, especially the latent heat flux, which consequently reduce the Convective Inhibition Energy (CINE), increase the buoyancy and the Convective Available Potential Energy (CAPE) of the lower troposphere (not shown here). Rain rate also begins to increase slightly. The cross-equatorial flow and upper tropospheric circulation during this stage remain unchanged from those of the dry season.

The developing stage starts with the reversal of cross-equatorial flow in the western Amazon from southerly (during the dry season) to northerly about 45 days before onset. This wind reversal increases moisture transport from the Caribbean Sea, and leads to moisture convergence. As a result of increasing moisture transport, the total moisture gain doubles over the Southern Amazon region, compared to the initiating phase. The enhanced moisture increases the probability of convection and consequently increases of

geopotential height at 200-hPa. In the upper troposphere, the positive energy conversion function suggests that divergent kinetic energy resulting from the stretching of the atmosphere column is transformed into rotational kinetic energy, consequently spins up the anticyclonic circulation. The stretching effect also reinforces the low-level convergence. This positive feedback accelerates the establishment of a circulation pattern favorable for the onset of the wet season.

The maturing stage begins with the onset of the Amazon rainy season and lasts about 30 to 60 days after the onset, when precipitation and 200-hPa geopotential peak. Presumably due to an increase of cloudiness which reduces the surface solar radiation, the increase of lower-level potential energy dissipates. The increase of rainfall and further development of the wet season circulation pattern appear to be dominated by the positive feedback between the upper-level atmospheric anticyclonic circulation and the lower troposphere convergence. The South American monsoon circulation matures during this phase.

Our results have offered a clarification for the apparent discrepancy in literature regarding the relative importance of the surface evaporation and large-scale moisture transport in determining the wet season onset. The results suggest that the increase of surface evaporation is key for initiating the transition from dry to wet seasons, although the large-scale moisture transport becomes a more important moisture supplier during the wet season. Hence, if the increase of surface evaporation is significantly weakened during the initiating phase, for example, increase of runoff due to change of land surface

type or decrease of rainfall in previous seasons, the onset of the wet season would probably be delayed. The changes in the large-scale circulation, such as those due to SST changes in the adjacent tropical Pacific and Atlantic, could directly influence the developing and maturing phases of the transition through their control over weakening of the moisture transport or the transition of upper tropospheric circulation. They can also indirectly influence the surface fluxes through their control of rainfall and cloudiness during dry seasons and the initiating phase of transitions.

CHAPTER 4

INTERANNUAL VARIATIONS OF WET SEASON ONSET OVER TROPICAL SOUTH AMERICA

The previous Chapter provides general evolutions of large-scale atmospheric and land surface conditions from dry to wet season over tropical South America. However, the climatology of the transition shown in Chapter 3 cannot explain discrepancies as large as three months for the onset dates of the rainy season on an interannual scale (Marengo et al 2001; Chapter 3). This chapter explores how the large-scale conditions mentioned above cause the deviations from the climatological wet season onset. This will also verify the mechanism presented in Chapter 3.

Chapter 3 demonstrates that in general, wet season onset begins from the increase of land surface fluxes that destabilizes the lower troposphere and initiates the seasonal increase of rainfall. The latter accelerates the transition of the large-scale circulation and leads to the onset of the wet season. This implies that changes in land surface fluxes, in addition to the externally forced atmospheric large-scale circulation change, could accelerate or delay the wet season onsets on an interannual scale. To verify this contention, we have selected 1979, 1984, and 1986 as examples of earlier or delayed onsets during the period of our analysis (1979–1993). These years are chosen because their onset dates (pentad 49 at 1979, pentad 73 at 1984 and 1986) differ from the fifteen-year average onset date (about pentad 62.5) by more than one month (Table 1). We also

use 1990 as an example of a normal onset year. The data used here and the domains analyzed in the Chapter are the same as in Chapter 3. All variables are analyzed according to their absolute pentads instead of relative pentads. We used the absolute pentads here to compare the relatively earlier and later change of the key variables during the transition in different years.

4.1 Interannual Variations Of The Wet Season Onset

4.1.1 Normal Onset

In a "normal" onset year 1990, the Bowen ratio, i.e. the ratio of the sensible and latent heat fluxes, ranged between 0.4 and 0.6 during the dry season and between 0.2 and 0.35 during the wet season (Fig. 4.1a). This is within the range of its observed values at the ABRACOS (Manzi and Planton 1996; Dias and Regnier, 1996). Since the ERA land surface fluxes are somewhat uncertain, we can only qualitatively discuss their differences between normal, early, and late onsets. In 1990, surface sensible flux averaged over the Southern Amazon region began to increase in early June (pentad 30, Fig. 4.1b), and surface latent flux in middle July (pentad 38, Fig. 4.1c). Following the increase of surface latent flux, humidity at 850-mb (q_{850mb}, Fig 4.2a) and CAPE all increased (Fig. 4.3b), and CINE decreased rapidly in early August (pentad 44; Fig. 4.3a). Precipitation began to increase from pentad 45. The V-index reversed in mid-October (pentad 57; Fig. 4.4a) and the 200-mb geopotential height began to increase in late September (pentad 53;

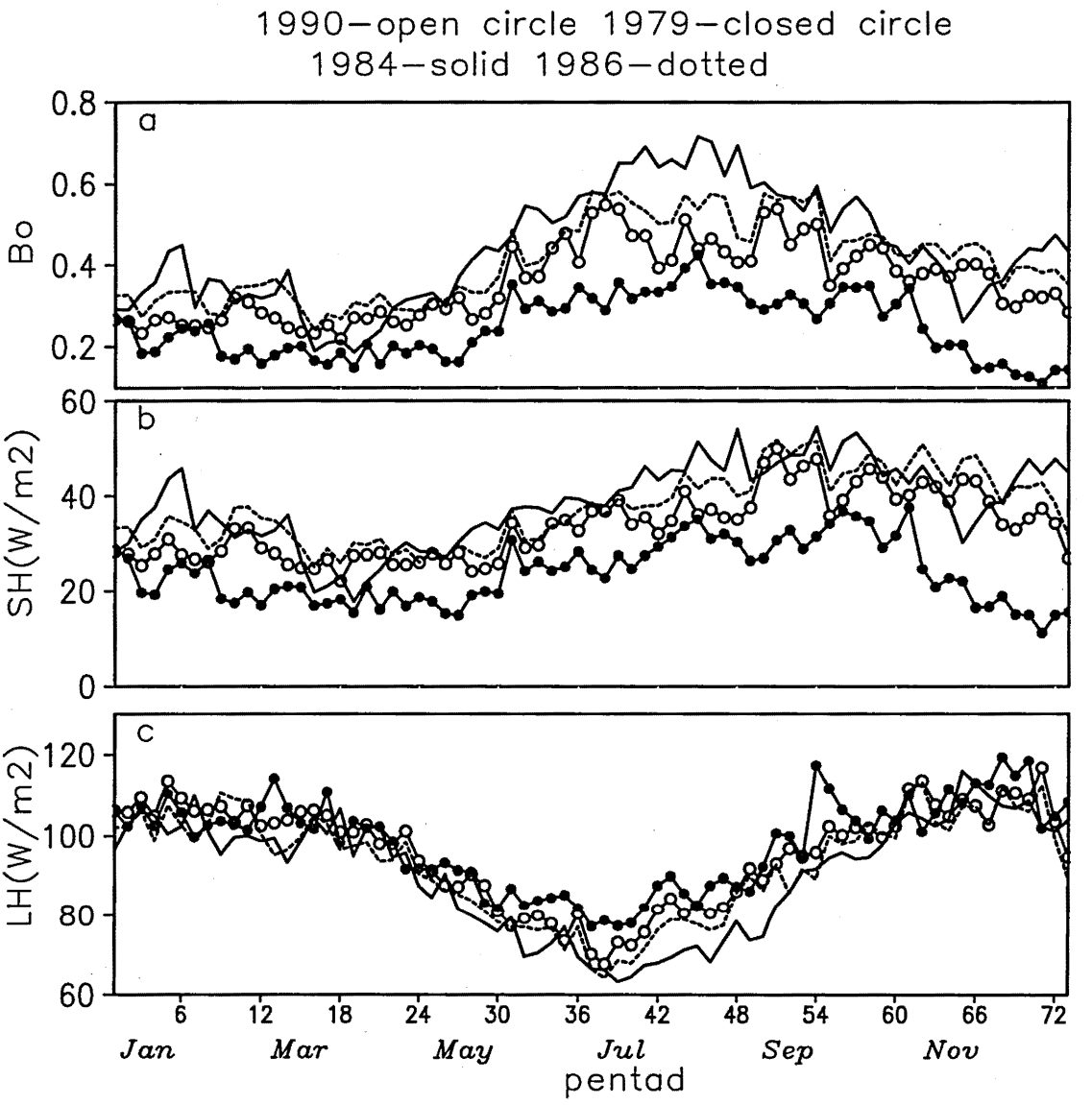

Figure 4.1. Annual cycles of area averaged a) Bowen ratio; b) surface sensible fluxes; c) surface latent fluxes for 1990 (curve with open circles), 1979 (curve with closed circles), 1984 (solid curve) and 1986 (dotted curve), respectively, for the Southern Amazonian domain. Unit of the fluxes is W m^{-2}.

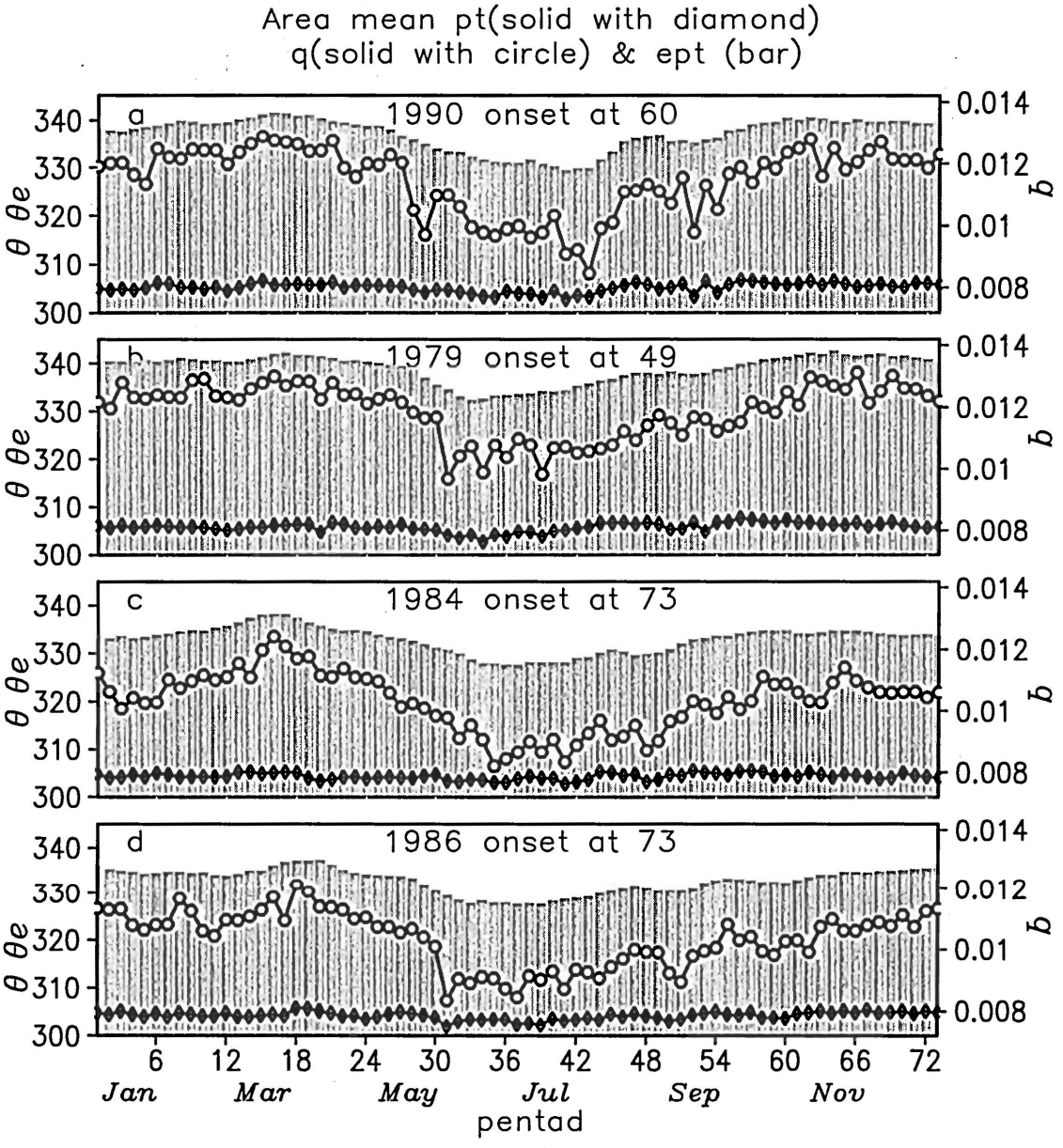

Figure 4.2. Annual cycles of area averaged θe at 850-hPa (bars, unit: K), potential temperature θ at 850-hPa (diamonds, unit: K) and q at 850-hPa(open circles, unit: kg kg^{-1}) for a) 1990; b) 1979; c) 1984; and d) 1986,respectively.

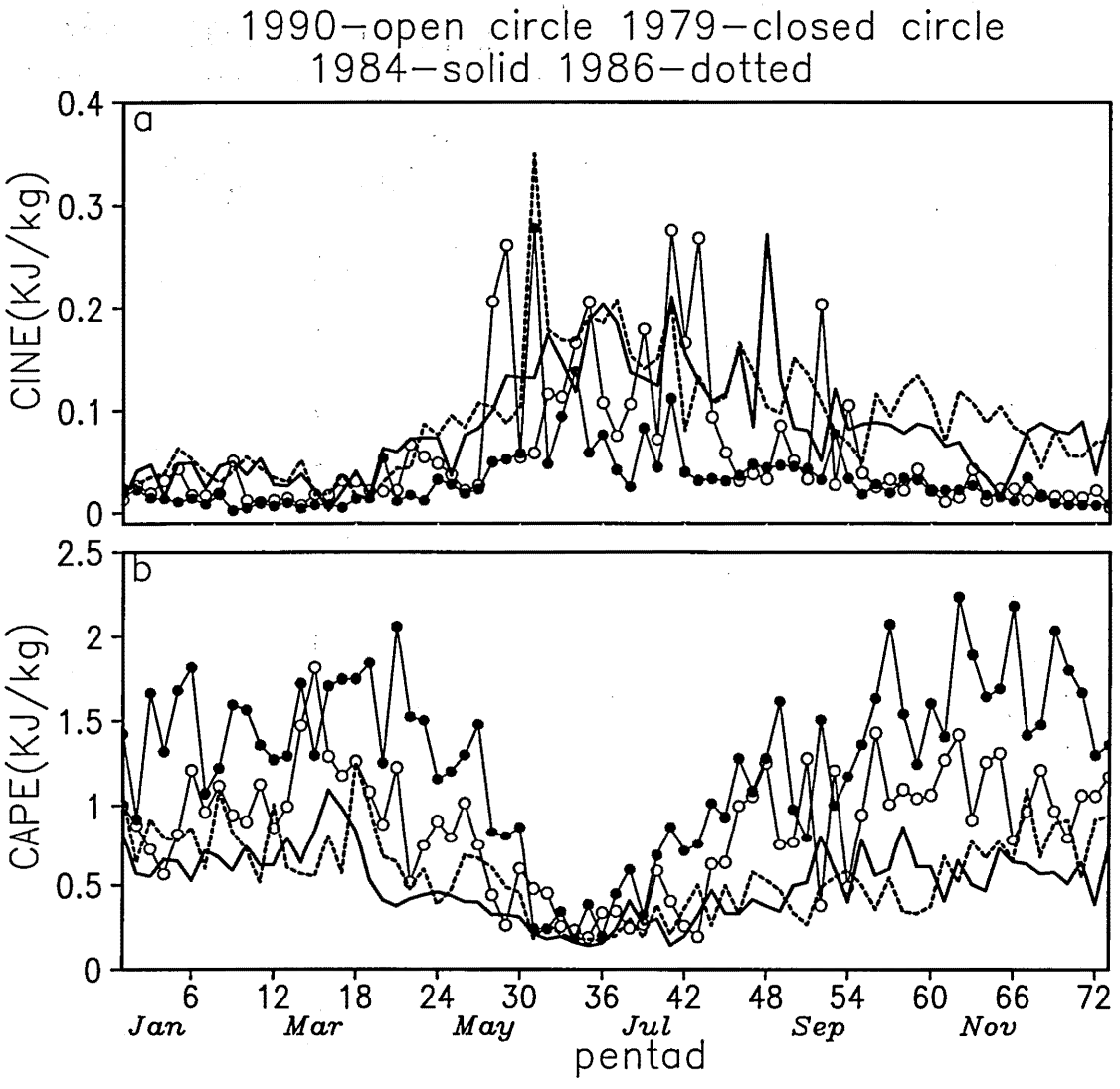

Figure 4.3. Annual cycles of area averaged a) CINE; and b) CAPE of 1990 (open circles), 1979 (closed circles), 1984 (solid curve) and 1986 (dotted curve), respectively. The unit is kJ kg^{-1}.

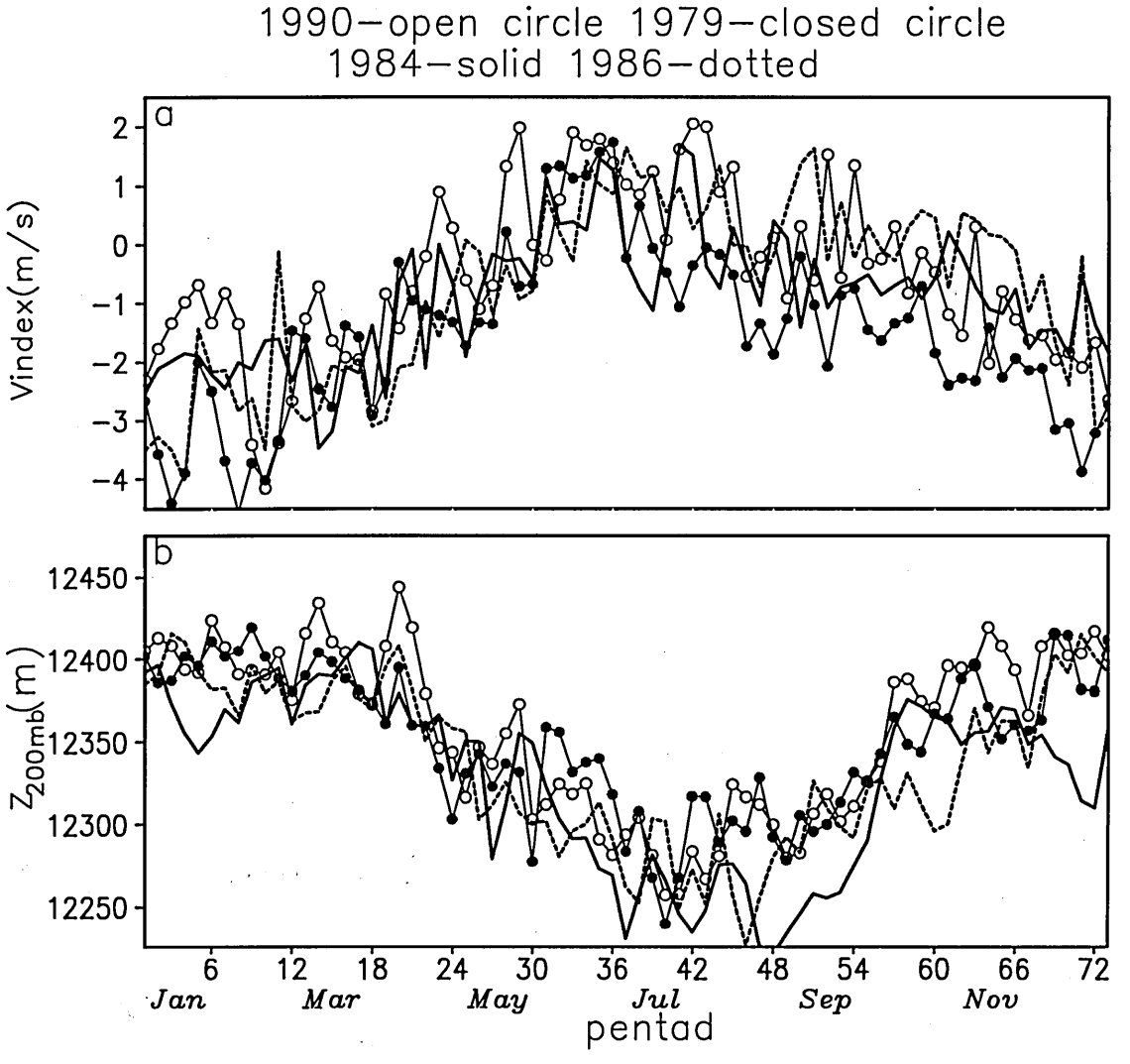

Figure 4.4. Annual cycles of area averaged a) the V-index (unit: m s^{-1}), and b) 200-mb geopotential height over the area of 5°–30°S 45°–75°W (unit: meter) for 1990 (open circles), 1979 (closed circles), 1984 (solid curve) and 1986 (dotted curve), respectively.

Fig. 4.4b). Precipitation increased quickly with the northerly cross-equatorial flow and reached the onset criteria 6.1 mm day^{-1} at pentad 60 (Fig. 4.5). The precipitation over the southern Amazon region also showed approximately 20-30 days intraseasonal variations as in Asian monsoon area. The process of normal onset year 1990 is consistent with that of wet season onset climatology in Chapter 3, i.e. the transition is mainly initiated by increases of surface latent heat flux and local driven precipitation. The latter provides an effective forcing for the reversal of the cross-equatorial flow, which causes net large-scale moisture convergence to the Southern Amazon region.

4.1.2 Early Onset

In 1979, the wet season began during August 28–September 2 (Table 1), about two months earlier than the averaged onset date (November 2–6). Compared to the dry season of 1990, the Bowen ratio was as much as 40% lower during August and September (Fig. 4.1a), as a result of lower surface sensible heat flux (by ~ 25% or 10 Wm^{-2}, Fig. 4.1b) and higher latent heat flux (by ~10% or 10 Wm^{-2}, Fig. 4.1c). Specific humidity at 850-mb (q_{850mb}) followed the higher surface latent flux, and was also 10% higher (Fig. 4.2). Evidently, the Bowen ratio was lower, the land surface was wetter and the lower troposphere was more humid during the 1979 dry and early transition seasons. CINE in June was 25% lower (Fig. 4.3a), and reduced quickly to 25-50% of its normal dry seasonal values in early July (pentad 36), before the northerly reversal of the V-index (Fig. 4.4a). In contrast, CAPE (Fig. 4.3b) and the 200-mb geoptential height (Fig. 4.4b)

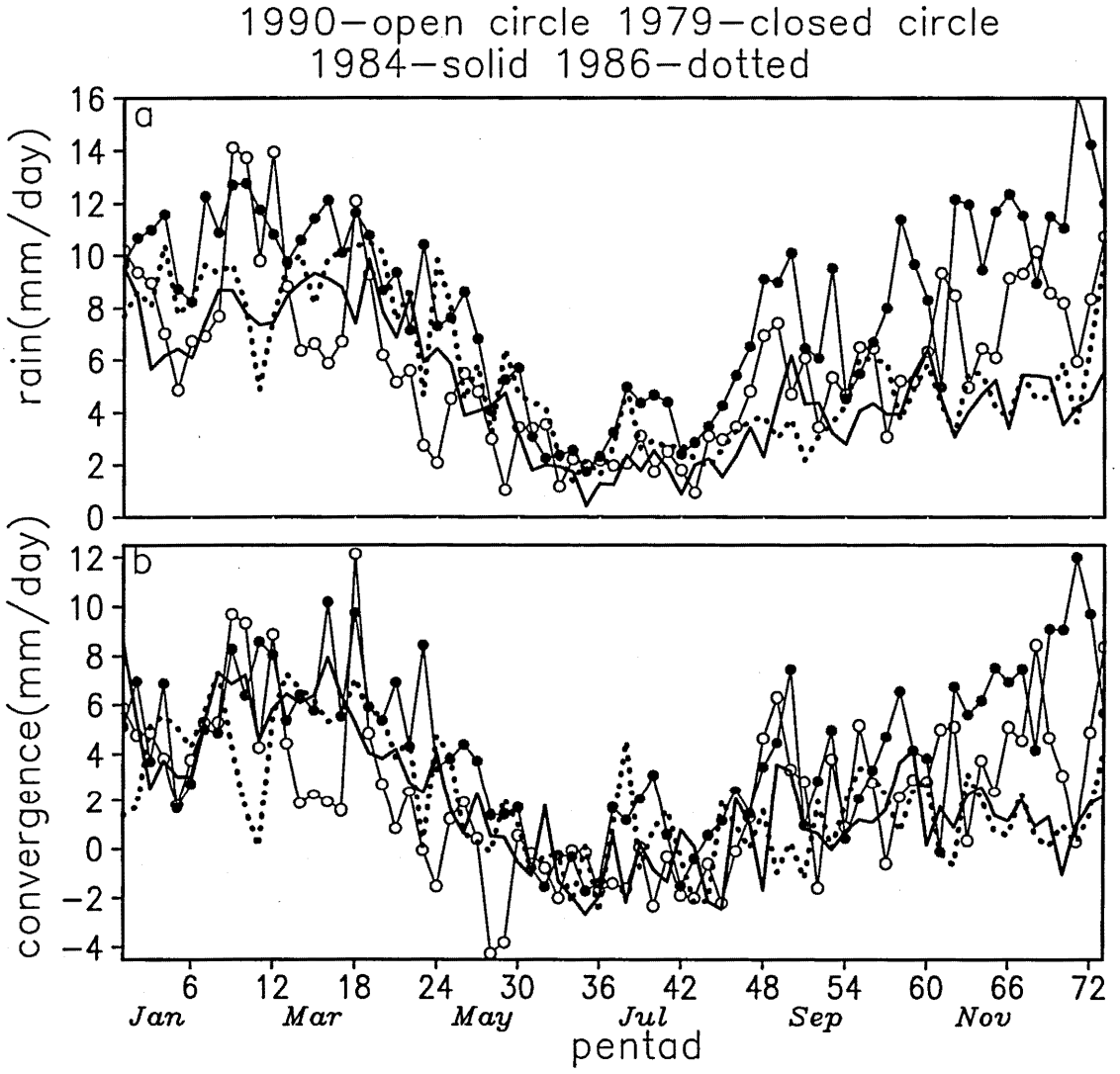

Figure 4.5. Annual cycles of area averaged a) rainrate (mm day^{-1}); and b) moisture convergence (mm day^{-1}) for 1990(open circles), 1979 (closed circles), 1984 (solid curve) and 1986 (dotted curve), respectively.

were similar to those of 1990 during the peak dry season, suggesting that the middle and upper troposphere in the dry season were as stable as in a normal dry season. Thus, wetter land surface and higher surface latent heat flux must contribute to the higher q_{850mb} and lower CINE found in the 1979 dry and early transition season.

The transition of the large-scale circulation also began earlier in 1979 than that in 1990. The V-index reversed to northerly in late July (Fig. 4.4a) almost three months earlier than in 1990. In middle August (pentad 45) when the northerly V-index increased to 2 m s^{-1}, the increase of q_{850mb}, θ_e at 850mb (Fig. 4.2b) and CAPE (Fig. 4.3b) also accelerated. Clearly, the earlier transition of the large-scale circulation also contributes to the earlier wet season onset in 1979. Although our diagnostic results cannot directly determine what causes the earlier reversal of the V-index in 1979, the warm land-surface temperatures caused stronger continent-ocean surface temperature differences in 1979 than in 1990 throughout most of the transition period (not shown). Thus, both the earlier increase of rainfall and the warmer land surface temperature may contribute to the earlier northerly reversal of the cross-equatorial flow in 1979.

Our analysis of the 1979 case suggests that a wetter land surface in the dry season cause an abnormally lower CINE, and thus promote an earlier and more rapidly increase of rainfall during the early phase of the transition. The anomalous rainfall and the earlier reversal of the cross-equatorial flow apparently led to the earlier wet season onset.

4.1.3 Late Onsets

Compared to the "normal" 1990, the wet season onsets were delayed by almost two months (Table 1) in both 1984 and 1986. Surface latent heat flux in both these years began to increase in early July (pentads 38 and 39), as it did in 1990 (Fig. 4.1c). However, the sensible heat flux was higher and the latent heat flux was lower, especially during the 1984 dry season, so the Bowen ratio was higher than normal in July and October by as much as 40% higher in 1984 and 20% higher in 1986 (Fig. 4.1a). These surface heat flux anomalies clearly indicate a drier land surface, especially in 1984. As expected from such dry land surface conditions, CINE was 2 to 3 times higher during August to middle September of 1984 and 1986 (Fig.4.3a). CINE remained higher than in 1990 through the rest of the transition until the wet season onset.

Figure 4.6 shows the composite CAPE and CINE during the transition, where CAPE and CINE are computed as in Williams and Renno (1993). During the fifteen years of our analysis, the wet season onsets appear to occur only after CINE reduces to 50 J kg^{-1} or less (Figures 4.3a and 4.6). CINE also remains lower than this value throughout the wet season. This result from ERA is consistent with that estimated from multi-year radiosonde data for Southern Amazon region (Fu et al., 1999). Thus, a low enough CINE, for example, 50 J kg^{-1} or less may be a necessary condition for the wet season to occur over Amazonia. If so, CINE in both 1984 and 1986 were too high for wet season onset from June to the end of December. This excess CINE alone can generally explain the delay of the wet season onsets in both 1984 and 1986.

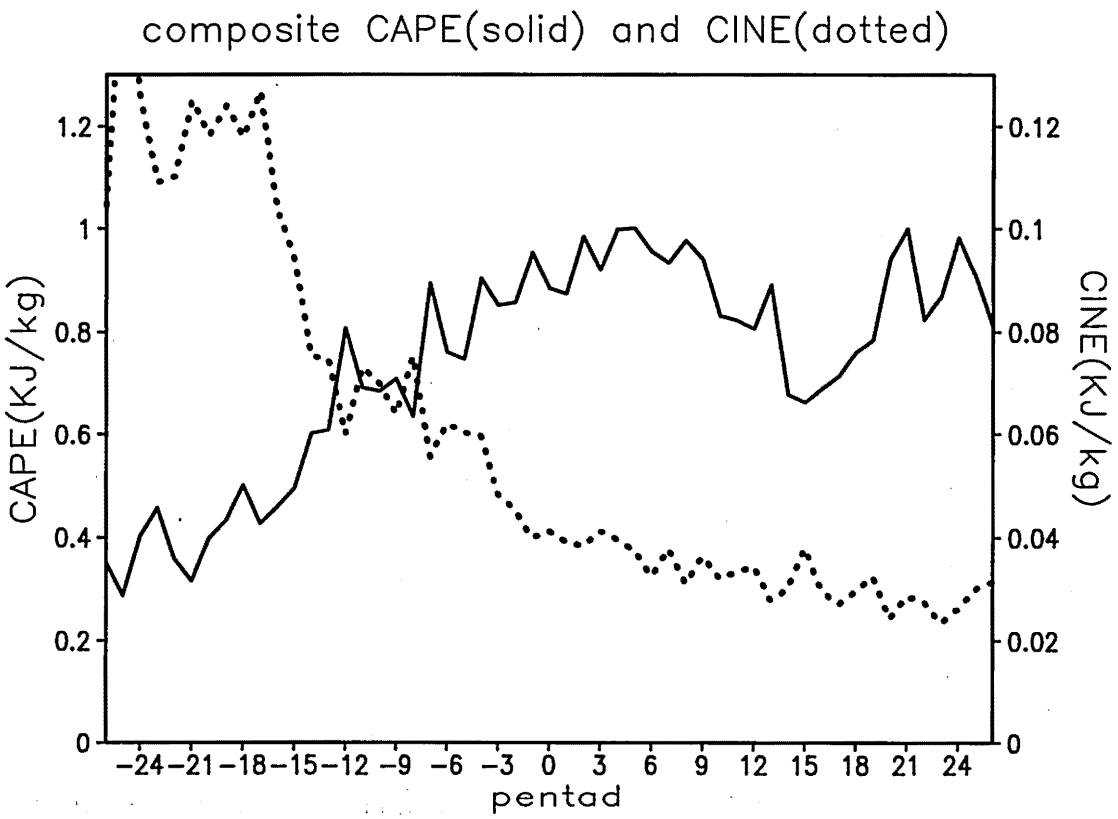

Figure 4.6. Fifteen-year composite of CAPE (solid, unit: kJ kg^{-1}) and CINE (dotted, unit: kJ kg^{-1}) over Southern Amazon region.

The large-scale circulation may have also influenced the wet season onset during the developing phase. The anomalous land surface dryness was stronger in 1984 than in 1986, but the delays of the wet season onset appear to be the same. As shown in Fig. 4.5a, the V-index reversed to northerly in early September in 1984 and early December in 1986. Although the northerly V-index in 1984 remained weak relative to that of 1990 until late November (pentad 65), it could partially offset the influence of the stronger land surface dryness and contribute to a rapid decrease of CINE in early September (Fig. 4.3a). The 200-mb geopotential height also increased rapidly starting from the end of September 1984 (the 54th pentad; Fig. 4.4b), following the northerly reversal of the V-index. Thus, the earlier initiation of the large-scale circulation transition in 1984 may have partially offset the effects of the stronger surface dryness.

4.2 Discussion

4.2.1 Impact Of Land Use On The Precipitation Regime Over The Amazonia

Our analysis in Chapter 4 suggests that land surface conditions during dry and early transition seasons can contribute significantly to the interannual changes of the wet season onset. For example, the humid surface conditions in the 1979 dry season supported higher surface latent fluxes, weaker CINE, and stronger CAPE, and in turn a stronger and quicker increase of convection. These factors and the earlier reversal of the cross-equatorial flow lead to an earlier increase of rainfall and geopotential height in the upper troposphere during the transition, and hence an earlier wet season onset.

Conversely, the lower surface latent flux and drier lower troposphere during dry seasons in 1984 and 1986 appear to cause higher CINE and lower CAPE during the transition, and therefore a delayed wet season onset in both years, even with the normal reversal of the cross-equatorial flow in 1984. On the other hand, the earlier reversal of the cross-equatorial flow in 1984 may have partially offset the delay expected from the stronger land surface dryness. Overall, our results imply that a drier land surface during the dry season should delay, not accelerate the wet season onset over Amazonia, although it should be noted that the surface conditions of the dry and transition seasons are largely a result of historic and current atmospheric conditions.

Previous land use studies have consistently shown that the removal of the rainforest reduces canopy interception of precipitation, increases runoff, and increases the exposure of the surface soil to solar radiation (e.g., Salati and Vose 1984; Dickinson and Henderson-Sellers 1988; Nobre et al., 1991; Hodnett et al., 1996; Souza et al., 1996; Werth and Avissar 2002). The loss of deep roots found in the rainforest (e.g., Dawson 1993; Nepstad et al., 1994) would disconnect surface soil from moisture in underlying deep soil. All these changes tend to accelerate the loss of soil moisture immediately after rain events, consequently reducing the surface wetness and latent heat flux during the dry season (e.g., Nobre et al., 1996). Based on the mechanism suggested by our analysis, with forest removed, the transition from dry to wet season should be delayed and weakened, thereby increasing the length of the dry season. By the same token, such changes would also amplify and prolong droughts, such as those caused by El Niño.

Compared to the areas with rainforest, the lower soil water storage would further reduce the surface latent heat flux during the droughts, thus require stronger moisture transport to support wet season onset. In reality, the influence of land use on the wet season onset and the length of dry season could depend on the patterns of land use and characteristic climate and ecological conditions that vary within the Amazonia. Thus, the general hypothesis inferred from our results must be tested more thoroughly using global and regional climate models. These inferences may not be applicable for the easternmost Amazonia, where oceanic influences dominate the precipitation climatology.

It is also possible that basin-scale land use could so substantially decrease the surface soil moisture and land surface latent heat flux during dry and transition seasons that the increase of sensible heat and of continent-ocean surface temperature gradient would become the main driver of the cross-equatorial flow reversal, as found for the Australia monsoon. With such changes, the diabatic heating in the middle troposphere produced by local rainfall in the early phase of the transition would be absent. The wet season onset could be delayed to summer, instead of spring, as found for the Australia monsoon. Further more, the smaller temperature contrast between Amazonia and the tropical Atlantic Ocean compared to the continent-ocean contrast of the Austro-Asian monsoon systems implies a weaker seasonal reversal of the continent-ocean temperature gradient. Thus, a shift from predominately surface latent heat flux to sensible heat flux as the main initiator of the transition could substantially delay the wet season onset, resulting in a climate regime with a much longer and drier dry season.

4.2.2 Potentials Of LBA Observations For Determining The Influence Of Land Surface Fluxes On Seasonal Transitions Of The Amazonian Rainfall

Although our results derived from ERA may clarify how to best use LBA and pre-LBA *in situ* observations to investigate the processes that determine the wet season onset, the ERA results may be inaccurate as to quantitative changes of the land surface fluxes. In particular, the surface fluxes and their climate variability during dry and transition season as represented by ERA need to be evaluated by multi-year observations as obtained by combining ABRACOS and LBA. In addition, the comprehensive and year-round *in situ* LBA measurements represent the best available ground "truth" over the Southern Amazonia for land surface fluxes from ground to canopy level, as well as soil moisture at various depths for different vegetation types. These LBA observations can be used to clarify the physical and biological processes that control surface fluxes and soil moisture during the transition seasons, and their interannual variations. As the LBA tower observations accumulate, especially through El Niño-Southern Oscillation cycles, we will be able to evaluate changes in the land surface fluxes for at least several areas within the Amazonia. They can also be used with satellite observations to examine the influences of atmospheric condition, such as rainfall and cloudiness, on the land surface conditions during dry and transition seasons. More importantly, the progress made by LBA in understanding the factors that control surface soil moisture and surface fluxes could lay the foundation for us to determine the influences of pre-seasonal and current

rainfall on these land surface properties in our large-scale diagnostic studies of precipitation climatology.

4.3 Summary

Our analysis of Chapter 4 further supports that the transition from dry to wet season in the Southern Amazonia is initially driven by increases of surface heat fluxes, especially latent heat flux. These fluxes rapidly reduce CINE and increase CAPE, and consequently provide a favorable condition for more rainfall even before the large-scale circulation has changed. The increase of rainfall presumably initiates the reversal of the cross-equatorial flow, thus leading to large-scale net moisture convergence over the Southern Amazonia. The analysis of early and late wet season onsets on an interannual scale shows that a longer dry season with lower rainfall causes lower surface latent heat flux in the earlier transition periods. This results in a higher CINE and a lower CAPE, which delays and weakens the initial increase of rainfall, thus the transition of the large-scale circulation. Conversely, a wetter dry season leads to a higher surface latent heat flux and a weak CINE, providing a necessary condition for an earlier increase of local rainfall and a sooner wet season onset.

The removal of the rainforest would result in a more rapid loss of soil moisture after rain events and thus drier surface soil and lower surface latent heat flux during the dry and transition seasons. If we assume that the changes of land surface fluxes due to land use are comparable to the differences between forest and pasture observed by ABRACOS

(e.g. Nobre et al. 1996) and LBA, then these changes would be comparable or greater than those interannual changes between the early and late onsets. Thus, increased land use could delay the wet season onset and prolong the dry season by as much as several months given similar large-scale atmospheric circulation pattern to today's. These inferences, if they can be validated by LBA observations, strongly suggest that more effort should be made to understand the impact of land use on the dry and transition seasons. Changes of precipitation during these periods may not only have greater ecological and economic impacts than a moderate reduction of wet season rainfall, but also have not received adequate attention.

Our results in Chapter 4 suggest that the influence of excess soil moisture on an early wet season onset can be different than that of dry soil on a late wet season. The land surface wetness and static instability in the lower troposphere only provide a necessary condition, not a sufficient condition, for wet season onset. Thus, a drier land surface delays the wet season onset, whereas a wet land surface during the dry season does not necessarily result in an earlier onset when lack of suitable triggering factors as we will show later in the next Chapter.

CHAPTER 5

THE TRIGGERING IMPACT FOR WET SEASON ONSET OVER TROPICAL SOUTH AMERICA: MID-LATITUDE INFLUENCES

The results of Chapter 3 and Chapter 4 address large-scale conditions needed for the wet season onset over tropical South America. However, this is not sufficient to determine the exact onset date. As we will show later, the land surface conditions and large-scale atmospheric conditions were favorable for early onset in 1982, but the real onset date (pentad 68) is about 30 days later than the climatological onset pentad (pentad 62.5). The one month delay of the onset date for 1982 could not be explained using land surface conditions and atmospheric thermodynamic conditions such as CAPE and CINE.

The onset of the monsoon rains is usually triggered by the intraseasonal variability of the atmospheric circulation (Webster et al, 1998). Previous studies have shown that when large-scale conditions for Asian monsoon systems are ready, such as a sufficiently strong temperature contrast due to the seasonal increase in solar insolation (e.g. Webster 1987), the actual onset may be triggered by a transient event such as a cold surge (e.g. Chang and Chen 1995), a synoptic system, or the Madden-Julian oscillation (MJO; Madden and Julian 1994). The earliest onset of the Asian summer monsoon occurs in early to middle May over the South China Sea. The arrival of a midlatitude trough/front appears to lead to increased deep convections along a southwestward extension of the cyclogenesis zone in the equatorial Indian Ocean and cause the onset of the South China

Sea summer monsoon (Chang and Chen, 1995). In the western Pacific and Indian oceans, the MJO is an important source of intraseasonal variability, and has been implicated as a trigger for the onset of the Indian (Webster 1987) and Australian (Hendon and Liebmann 1990) monsoons, as well as a factor in their active-break cycles.

Observations have shown that wet season onset over South America begins in the northwestern part of South America, expands southward to southeastward from the western Amazon to southeastern Brazil (about 20-25 degree latitudinal) within a week or two in the austral Spring and finally progresses eastward to the northeastern Brazil and the entire basin (e.g. Kousky 1988; Sugahara 1991). Horel et al. (1989) suggested that the rapid onset, sometimes on a 5-day period, is of dynamical origin rather than a response to the annual variation in solar zenith angle. Over the Amazon region, the MJO does not emerge as a prominent instigator of the onset mechanism. It is generally much weaker over South America than in the Asian-Australian sector, although it does modulate the South American LLJ and the SACZ (Liebmann et al 2003).

Mid-latitude cold surges often penetrate into subtropical and tropical South America along the east of the Andes all year around. From a statistical perspective, the cold surges are the dominant synoptic-scale mode of circulation and temperature variability over subtropical South America (Kousky and Cavalcanti 1997; Vera and Vigliarolo 2000). The structure and influence of the cold front systems on precipitation during austral winter and summer have been investigated by Marengo et al (1997), Garreaud and Wallace (1998), Vera and Vigliarolo (2000) and Vera et al. (2002). These strong cold

surges may account for about 50% of the total summertime precipitation south of 25°S, about 30% over the western edge of the Amazon basin and 20% over the northeast coast of South America when the convective bands propagate equatorward (Garreaud and Wallace 1998). The mean monthly distribution of the frequency of frontal passage between 5°S and 20°S is the highest during the transition season (October-November) according to Oliveira (1986). Whether these mid-latitude cold air systems could trigger the transition from dry to wet seasons as in the East-Asian monsoon region remains unclear, however.

The unique southeastward expansion of the deep convection area from western Amazonia over South America seems to resemble the propagating passage of a cold air intrusion. However, whether such a cold air intrusion could indeed influence the wet season onset over South America has not been previously investigated. In this Chapter, we will explore its role as a possible trigger of the wet season onset. This will lead to a more precise determination of the wet season onset, and consequently a clearer understanding of what causes such large discrepancies in the onset dates interannually (Marengo et al. 2001).

5.1 Methods

Since the lifetime of cold air intrusions is usually on the order of 5-12 days (Marengo et al. 1997; Garreaud 2000), daily time resolution of ERA data is used to discern the cold air intrusion cases. The large-scale thermodynamic and dynamic fields

remain in pentad resolution for the purpose of representing the wet season onset as seen in Chapters 3 and 4. Based on the onset criteria defined in Chapter 3 for the period of 1979-1993 (Table 1), the onset dates for 11 out of 15 years occurs within October and November. The influence of cold air intrusions on wet season onset has been examined for October to November as the climatology background. Cold air is defined according to Garreaud (2000) but modified due to the large interannual change of the wet season onset dates. Specifically, we choose the 24-hour sea level pressure tendency (δSLP) as the key variable for identifying the steep rise in SLP at the leading edge of the cold air. The cold air index domain (referred to as the index area thereinafter) is centered at 25°S and 57.5°W with 5° x 5° grid longitude and latitude. This index area has been shown to mostly capture the cold front and its remainders based on a climatological dataset (Garreaud and Wallace 1998; Garreaud 2000). The initial set of cold air episodes was taken as the days that δSLP is within the top 10% of the seasonal frequency distribution for those years which onsets occurred in Oct. to Nov.. To make sure the SLP increase is actually associated with the passage of a cold air incursion, we only retain those episodes in which SLP is higher than 1018-hPa and temperature drops at least 8°C after the whole process. The choices of 1018-hPa and 8°C are based on the climatology for October-November for all 15 years. We also combine the evolution of 925-hPa geopotential height to verify the cold air incursion process. For the rest of years, cold air episodes are defined using the above δSLP, SLP and temperature criteria obtained for Oct.-Nov.. Fig.

5.1 showed the time series of δSLP, SLP and 925-hPa temperature for the transition period of 1979 as an example, together with the selected episodes. In 1979, the wet season onset occurred at pentad 49, which is defined as August 29 to September 2. There is a strong cold air intrusion beginning on August 29 which lasts for about 6 days.

Based on the criteria of δSLP, SLP and 925-hPa temperature as well as geopotential height at 925-hPa for the fifteen years, we found strong or weak cold air intrusions associated with all wet season onsets except for the two late onset years 1984 and 1986. This is because these two late onsets took place at the year's end when sufficiently strong cold air intrusions are unlikely to occur. The climatological influence of cold air penetrations on wet season onset over tropical South America is represented by a composite of the large-scale circulation change associated with the cold air intrusions. Day 0 of a composite field is the average for that field from all the days when cold air intrusions are first identified immediately preceding wet season onset. Composite fields for day n (for n = -2, –1, +1 and +2) are defined as the average of the fields using n days before or after each original day 0. The associated circulation, convective activity and thermodynamic features are characterized by the composite analysis.

Linear regressions of SLP and 925-hPa temperature against precipitation are used to measure the influence of cold air intrusions on precipitation amount over South America. This statistical method is able to identify the spatial patterns of precipitation change due to the SLP increase and the temperature decrease associated with the cold front passage.

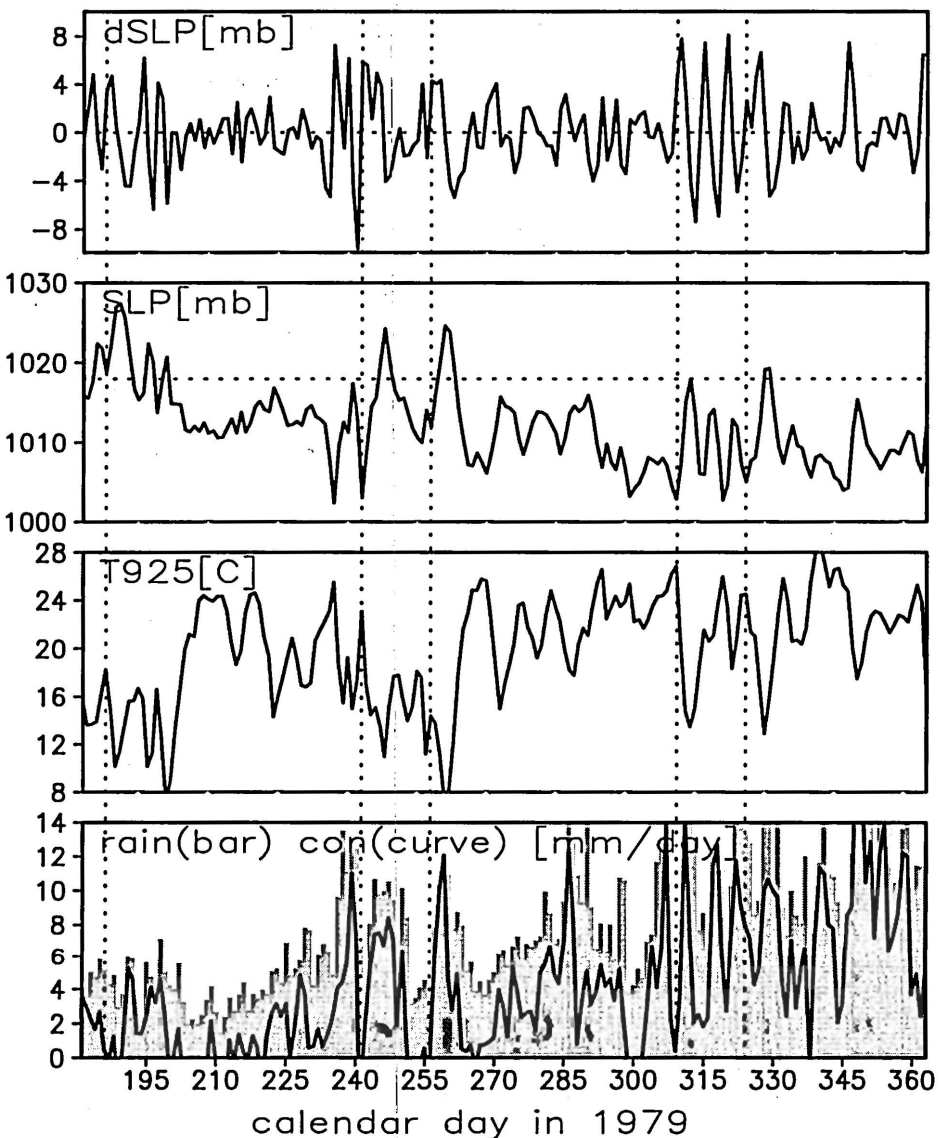

Figure 5.1. Daily mean values of 24-h sea level pressure tendency (δSLP, upper panel), sea level pressure (middle upper panel), 925-hPa air temperature (middle lower panel) averaged over the 5 ° x 5° cold air index area centered at 25°S 57.5°W as well as averaged rainrate (bar) and moisture convergence (curve) over the Southern Amazon domain (5°–15°S, 45°–75°W) (lower panel). Horizontal line in the middle upper panel indicated one of the criteria, SLP, for identifying cold air episodes. The vertical dashed lines indicate day 0 for the selected cold surges according to Garreaud (2000).

5.2 Results

5.2.1 Role Of Cold Air Intrusions In A Climatological Transition

Cold air intrusions usually influence precipitation through convergence ahead of the front and the uplifting of warm air (Aguado and Burt, 1999). Exploring a possible connection between cold air intrusions and precipitation change over South America during the transition period, Fig. 5.2a shows the correlation of ERA precipitation field with SLP index, using daily data in October and November for the fifteen years. Areas with significant positive correlations are found in the western Amazon and SACZ, while significant negative correlations are observed in the subtropics. Since SLP increases and temperature decreases simultaneously during a cold air intrusion, significant negative correlations between the temperature and the precipitation fields appear in the western Amazon and SACZ (Fig. 5.2b) as expected. This suggests that precipitation increases over western Amazon and decreases over most of the subtropics when a cold front approaches. The enhanced convection that precedes the cool surges is consistent with the intense low-level wind convergence embedded in a conditionally unstable environment (Garreaud and Wallace 1998). On the other hand, SLP and temperature changes related with cold surges during the transition season leave a clear imprint on convection over the SACZ, also pointed out by Lenters and Cook (1995).

The composite fields of low-level wind anomalies and equivalent potential temperature (θ_e) anomalies at 925-hPa for the cold air episodes before the wet season onsets are presented in Figure 5.3. The composite anomalies are calculated as the

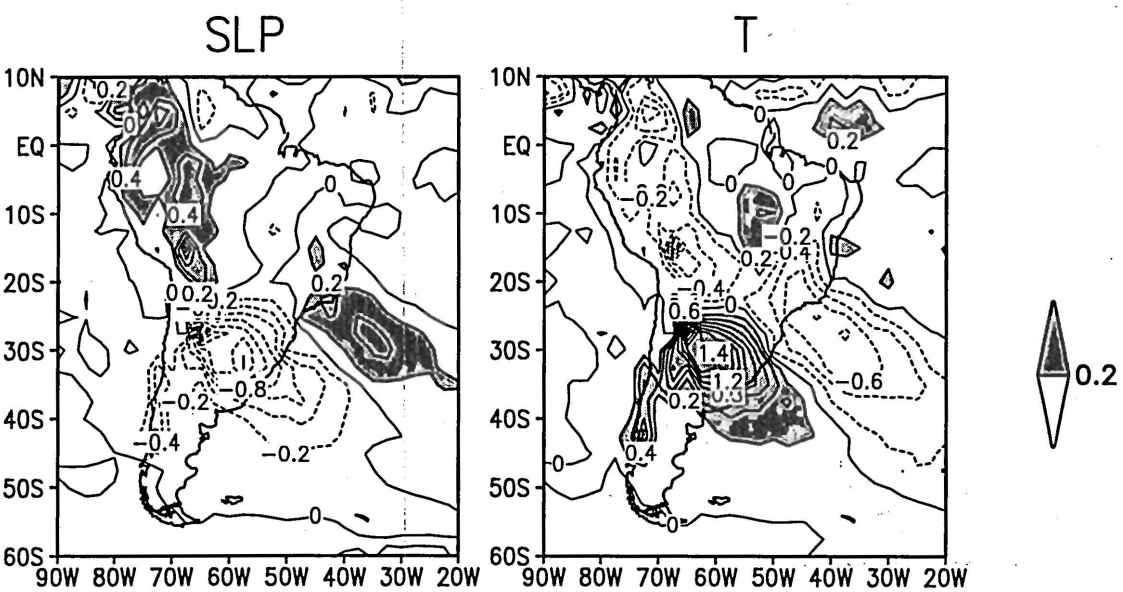

Figure 5.2. Linear regression coefficient for daily precipitation associated with 15-yr daily mean (a) Sea Level Pressure (hPa), and (b) temperature at 925-hPa (K). Contour interval is 0.2 mm day^{-1}, negative coefficients are plotted using dashed lines.

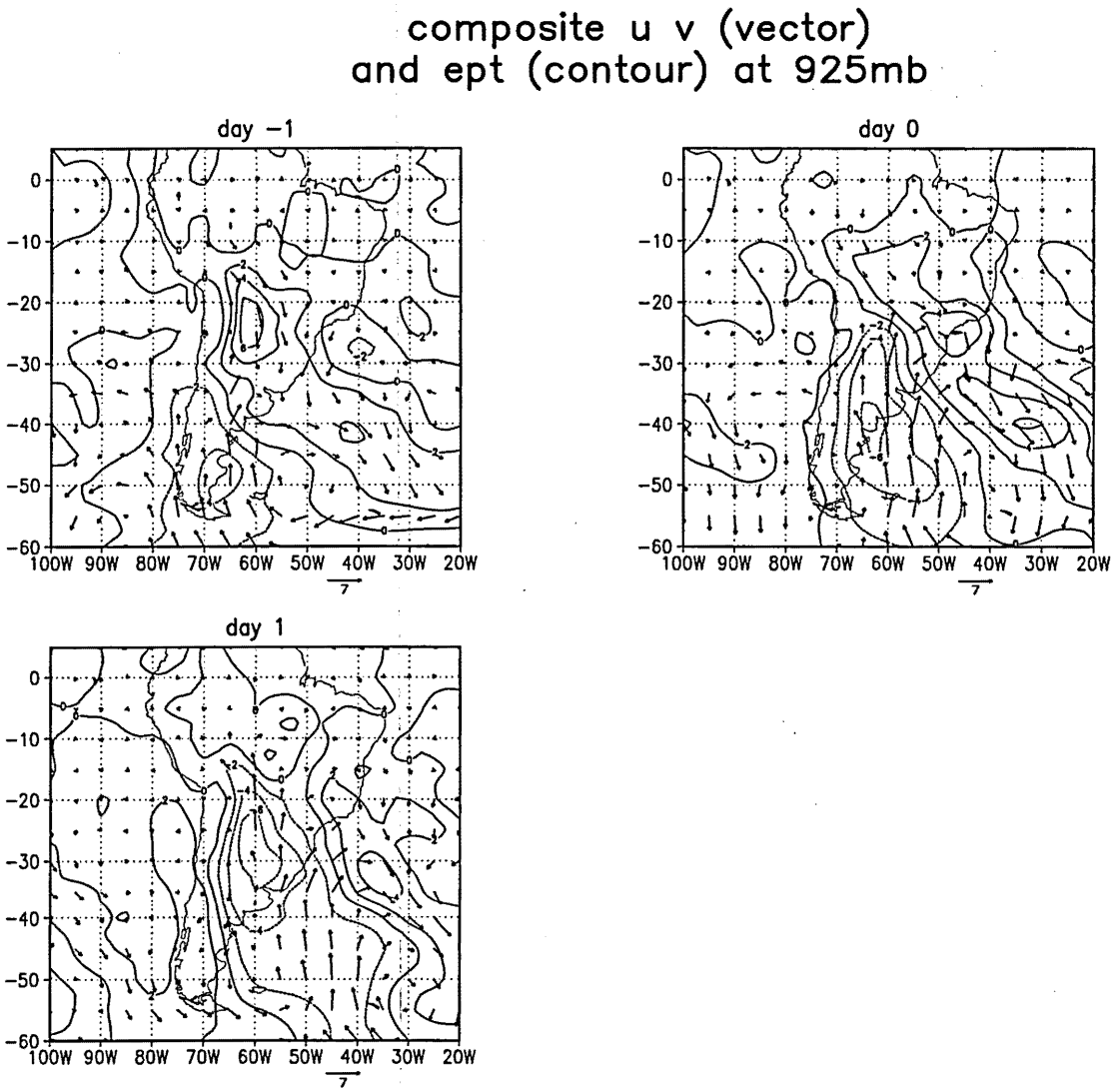

Figure 5.3. Composite maps of 925-hPa winds (vectors) and equivalent potential temperature anomalies (contoured every 2 K) for cold surges.

composite fields minus the corresponding mean fields for all the cold air episodes. The anomalies of the meridional wind and θ_e clearly reveal the equatorward advance of southerly winds and cold air. The negative θ_e anomalies can penetrate equatorward to 10-15°S after the cold air passes through the index area. Fig. 5.4 shows the composite 294 K temperature contour migration during the cold air intrusion process. The temperature contour withdraws from about 35°S at day –1 to about 25°S when the cold air approaches the index area, and then recedes further north to about 20°S one day after the cold air breaks up. In addition to the circulation and temperature changes, the precipitation also changes, as is demonstrated in Fig. 5.5. Fig. 5.5 shows the composite sequences of the precipitation anomalies before, during, and after the cold air intrusion. The enhanced convection as shown by the positive value of the precipitation anomalies is located at the leading edge of the cool air. It moved from the southern subtropics 30-35°S to the lower latitudes (as far north as 5-10°S although the major convective area is located near 10-20°S). The band had longitudinal scale of about 3000 km. The enhanced convection ahead of the cool surges is consistent with the intense low-level wind convergence embedded in a conditionally unstable environment (Garreaud and Wallace 1998). This synoptic-scale band was limited by the eastern slope of the Andes and extended into the South Atlantic Ocean with a northwest-southeast orientation. The spatial pattern of the enhanced precipitation seems to agree with the onset migration of the wet season over South America, suggesting that the wet season onset may be triggered by such cold surge systems.

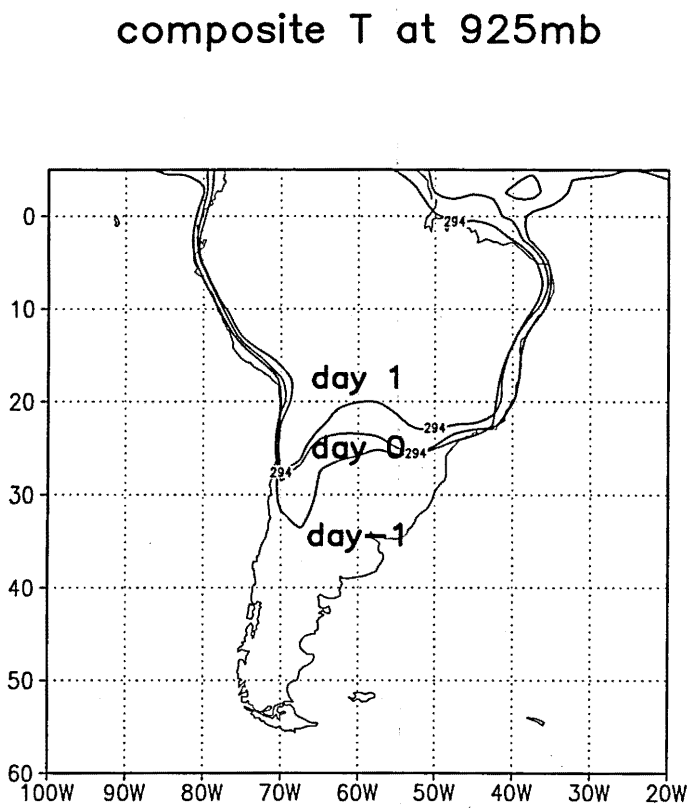

Figure 5.4. The migration of composite 925-hPa temperature 294K during the cold air intrusion.

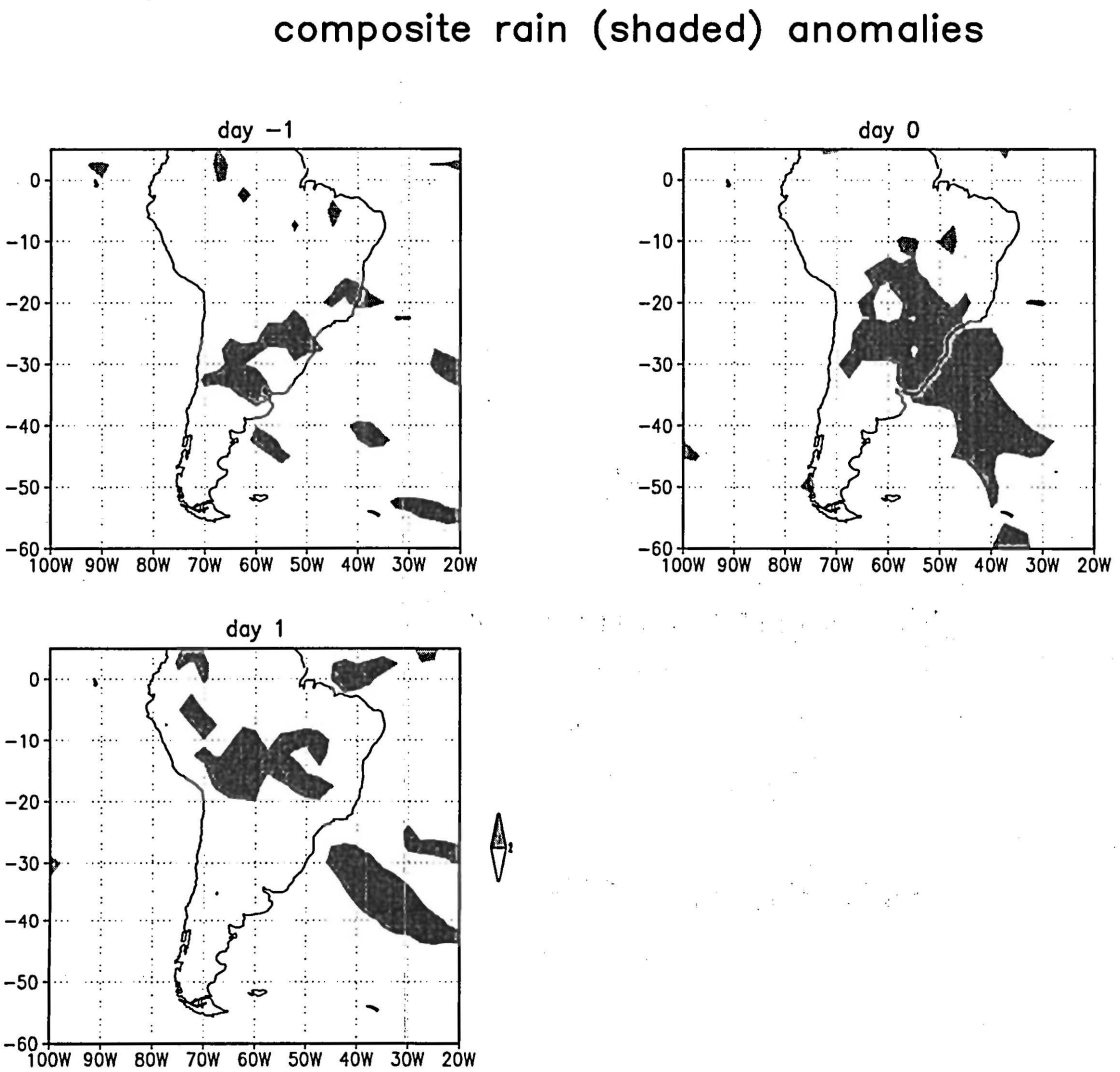

Figure 5.5. Composite maps of precipitation anomalies for cold air intrusion passage.

5.2.2 Influence Of The Cold Air Intrusion On The Early And Late Onsets

On a statistical basis, the wet season over tropical South America often begins with a short period of transition from a dry atmosphere with infrequent precipitation event to a more humid atmosphere with more frequent rainy events. Figures 5.3 and 5.5 suggest that cold air intrusions enhance convective precipitation through low-level wind convergence, thus contributing to this rapid transition. However, cold air incursions occur in all seasons. What determines which cold air incursions trigger the wet season onset? The wet season onset not only depends on a cold air intrusion over tropical South America but also depends on the large-scale circulation over the region. When large-scale conditions are not ready to sustain frequent deep convection, cold air intrusions alone cannot maintain frequent and strong rainfall. What is the right combination of cold air triggers and the large-scale conditions for wet season onset?

Possibilities for such a combination can be illustrated by comparing the following three onsets: the early onset year 1979 (onset at pentad 49, around August 19 to September 2), a relatively late onset year 1982 (onset at pentad 68, from December 2 to December 6), and a "normal" onset year 1983 (onset at pentad 60, between October 23 and October 27) as an example for normal onset year.

Figure 5.1 shows the frequency of cold air intrusions in 1979. Right before the wet season onset at pentad 49 (i.e. day 241-245), a strong cold air event passed through the index area. It started at day 238, although the maximum SLP increase and temperature drop occurred at the onset date (i.e. day 241; August 29). Figure 5.6 shows the sequential

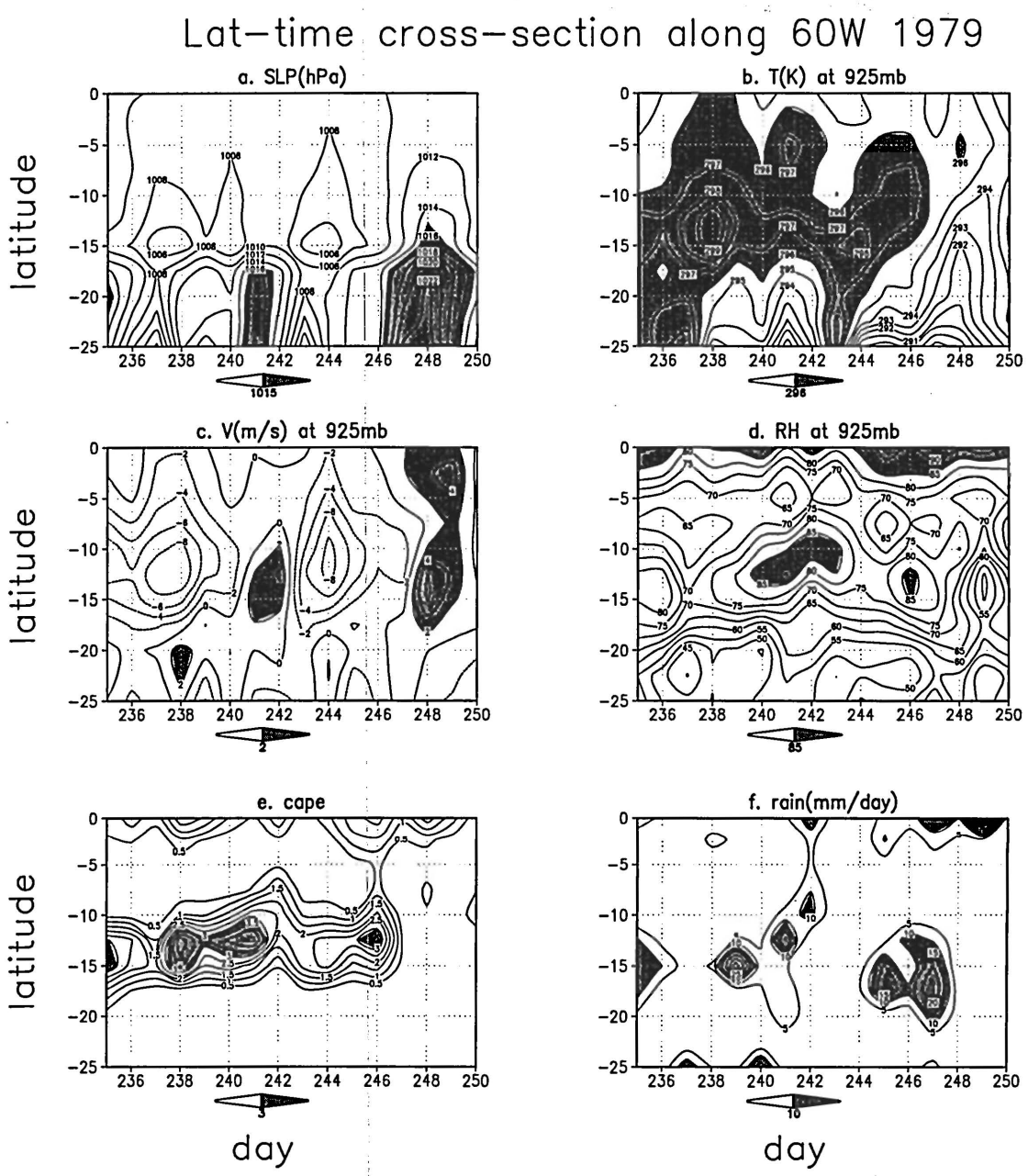

Figure 5.6. Latitudinal-time cross –section along 60°W of (a) Sea level pressure (hPa), (b) temperature (K) at 925 hPa, (c) meridional wind (m s^{-1}) at 925 hPa, positive values represent southerly, (d) relative humidity at 925hPa, (e) CAPE (KJ kg^{-1}), and (f) rain rate (mm day^{-1}) in 1979. x coordinate is calendar day, y-coordinate is the latitude.

variation of SLP, temperature at 925-hPa, V-index, relative humidity at 925-hPa, CAPE and precipitation along 60°W as the cold surges passed the index area. Cold air penetrated into the Amazon region, as is shown by increased SLP and decreased temperature starting from 3 days before the onset (Figs. 5.6a and 5.6b). CAPE also increased rapidly (Fig. 5.6e) from day -3 to day +1, and the meridional wind changed from northerly to southerly (Fig. 5.6c), causing moisture convergence (Garreaud and Wallace 1998) over 8°S to 18°S starting from day 238 (not shown here). Precipitation increased from 5 mm day^{-1} to 10 mm day^{-1} averaged over the entire area (Fig. 5.6f). The relative humidity increased from 65% to 85% and remained high afterwards (Fig. 5.6d). After the cold air intrusion, wet season onset began at pentad 49 corresponding to calendar days 241-245. This means that the cold air helped to release the potential energy of the atmosphere and increase the moisture convergence and precipitation to trigger the onset. Through all the 15 years, the early onset years including 1980 (onset at pentad 57 i.e. Oct. 8- Oct. 12) and 1981 (onset happened at pentad 59, i.e. Oct. 18-Oct. 22), appear to be triggered by similar cold air incursions.

Compare to a "normal" onset in 1983 (pentad 60; day 296 to 300), the wet season onset of 1982 occurred relatively late (at pentad 68; day 336 to 340). The large-scale environments for these two years are compared to that of 1979. Fig. 5.7 shows the land surface conditions for all three years. The sensible heat flux for 1982 is lower and latent heat flux is larger, leading to a lower Bowen ratio. Shown in Fig. 5.8, the increase of CAPE began at pentad 42 in 1982, the same as in the "normal" onset year 1983, but the

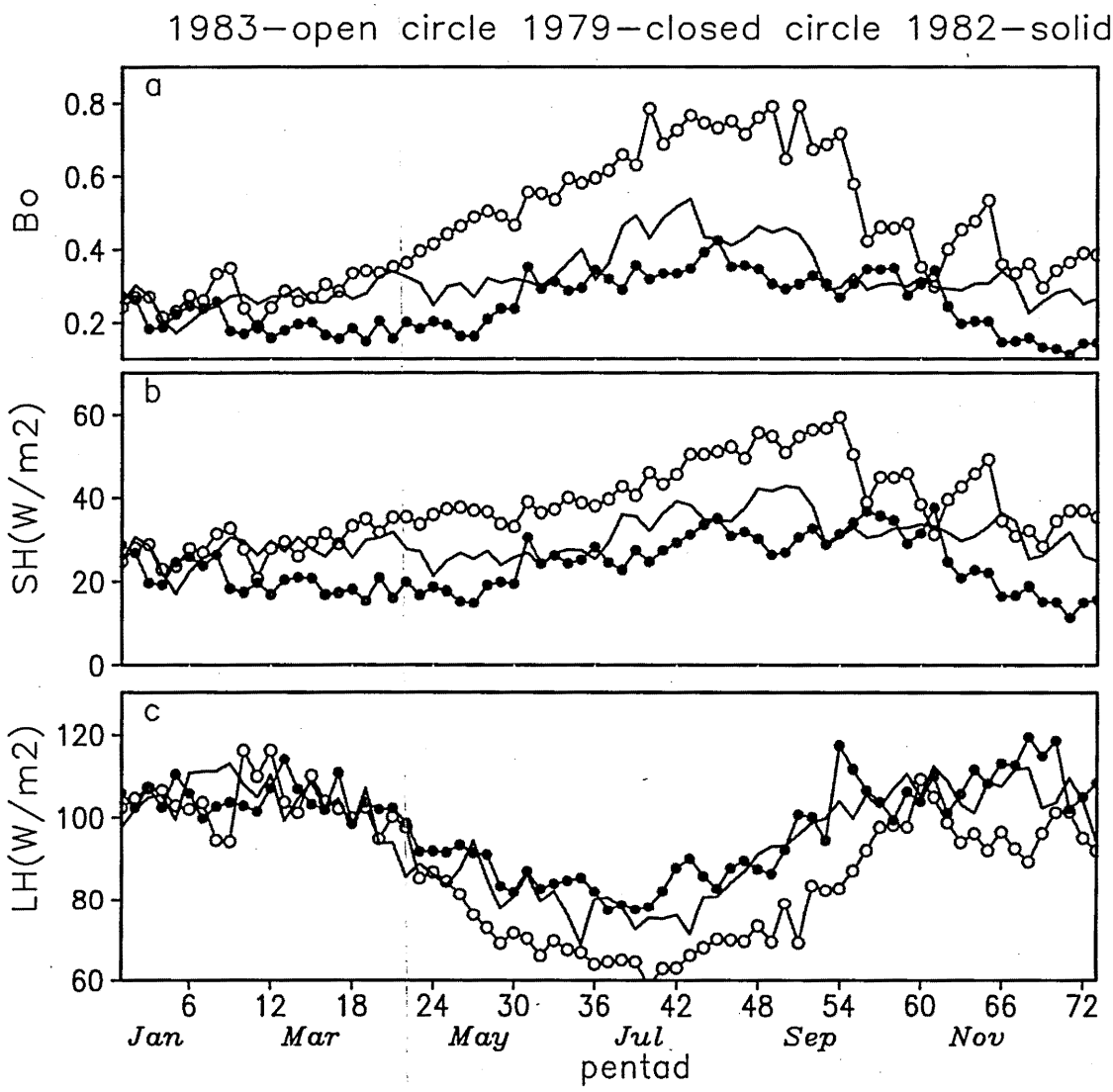

Figure 5.7. Areal averaged Bowen ratio (upper panel), Sensible heat flux (middle panel, W m^{-2}) and latent heat flux (lower panel, W m^{-2}) over (5°–15°S and 45°–75°W) in normal year 1983 (open circle), early onset year 1979 (closed circle), and relatively late onset year 1982 (solid).

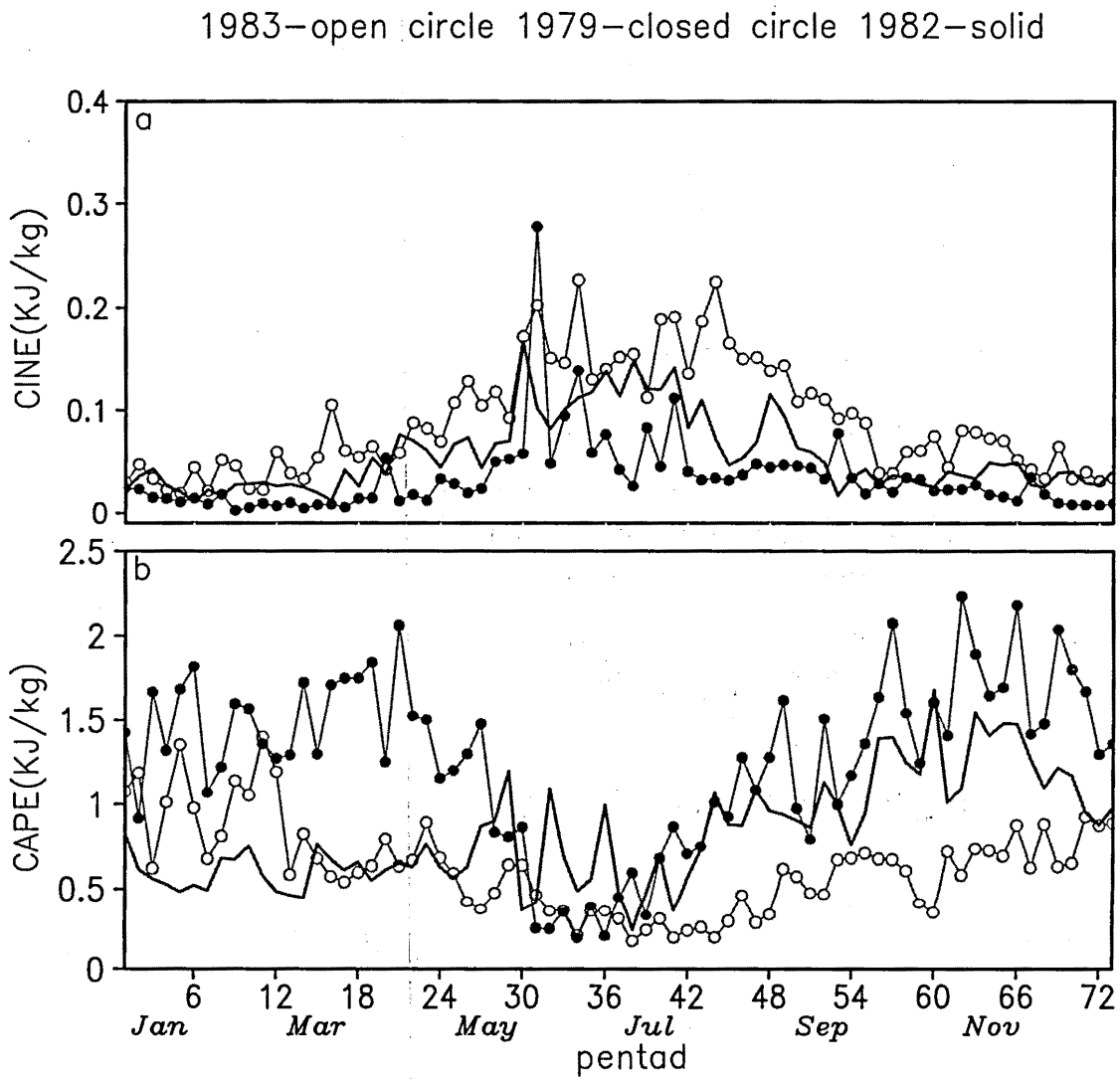

Figure 5.8. Areal averaged CINE (upper panel, KJ kg^{-1}), and CAPE (lower panel, KJ kg^{-1}) over (5°–15°S and 45°–75°W) in normal year 1983(open circle), early onset year 1979(closed circle), and relatively late onset year 1982 (solid).

magnitude in 1983 is about 75% higher. CINE decreases at pentad 45 in 1982, as in 1983, although its value is about 30% lower before pentad 66. These land surface conditions and atmospheric conditions suggest that the atmosphere was more favorable for early onset of deep convection in 1982 than in 1983; however, the actual wet season onset was about 40 days later in 1982. Therefore, the land surface conditions and atmospheric static instability alone cannot fully control when the wet season begins.

Figure 5.9 shows the sequences of SLP, temperature at 925-hPa over the index area, and domain averaged precipitation and moisture convergence over Southern Amazon region (5-15°S, 75-45°W) for 1982 and 1983. Based on the definition of a cold air intrusion, there is only one cold surge that passes through the index domain (Figs 5.9a and 5.9b) during day 247 to day 249 (pentad 50) in 1982, 88 days before the onset. The cold air intrusion for 1982 did increase moisture convergence over the Southern Amazon region but the background atmosphere was too stable to support wet season onset at this early stage of the transition. The other two cold surges which occurred at day 260 (pentad 52) and day 270 (pentad 54), are relatively weak and could not reach the central Amazon as shown in Fig. 5.10. Figure 5.10 also shows that subsidence dominated over the Amazon region during these two weak cold air intrusions. The relative infrequency and weakness of cold air penetrations may cause the late onset of the wet season in 1982. We note that 1982 is a strong El Niño year. The case study (Fig. 5.11) of the 200-hPa circulation in 1982 showed that for this year, the subtropical jet stream was about 5m s^{-1} (about 20%-30%) stronger than in 1983 (not shown here) and about 5° north of its

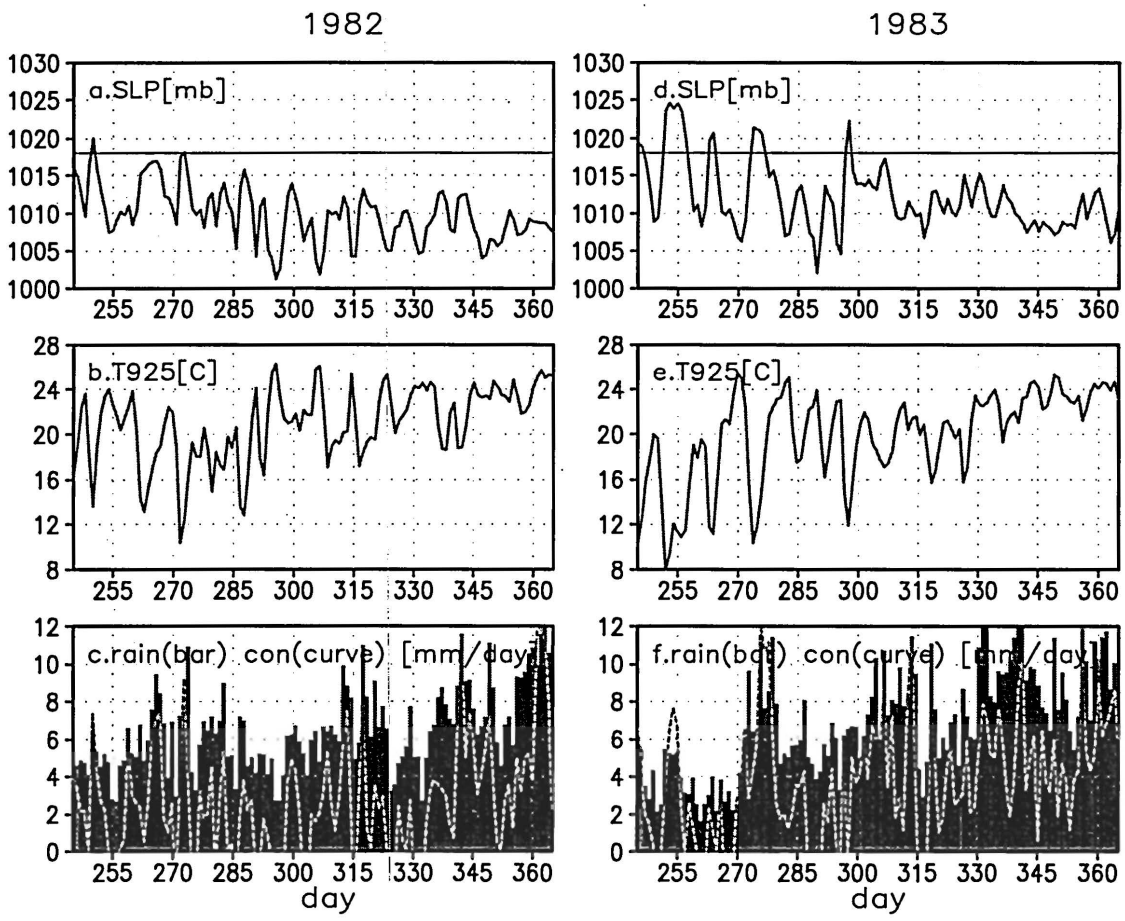

Figure 5.9. Comparison of SLP (upper panels, hPa), 925-hPa air temperature (middle panel, °C) over cold air index region, and rainrate (lower panel, bar, mm day^{-1}), moisture convergence (lower panel, curve, mm day^{-1}) over Southern Amazon domain (5°–15°S, 45°–75°W) between 1982 and 1983.

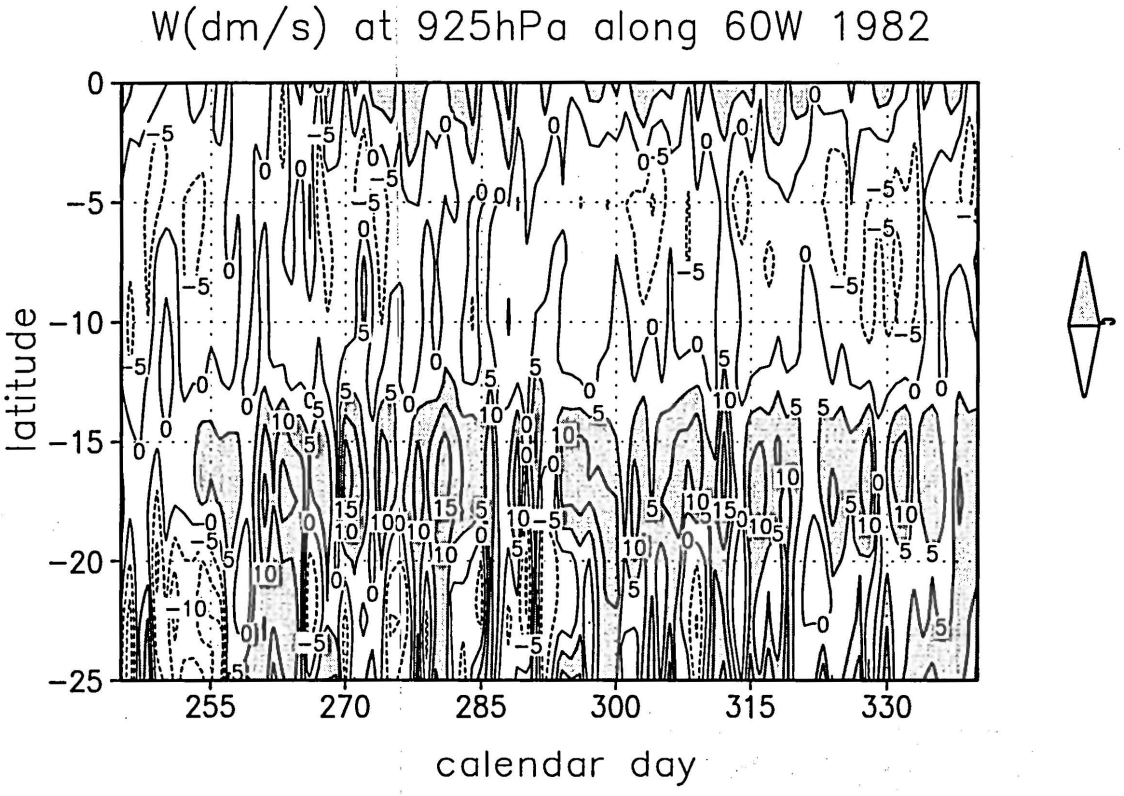

Figure 5.10. 925-hPa vertical velocity (dm s^{-1}) change with time along 60°W in 1982, positive values represent the upward motion, x coordinate is calendar day, y-coordinate is the latitude.

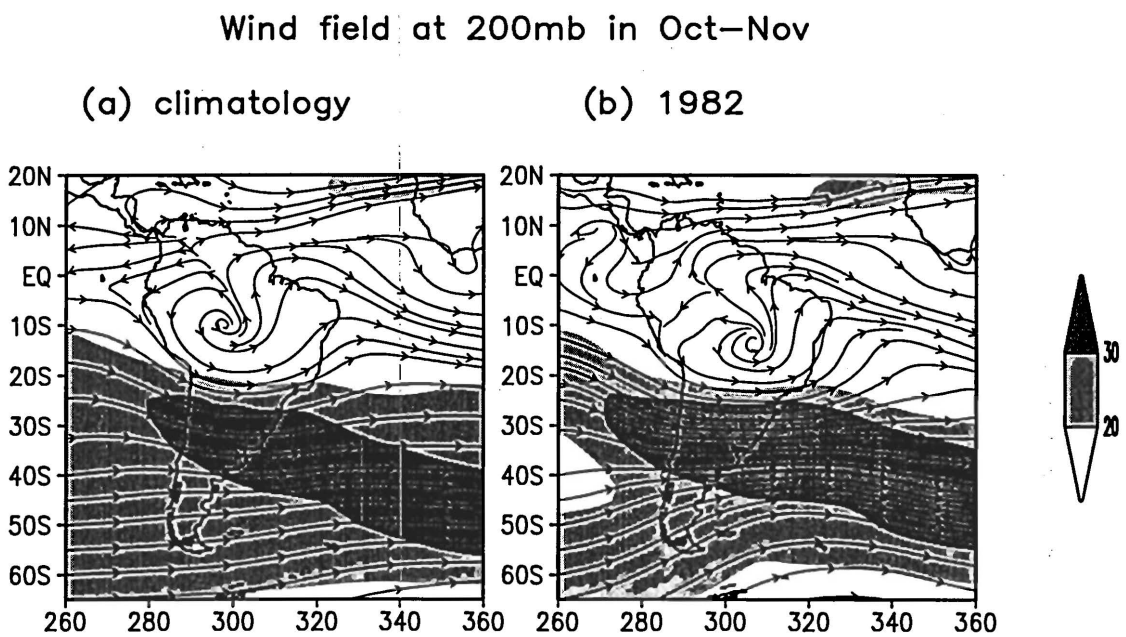

Figure 5.11 Comparison of wind field at 200-hPa averaged in Oct-Nov for (a) fifteen years climatology; and (b) 1982. Light and dark shaded areas represent wind speed which are larger than 20 m s^{-1} and 30 m s^{-1} respectively.

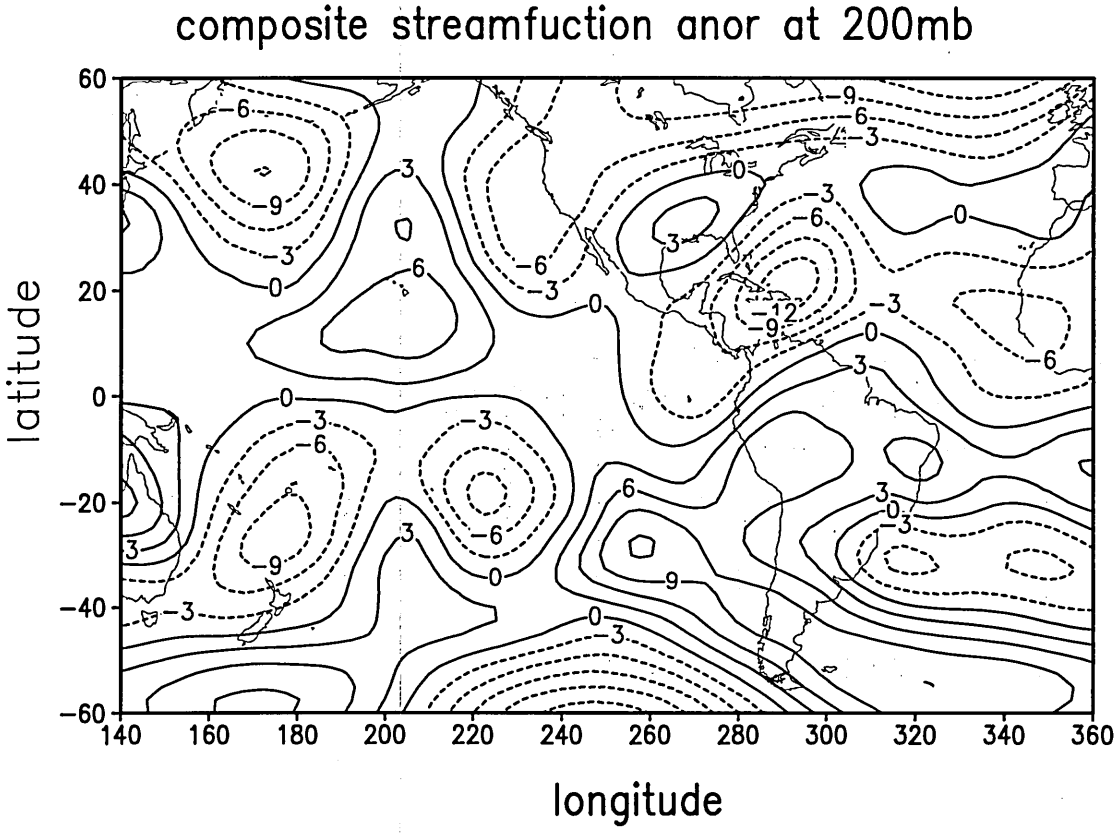

Figure 5.12. The 200-hPa streamfunction anomaly composite in November for 4 El Niño years 1982,1986,1987 and 1992. Contour interval is 3 x 10^6 s^{-2}. The anomaly is calculated as the composite of 4 El Niño years minus the 15-year mean.

climatological position during the transition months of October and November. The abnormal strength and equatorward position of the subtropical jet stream in 1982 is unfavorable to the equatorward penetration of frontal systems and convective complexes, which can normally reach central South America (Coelho and Ambrizzi 2000; Garreaud 2003).

In 1983, several episodes of cold air are apparent during the transition period. The earlier cold surges led to the increase of moisture convergence over the Southern Amazon domain (Fig 5.9f). Right before the wet season onset in 1983, on day 295, the cold air passed through the index area, lifting the moisture air and leading to the precipitation and a realization of the onset criteria at pentad 60 (i.e. day 296-300). The increased frequency and strength of equatorward cold air intrusions seem to contribute an earlier onset for 1983 compared to that observed in 1982.

5.3 Discussion

We have analyzed the large-scale processes necessary for wet season onset in Chapters 3 and 4. However, such large-scale thermodynamic conditions alone, sometimes, cannot determine when the wet season onset occurs. A lack of the triggering factors can delay the wet season onset as in 1982, even when the land surface conditions and local atmospheric condition seems ready.

Cold air incursions appear to be more critical for the early onset years, when both the land surface and large-scale transport are already destabilized. For example in 1979, since the atmosphere reaches a conditional unstable state relatively early, when a cold air comes, it lifts the air above the Lifting Condensation level (LCL) and causes an increase of moisture convergence, resulting in precipitation (Garreaud 2000). On the contrary, in 1982, without frequent and sufficiently strong cold air intrusions triggering the atmosphere to release potential energy, the wet season begins about 40 days later than the normal onset year 1983 even though the large-scale thermal and dynamic conditions seem favorable to an early wet season onset in 1982. Under these circumstances, cold air intrusions appear to be critical for wet season onset, presumably because the maximum insolation has not yet moved into southern Amazonia to drive local thermal convection.

For late onset, cold air intrusions may not be the only trigger of the wet season onset. For example, there are not apparent cold air penetrations prior to the wet season onset over Southern Amazon region in 1984. The wet season onset is probably the result of a local thermally driven precipitation that occurs when large-scale circulation is ready.

El Niño appears to influence the wet season onset through the variation of the subtropical jet stream (Grimm et al. 2000; Paegle et al. 2002). Our composite results show that the subtropical jet stream is abnormally strong and further north than usual during El Niño years based on 15-year ERA data (Fig. 5.12). This agrees with Grimm et al. (2000), who used National Center for Environmental Prediction (NCEP) reanalysis data. The anomalous strength and position of the subtropical jet stream are unfavorable

for cold air incursions into tropics, and therefore lead to less (more) precipitation over the Amazon (subtropics) (Coelho and Ambrizzi 2000; Coelho et al. 2002). In addition to the subtropical jet stream, the sea level pressure gradient from the North Atlantic and the tropical Amazon region is related with El Niño. During El Niño years, SLP in the North Atlantic is lower (Nobre and Shukla 1996) and tropical South American surface atmospheric pressure is higher (Poveda and Mesa 1997), which leads to a reduction in the gradient between the North Atlantic and northern South America. This weakening of the pressure gradient probably leads in turn to a late reversal of the V-index, and therefore a later start to moisture convergence over the Amazon region. In our 15-year dataset, we only find one case like this, in 1986. The overall influences of El Niño on wet season onset over tropical South America need to be further studied (Marengo and Hastenrath 1993) since El Niño years (1982, 1986, 1987 and 1992) tend to have late onset dates (Table 1).

5. 4 Summary

We have observed a close relationship between cold air intrusion and wet season onset over tropical South America. Our results suggest that during the transition period of October-November, enhanced precipitation due to cold air penetration is found in the western Amazon and SACZ, where precipitation decreases are mainly confined to the subtropics. This spatial pattern of enhanced precipitation and the 5-12 days temporal scale of cold surges over South America suggest that cold air intrusions may trigger wet

season onset and cause the rapid, southeastward expansion of the rainy area from the western Amazon to southeastern Brazil during the transition.

Comparisons among an early onset year 1979, a normal onset year 1983 and a relatively late onset year 1982 suggest that the triggering impact of cold air incursions is sometimes critical for determining when the onset happens. During the transition period of the early onset years, local land surface and atmospheric conditions are already destabilized for deep convection at early stages, but the triggering mechanism appears to be necessary for the release of potential energy, intense moisture convergence and enhanced deep convection that lead to wet season onset. On the contrary, without the triggering influence of frequent and sufficiently strong cold surges, the wet season onset of 1982 is about 30 days later than the climatology even though the land surface and large-scale conditions were favorable for early onset. The cold air intrusion immediately preceding wet season onset in 1983 appears to trigger a normal onset date (pentad 60^{th}) even though the land surface and atmospheric conditions are more unfavorable to early onset than in 1982.

El Niño years tend to exhibit a northward shift and higher intensity in the subtropical jet stream over South America. The abnormal strength and position of the subtropical jet stream, such as in 1982, tends to block moisture convergence into tropical South America and confine cold air to the subtropical region, leading to less (more) precipitation over the Amazon basin (subtropics), a result that was also reported by Lenters and Cook (1997), Coelho and Ambrizzi (2000), and Coelho et al. (2002).

CHAPTER 6

CONCLUSION, DISCUSSION, AND OUTLOOK

6.1 Conclusion

In this Dissertation, we have studied the mechanism responsible for the wet season onset over tropical South America as schematically illustrated in Figure 6.1. We first studied the climatological wet season onset using a composite analysis of different atmospheric fields and land surface conditions on the basis of 15 years of ERA data (Chapter 3). The results suggest that the primary driving force of the transition varies as the transition progresses through three phases. During the initiating phase, land surface fluxes dominate the increase of atmospheric moisture and moist static energy in the lower troposphere; large-scale moisture transport and upper tropospheric geopotential remain more or less unchanged from the dry season. During the developing phase, moisture transport becomes increasingly important in driving the transition, and the dynamic feedbacks to the stretching of the atmospheric column dominate in this phase. The maturing phase features a buildup of the Bolivian High, and precipitation reaches its peak.

The mechanism was then applied to explain the interannual variations of the onset of the rainy seasons (Chapter 4). The results confirm the importance of land surface fluxes, especially latent heat flux during dry and early transition seasons, to the wet

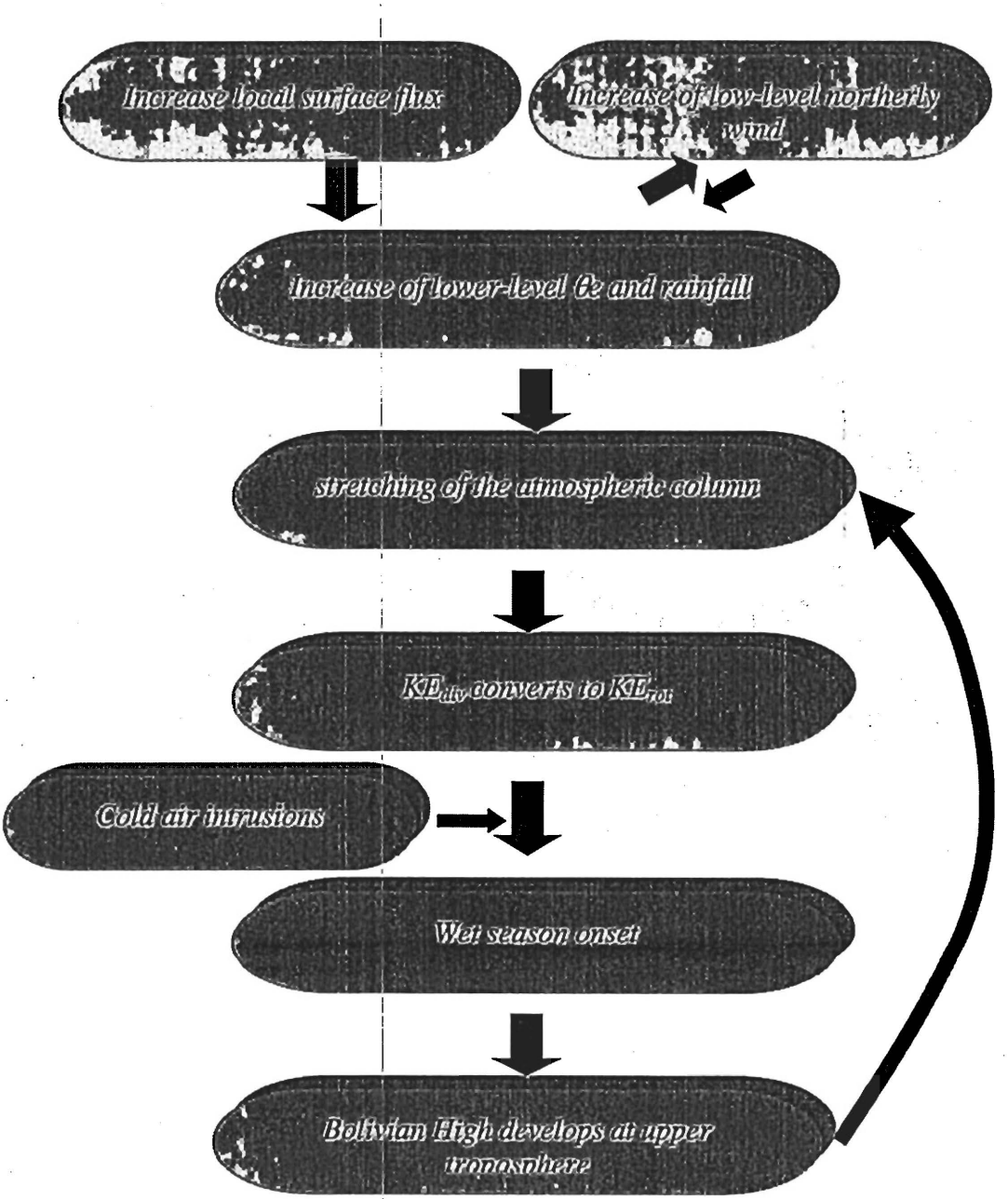

Figure 6.1. Schematic diagram of the onset of the wet season over tropical South America. Arrows indicate the onset progress.

season onset. Specifically, a longer dry season with lower rainfall causes lower surface latent heat flux in the earlier transition periods. This results in a higher CINE and a lower CAPE, delays and weakens the initial increase of rainfall, and delays the transition of the large-scale circulation. Conversely, a wetter dry season leads to a higher surface latent flux and a weaker CINE, providing a favorable condition necessary for an earlier increase of local rainfall and thus an earlier wet season onset.

Finally, the triggering mechanism of cold air intrusion from mid-latitude for the wet season onset was analyzed (Chapter 5). When a large-scale background (described in Chapters 3 and 4) is already destabilized for deep convection, cold air penetration into tropical South America can cause the rapid, southeastward expansion of enhanced precipitation through the increase of moisture convergence. Our comparisons among early, normal, and late onsets on an interannual scale further suggested that such cold air intrusion helps to enhance the moisture convergence and deep convection, and therefore precipitation reaches the onset criteria. On the contrary, without frequent and sufficiently strong cold air incursion, wet season onset can be delayed even though the large-scale environmental conditions have already destabilized.

6.2 Comparison For The SASM Onset And The Asian Summer Monsoon Onset

South America was not considered a monsoon region because of its lack of climatological wind shifts from summer to winter (e.g., Ramage 1971; Ayoade 1983). However, Zhou and Lau (1998) have demonstrated that, when annual means are removed, the

patterns of seasonal change for the atmospheric circulation over South America are similar to those of a monsoon system. Our analyses have further suggested that the reversal of the cross-equatorial meridional flow and transport of moisture, the sources and transformation of energy, and the evolution of the 200 hPa geopotential height over South America are similar to those of the South Asian monsoon. Like cold surges triggering the onset of the South China Sea summer monsoon (Chang and Chen 1995), cold air intrusion can also trigger the wet season onset over tropical South America and lead to the rapid, southeastward expansion of the rainy area from the western Amazon to Southeast Brazil during the transition season.

The most noticeable differences are that the increase of land surface latent heat flux can increase rainfall, which presumably contributes to the cross-equatorial flow and moisture convergence. The relatively high surface latent heat flux and zonal moisture convergence can maintain a relatively wet dry season. Because of the impact of surface latent heat flux on the moist static energy, the development of a continental-scale thermal low due to the increase of sensible heat flux, as in the classic monsoon onset process (Kawamur et al. 2002), is not dominant over the Amazon. Such differences contribute to the three-month changes of the onset dates on an interannual scale (Marengo et al. 2001; Li and Fu 2003) over South America. The above differences are reasonable, considering the contrasts in geographic location, topography, and land-surface type between South America and South Asia. These contrasts include:

6.2.1 The Weaker Differential Heating Between The Continent And Adjacent Oceans

The Altiplano Plateau is about one-twelfth the horizontal area and half the altitude of the Tibetan Plateau, although the sensible heat flux at the surface appears to be comparable between the two regions (Rao and Erdogan 1989). The tropical location of the Amazon basin, representing the bulk of the South American land mass, leads to a warmer and more humid winter climate than that of the subtropical Indian subcontinent. This contributes to a weaker and less effective differential heating between the South American continent and the adjacent Atlantic Ocean than for the South Asia monsoon. Despite the strong contrast (as much as 5°C) between the SSTs of the eastern Pacific cold tongue and land-surface temperatures of the South American continent (Oliver and Fairbridge 1987), the link between these two regions is weak (e.g., Grimm and Silva Dias 1995; Fu et al. 2001) because the Andes blocks the low-level flow between the two regions. Conversely, the atmosphere is significantly more humid and less stable during the dry season in tropical South America. Thus, the transition can be initiated by relatively small variations of land-surface conditions, compared to the large variations required by the Asian monsoon.

6.2.2 The Greater Importance Of Humidity

Radiosonde observations have shown that, even during the dry season, the atmosphere over the Amazon is almost statically neutral. The results presented in Chapters 3 and 4 demonstrated that main thermodynamic changes from the dry to the wet seasons

are mainly caused by increasing humidity (Fu et al. 1999; Betts and Jakob 2002). Over the Amazon, the prevailing easterly wind transports warm and humid air from the equatorial Atlantic (Satyamurty et al. 1998). The rainforest is also able to support greater surface latent heat flux than do the savanna, shrub, and barrens that dominate the land surface on the Indian subcontinent. Hence, convective instability can be reached with relatively small increases in humidity. Numerical experiments demonstrated that the direct mechanical and sensible heating effects of the Andes on the origin of the Bolivian high are secondary compared to the precipitation over the Amazon basin, central Andes, and South Atlantic convergence zone (Kleeman 1989; Lenters and Cooks 1997). In contrast, the formation of the Tibetan High, driven primarily by sensible heat flux (e.g., Li and Yanai 1996), and the reversal of the low-level flow are needed to initiate the increase in precipitation over South Asia.

6.3 Future Directions

I plan to pursue the following research topics to improve and expand my thesis work in the future:

- The realism of surface fluxes and soil moisture during the transition seasons (with more LBA observational data available) and their interannual variations (as reported in the ERA datasets) need to be evaluated, although the role of land surface in driving the transition from dry to wet season (derived from ERA) is physically plausible.

- SST influences on the adjacent oceans, especially ENSO influences on the wet season onset, need to be further studied with the release of 40-year ECMWF reanalyses. This not only includes more cases, but also can verify the results we have presented. The study of interannual variations for the onset date over the region also will help to understand the contributions of land surface and large-scale atmospheric conditions to the wet season onset.
- Numerical simulation will be useful in verifying the mechanism of the wet season onset over tropical South America. This includes a) quantifying the influences of land surface fluxes due to the change of soil moisture, as well as the influence of the precipitation of the previous dry season on the initiation of thermally driven rainfall; and b) testing the triggering impact of cold air intrusion on the enhanced precipitation during the transition season. This may determine the combination of the cold air triggers and the large-scale condition for the wet season onset, as well as its three-dimensional large-scale structure and the mechanism responsible for the enhanced precipitation right before the rainy season.

REFERENCES

Aceituno, P., 1988: On the functioning of the Southern Oscillation in the South American sector, Part I: Surface climate. *Mon. Wea. Rev.*, **116**, 505–524

Adams, D. K. and A. C. Comrie, 1997: The North American Monsoon, *Bull Amer. Meteor. Soc.*, **78**, 2197-2213

Aguado, E. and J E Burt, 1999: *Understanding weather and climate*, 474pp, Prentice Hall, Upper Saddle River

Ayoade, J. O., 1983: *Introduction to Climatology for the Tropics*. Vail-Ballou Press Inc., New York, 258 pp.

Badan-Dangon, A. C., C. E. Dorman, M. A. Merrifield, and C. D. Winant, 1991: The lower atmosphere over the Gulf of California, *J. Geophys. Res.*, **96**, 877-896

Barlow, M., S. Nigam, and E. H. Berbery, 1998: Evolution of the North American Monsoon System. *J. Climate,* **11**, 2238–2257

Barnett, T. P. L. Dumenil, U. Schlese, E. Roekler and M. Latif, 1989: The effect of Eurasian snow cover on regional and global climate variations, *J. Atmos. Sci.,* **46**,661-685

Betts, A. K., and C. Jakob, 2002: Evaluation of the diurnal cycle of precipitation, surface thermodynamics, and surface fluxes in the ECMWF model using LBA data. *J. Geophys. Res.*, **107**, LBA 12-1–10

Bowen, B. M., 1996: Rainfall and climate variation over a sloping New Mexico plateau during the North American monsoon, *J Clim.*, **9**, 3432-3442

Bryson, R.A. and F. K. Hare 1974: The climates of North America, *World Survey of Climatology*, **2**, *Climates of North America*, R. A. Bryson and F. K. Hare, Eds. Elsevier, 1-36

Cavazos, T., A. C. Comrie, and D. M. Liverman, 2002: Intraseasonal variability associated with wet monsoons in Southeast Arizona, *J Clim.*, **15**, 2477-2490

Chang, C.-P., G. T.J. Chen,1995: Tropical Circulations Associated with Southwest Monsoon Onset and Westerly Surges over the South China Sea, *Mon. Wea. Rev.,*. **123**, 3254–3267

Charney, J. G. 1975: The dynamics of deserts and droughts in the Sahel, *Q. J. R. Meteor. Soc.*, **101**, 193-202

Chu, P. S., 1985: A contribution of the upper-air climatology of tropical South America. *J. Climatology,* **5,** 403–416.

Coelho C.A.S., and T. Ambrizzi, 2000: Climatological studies of the influences of El Niño Southern Oscillation events in the precipitation pattern over South America during austral summer. *Sixth International Conference on Southern Hemisphere Meteorology and Oceanography* , **1** , 149-150, Santiago - Chile

Coelho C.A.S., C.B. Uvo and T. Ambrizzi, 2002: Exploring the impacts of the tropical Pacific SST on the precipitation patterns over South America during ENSO periods, *Theor. Appl. Climatol.*,**71**,185-197

Covey, D. L., and S. Hastenrath, 1978: The Pacific El Niño phenomenon and the Atlantic circulation. *Mon. Wea. Rev.*, **106,** 1280–1287.

Cox, P.M., Betts, R. A., Jones, C.D.; Spell, S.A. and Totter dell, I.J., 2000: Acceleration of global warming due to carbon-cycle feedbacks in a coupled climate model, *Nature*, **408**,184-190

Dall'Dlio, A, Salati, E, Azevedo, CE, and Matsui, E, 1979: Model de fracionamento isotopico da agua na Bacia Amazonica, *Acta Amazon*, **9**, 675–687.

Das, P. K., 1972: The monsoons, St. Martin's Press, 162pp

Dawson, T. E., 1993: Hydraulic lift and water use by plants: Implications for water balance, performance, and plant-plant interactions, *Oecologia*, **95**, 565–574.

Dias, MAFS, and Regnier, P, 1996: Simulaiton of mesoscale circulations in a deforestated area of Rondônia in the dry season, *Amazonian Deforestation and Climate,* Gash, JHC, Nobre, CA, Roberts, JM, and Victoria, RL Eds., John Wiley & Sons, 531-547.

Dickinson, R.E., and Henderson-Sellers, A, 1988: Modeling tropical deforestation: A study of GCM land-surface parameterization. *Quart. J. Roy Meteor. Soc.,* **114,** 439 – 462.

Ding, Y. H., 1991: Advance Synoptic Meteorology, Meteorology Press, 792pp

Douglas, M. W., R. Maddox, K. Howard, and D Reyes, 1993: The Mexican monsoon, *J Clim.*, **6**, 1665-1667

Eltahir, E. A. B., 1998: A Soil Moisture-Rainfall Feedback Mechanism, 1. Theory and Observations, *Water Resources Research*, **34**, 765-776.

Entekhabi, D. and I. Rodriguez-Iturbe, 1994: An analytic framework for the characterization of the space-time variability of soil moisture, *Advances in Water Resources.*, **17**,35-45

Falls, R. 1970a: Some synoptic model-north-Australia, *Proceeding of the Symposium on Tropical Meteorology*, Honolulu: AMS and WMO

Falls, R. 1970b: Synoptic analysis and forecasting in the tropics of Asia and the southwest Pacific, *Proceeding of the Regional Training Seminar*, Singapore: WMO

Fein, J. S. and P. L. Stephens (Eds), 1987: Monsoons, New York, 632 pp

Fennessy, M. J., J. L., Kinter, B., Kirtman, L., Marx, S., Nigam, E., Schneider, J. Shukla, D. Straus, A. Vernekar, Y. Xue, J. Zhou, 1994: The Simulated Indian Monsoon: A GCM Sensitivity Study. *J. Clim.* **7**, 33–43.

Flohn, H. 1957: Large-scale aspects of the "summer monsoon" in south and east Asia, *J. Meteoro. Soc. Jpn*, **35**, 180-186

Flohn, H., and J. O., Struning, 1969: Investigations on the atmospheric circulation over Africa, *Bonner Meteor. Abhand.*, **10**

Fu, C. and J. Fletcher, 1985: The relationship between Tibet-tropical ocean thermal contrast and interannual variability of Indian monsoon rainfall, *J. Clim. Appl. Meteoro.* , **24**, 841-847

Fu, R., B. Zhu, and R. E. Dickinson, 1999: How do atmosphere and land surface influence seasonal changes of convection in the tropical Amazon? *J. Climate*, **12**, 1306–1321.

Fu, R., R. E. Dickinson, M. Chen, and H. Wang, 2001: How do tropical sea surface temperatures influence the seasonal distribution of precipitation in the equatorial Amazon? *J. Climate*, **14**, 4003–4026.

Gandu, A. W., and J. E. Geisler, 1991: A primitive equations model study of the effect of topography on the summer circulation over tropical South America. *J. Atmos. Sci.*, **48**, 1822–1836.

Gandu, A. W., and P. L. Silva Dias, 1998 Impact of tropical heat sources on the South American tropospheric upper circulation and subsidence, *J. Geophys. Res.* **103** , 6001-6015.

Gao, Y. X., M.C. Tang, S. W. Luo, Z. B. Shen and C. Li, 1981: Some aspects of recent research on the Qinghai-Xizang Plateau meteorology, *Bull Amer. Meteor. Soc.*, **62**, 31-35

Garreaud, R. D., 1998: Cold air intrusion into low-latitudes: Global perspective and regional analysis over South America, Ph.D. thesis, 161pp

Garreaud, R. D. and J.M. Wallace, 1998: Summertime Incursions of Midlatitude Air into Subtropical and Tropical South America, *Mon. Wea. Rev.* **126**, 2713–2733.

Garreaud, R. D. 1999: Cold Air Incursions over Subtropical and Tropical South America: A Numerical Case Study, *Mon. Wea. Rev.* **127**, 2823–2853

Garreaud, R. D. 2000: Cold Air Incursions over Subtropical South America: Mean Structure and Dynamics, *Mon. Wea. Rev.* **128**, 2544–2559.

Grodsky, S.A., and J.A. Carton, 2001: Coupled land/atmosphere interactions in the West African monsoon, *Geophys. Res. Letts.*, **28**, 1503-1506.

Gibbs, J. R., 1979: Mechanism controlling world water chemistry. *Science*, **170**, 1088–1090.

Gill, A. E., 1980: Some simple solutions for heat-induced tropical circulation. *Quart. J. Roy. Meteor. Soc.*, **106**, 447–462.

Grimm, A. M., and P. L. Silva Dias, 1995: Analysis of tropical-extratropical interactions with influence functions of a barotropic model. *J. Atmos. Sci.*, **52**, 3538–3555.

Grimm, A. M., V. R. Barros, and M. E. Doyle, 2000: Climate Variability in Southern South America Associated with El Niño and La Niña Events, *J. Climate,* **13**, 35–58.

Grodsky, S.A., and J.A. Carton, 2001: Coupled land/atmosphere interactions in the West African monsoon, *Geophys. Res. Letts.*, **28**, 1503-1506.

Gutman, G. J., and W. Schwerdtfeger, 1965: The role of latent and sensible heat for the development of a high-pressure system over the subtropical Andes in the summer. *Metero. Rundsch.*, **18**, 69–76.

Hartmann, D. L. 1994: *Global physical Climatology*, Academic Press, 411pp

Hastenrath, S., and L. Heller, 1977: Dynamics of climatic hazards in Northeast Brazil. *Quart. J. Roy. Meteor. Soc.*, **103**, *77–92.*

Hastenrath, S., 1990: The relationship of highly reflective clouds to tropical climate anomalies. *J. Climate,* **3**, 353–365.

Haylock M and J. McBride, 2001: Spatial coherence and predictability of Indonesian wet season rainfall, *J Clim.*, **14**, 3882-3887

He, H., J.W. McGinnis, Z. Song, and M. Yanai, 1987: Onset of the Asian monsoon in 1979 and the effect of the Tibetan Plateau, *Mon. Wea. Rev.*, **115**,1966-1995

Hendo, H. H. and B. Liebmann, 1990: A composite study of onset of the Australian summer monsoon, *J. Atmos. Sci.*, **47**,2227-224

Hodnett, MG, Oyama, MD, Tomasella, J, and Filho AOM, 1996: Comparison of long-term soil water storage behaviour under pasture and forest in three areas of Amazonia. *Amazonian Deforestation and Climate,* Gash, JHC, Nobre, CA, Roberts, JM, and Victoria, RL Eds., John Wiley & Sons, 57–77.

Horel, J. D., A. N. Hahmann, and J. E. Geisler, 1989: An investigation of the annual cycle of convective activity over the tropical Americas. *J. Climate*, **2**, 1388–1403.

Huffman, G. J., R. A. Adler, M. M. Morrissey, D. T. Bolvin, S. Curtis, R. Joyce, B. McGavock, and J. Susskind, 2001: Global precipitation at one-degree daily resolution from multisatellite observations. *J. Hydro.*, **2**, 36–50.

Kawamura R, Y. Fukutaa, H. Ueda, T. Matsuura and S. Lizuka, 2002: A mechanism of the onset of the Australian summer monsoon, *J. Geophys. Res.*, **107**, ACL5-1 ACL-15

Keller, M., R. Victoria, and C. Nobre, 2001: Answers sought to big questions about the Amazon region, *EOS*, **82**, 405–406.

Klevin, W. H., 1957: Principal tracks and frequencies of cyclones and anticyclones in the Northern Hemisphere, *U.S. Weather Bur., Res. Pap.* **40**

Kousky, V. E., 1988: Pentad outgoing longwave radiation climatology for the South American sector. *Rev. Bras. Meteor.*, **3**, 217–231.

Kousky, V. E., and I. Cavalcani, 1997: The principal modes of high-frequency variability over the South America region, Preprints, *Fifth Intl. Conf. on Southern Hemisphere meteorology & Oceanography*, Pretoria, South Africa., Amer. Meteor. Soc., 7B.2-7B.3

Krishnamurti, T. N., and Y. Ramanathan, 1982: Sensitivity of the monsoon onset to differential heating. *J. Atmos. Sci.*, **39**, 1290–1306.

Krishnamurti, T. N., M. C. Sinha, Bhaskar Jha, and U. C. Mohanty, 1998: A study of South Asian monsoon energetics. *J. Atmos. Sci.*, **55**, 2530–2548.

Kuo, H.L. and Y. F. Qian 1982: Numerical simulation of the development of mean monsoon circulation in July, *Mon. Wea. Rev.*, **110**,1879-1897

Lau, K.-M, and M-T. Li, 1984: The Monsoon of East Asia and its Global Associations—A Survey. *Bull. Amer. Meteor. Soc.* **.65**, 114–125.

Leighton, R. 1979: *Anticyclonicity and cyclonicity averages for 1965-1974*, Australian Bureau of Meteorology, Tech. Rep. No 35

Lenters, J. D., and K. H. Cook, 1995: Simulation and diagnosis of the regional summertime precipitation climatology of South America. *J. Climate,* **8,** 2988–3005.

Lenters, J. D., and K. H. Cook, 1997: On the origin of the Bolivian High and related circulation features of the South American climate. *J. Atmos. Sci.*, **54**, 656–678.

Leslei, L. M., 1980: Numerical modeling of the summer heat low over Australia, *J Appl. Meteor.,* **19**,381-387

Li, C., and M. Yanai, 1996: The onset and interannual variability of the Asian Summer Monsoon in relation to land-sea thermal contrast. *J. Climate*, **9**, 358–375.

Li, W, and Fu, R, 2002: Transition of the Large-scale Atmospheric and Land Surface Conditions from Dry to Wet Season over the Amazon. Revision for *J. Climate*

Liebmann, B., and J. A. Marengo, 2001: Interannual variability of the rainy season and rainfall in the Brazilian Amazon Basin. *J. Climate,* **14**, 4308–4318.

Liebmann, B, and Marengo, JA, 2002: Interannual variability of the rainy season and rainfall in the Brazilian Amazon Basin. *J. Climate,* **14**, 4308–4318

McBride, J. L. 1975: The effect of land-sea temperature contrast on short-term numerical forecasts, *Australian Meteor. Magazine*, **23**, 75-98

McBride, J. L. and T.D. Keenan, 1982: Climatology of tropical cyclone genesis in the Australian region. J. Climatol.,**2**, 13-33.

Madden, R. A., and P. R. Julian, 1994: Observations of the 40-50-day oscillation-A review, *Mon. Wea. Rev.,*. **122**, 814-837

Manzi, AO, and Planton, S, 1996: A simulation of Amazonian deforestation using a GCM calibrated with ABRACOS and ARME data. *Amazonian Deforestation and Climate,* Gash, JHC, Nobre, CA, Roberts, JM, and Victoria, RL Eds., John Wiley & Sons, 505-529

Marengo, J., A. Cornejo, P., Satyamurty, C. Nobre, and W. Sea, 1997: Cold Surges in Tropical and Extratropical South America: The Strong Event in June 1994, *Mon. Wea. Rev.* **125**, 2759–2786.

Marengo, J. A., B. Liebmann, V. E. Kousky, N. P. Filizola, and I. C. Wainer, 2001: Onset and end of the rainy season in the Brazilian Amazon Basin. *J. Climate,* **14**, 833–852.

Markham, C. G., and D. R. McLain, 1977: Sea surface temperature related to rain in Ceará, Northeastern Brazil, *Nature*, **265**, 320–323.

Masiño, P., and E. García, 1974: The climate of Mexico, *Climate of North America,* R. A. Bryson and F. K. Hare, Eds., **2**, *World Survey of Climatology*, Elsevier, 373-404

Moscati, M. C. D., and V. B. Rao, 2001: Energetics of the summer circulation over South America. *Annales Geophysicae*, **19**, 83–97.

Moura, A. D., and J. Shukla, 1981: On the dynamics of droughts in northeast Brazil: Observations, theory and numerical experiments with a general circulation model. *J. Atmos. Sci.*, **38**, 2653–2675.

Murakami, T., 1987: Orography and Monsoons, in *Monsoon*, edited by J. S. Fein and P. L. Stephens, John Wiley, New York, 331-364Namias, J., 1972: Influence of northern hemisphere general circulation on drought in northeast Brazil, *Tellus,* **24**, 336–342.

Namias, J., 1972: Space scales of sea-surface temperature patterns and their causes. *Fish. Bull.,* 70, 611–617

Nastrom, G. D., and F.D. Eaton, 1993: Onset of the summer monsoon over White Sands Missile Range, Puri, K., 1994: Modeling studies on the Australian summer monsoon, *Mon. Wea. Rev.*, **122**,2816-2821

Nepstad, DC, Carvalho, CR, Davidson, EA, Jipp, PH, Lefebvre, PA, Negreiros GH, da Silva, ED, Stone, TA, Trumbore, SE, and Vieira, S, 1994: The role of deep roots in the hydrological and carbon cycles of Amazonian forests and pastures, *Nature*, **372**, 666–669.

Nepstad, DC, Verissimo, A, Alencar, A, Nobre, C, Lima, E, Lefebvre, P, Schlesinger, P, Potter, C, Moutinho, P, Mendoza, E, Cochrane, M, and Brooks, V, 1999: Large-scale impoverishment of Amazonian forests by logging and fire, *Nature*, **398**, 505–508.

Nicholls, N., J. L. Mcbride, and R. J. Ormerod, 1982: ON predicting the onset of the Australian wet season at Darwin, *Mon. Wea. Rev.*, **110**, 14-17

Nishizawa, T., and M. Tanaka, 1983: The annual change in the tropospheric circulation and the rainfall in South America. *Arch. Metero. Geophys. Bioklmatol.,* **33**, 107–116.

NOAA Sciences Report, 2002: http://www.wrh.noaa.gov/flagstaff/science/monsoon.htm

Nobre, CA, Sellers, PJ, and Shukla, J, 1991: Amazon deforestation and regional climate change. *J. Climate*, 4,957–4, 988

Nobre, P., and J. Shukla, 1996: Variations of Sea Surface Temperature, Wind Stress, and Rainfall over the Tropical Atlantic and South America, *J. Climate,* **9**,2464–2479.

Nobre, C.A., Fisch, G., Rocha, H. R., Lyra, R. F. Rocha, E. P., Costa, ACL, and Ubarana, V. N., 1996: Observations of the atmospheric boundary layer in Rondônia. *Amazonian Deforestation and Climate*, Gash, JHC, Nobre, CA, Roberts, JM, and Victoria, RL Eds., John Wiley & Sons, 413-423.

Okabe, I. T., 1994: The North American monsoon, Ph.D. dissertation, Univ. of British Columbia,146pp

Oliver, J. E., and R. W. Fairbridge, 1987: *The Encyclopedia Of Climatology*. New York: Van Nostrand Reinhold Company, 986 pp.

Oliveris, A. S., 1986: Interactions between the South American frontal systems and the Amazonian convection, INPE-4008-TDL/239, Intsitute Nacional de Pesquisas Espaciais,115pp

Paegle, J., A. W. Robertson, and C.R. Mechoso,2000: Relationship between the North Atlantic Oscillation and river flow regiems of South America, Proceedings of 25th Annual Climate Diagnostics and Prediction Workshop,23-27 October 2000,Palisades,NY,323-326

Paegle, J., C. R., Mechoso, R. Fu, E. Hogo Bergery, W. C. Chao, T.-C. Chen, K. Cook, A. F. Diaz, D. Enfield, R. Ferreira, A. M. Grimm, V. Kousky, B. Liebmann, J. Marengo, K. Mo, J. D. Neelin, J. Paegle, A. W. Robertson, A. Seth, C. S. Vera, and J. Zhou, 2002: Progress in Pan American CLIVAR research: understanding the South American monsoon, Special issue on South American Monsoon System, *Meteor. Logica*, **27**, 3-33

Pedgley, D. E. and T.N., Krishnamurti, 1976: Structure and behavior of a monsoon cyclone over west Africa, *Mon. Wea. Rev.*, **104,** 149-167

Petersen, W. A. and S. A. Rutledge, 2001: Regional Variability in Tropical Convection: Observations from TRMM, *J. Clim.* **14**, 3566–3586

Polcher, J, 1995: Sensitivity of tropical convection to land surface processes. *J. Atmos. Sci.*, **52**, 3143–3161.

Poveda, G., and O. J. Mesa, 1997: Feedbacks between Hydrological Processes in Tropical South America and Large-Scale Ocean–Atmospheric Phenomena, *J. Climate,* **10**, 2690–2702

Ramage, C. S., 1971: Monsoon Meteorology, Academic Press, 296pp

Rao, G. V., and S. Erdogan, 1989: The atmospheric heat source over the Bolivian plateau for a mean January. *Bound. Layer Meteor.*, **46**, 13–33.

Rao, V. B., I. F. A. Cavalcanti, and K. Hada, 1996: Annual variation of rainfall over Brazil and water vapor characteristics over South America. *J. Geophys. Res.*, **101**, 26,539–26,551.

Rind, D, and Rossow, W.B., 1984: The Effects of Physical Processes on the Hadley Circulation. *J. Atmos. Sci.*, **41**, 479–507.

Ropelewski, C. F., and M. S. Halpert, 1989: Precipitation patterns associated with the high index phase of the Southern Oscillation. *J. Climate*, **2**, 268–284.

Rowntree, P. R., 1976: Response of the atmosphere to a tropical Atlantic Ocean temperature anomaly. *Quart. J. Roy. Meteor. Soc.*, **102**, 607–625.

Salati, E., A. Dall'Olio, J. Gat, and E. Matsui., 1979: Recycling of water in Amazon Basin: An isotope study. *Water Resour. Res.*, **15**, 1250–1258.

Salati, E, and P. B. Vose, 1984: Amazon Basin: A system in equilibrium, *Science*, **225**, 129–138.

Satyamurty, P., C. A. Nobre, and P. L. Silva Dias, 1998: Meteorology of the Tropics-South America, *Meteorology of the Southern Hemisphere*, Koroly D. J. and D. G. Vincent, Eds, AMS, 119-141

Serra, A. B., 1973: Statistical aspects of Northeast Brazil droughts. *Dept. National de Metero., Ministerio da Agricultula*, Rio de Janerio, 17 pp.

Shukla, J. and Y. Mintz, 1982: Influence of land-surface evapotranspiration on the Earth's climate, *Sciences*, **214**, 1498-1501

Shukla, J., and M. J. Fennessy 1994: Simulation and predictability of monsoons, in *Proc. International Conf. on Monsoon Variability and Prediction*, Tech. Rep. WCRP-84, 567-575, World Climate Research Program, Geneva, Switzerland

Shukla, J. and D. A. Paolina, 1983: The southern oscillation and lng range forecasting of the summer monsoon rainfall over India, *Mon. Wea. Rev.*, **111**, 1830-1837

Shuttleworth, W. J., 1991: The modellion concept, *Rev . Geophy.*, 585-606

Silva Dias, P. L., W. H. Schubert, and M. DeMaria, 1983: Large-scale response of the tropical atmosphere to transient convection. *J. Atmos. Sci.*, **40**, 2689–2707.

Souza, J.R.S., Pinheiro, F.M.A., Araujo, R.L.C., Pinheiro, H.S., and Hodnett, M.G., 1996: Termperature and moisture profiles in soil beneath forest and pasture areas in eastern Amazon, *Amazonian Deforestation and Climate,* Gash, JHC, Nobre, CA, Roberts, JM, and Victoria, RL Eds., John Wiley & Sons, 57–77.

Stensrud, D. J., R. Gall, S. Mullen, and K. Howard, 1995: Model climatology of the Mexican monsoon, *J Clim.*, **8**, 1775-1794

Stroppiana, D., S. Pinnock , and J. M. Gregoire,2000: The Global Fire Product: Daily fire occurrence from April 1992-December 1993 derived from NOAA-AVHRR data, *Int. J. Remote Sens.*, **21,** 1279-1288

Sugahara, S. 1991. Flutuações interannuais, sazonais eintrasazonais da precipitação no Estado de São Paulo (In Portuguese, with English abstract). Ph.D. thesis, Univ. of São Paulo, São Paulo.

Sultan B., and S. Janicot, 2002: The west African monsoon dynamics: Part II: the "pre-onset" and the "onset" of the summer monsoon, submitted to *J. Clim.*

Suppiah, R., 1992: The Australian summer monsoon: A review, *Prog. Phys., Geogr.*, **16**,283-318

Talley, L. 1998: Topic 8: Monsoons El Nino; Midlatitude variability

Tanaka, M., 1994: The onset and retreat dates of the austral summer monsoon over Indonesia, Australia and New Guinea, *J. Met. Soc. Jap.* , **72**, 255-266

Tang, M., and E. R. Reiter, 1984: Plateau moons of the Northern Hemisphere: A comparison between North America and Tibet, *Mon. Wea. Rev.*, **112,** 617-637

Tian, H., J. M. Melillo, D.W. Kicklighter, A.D.McGuire, J.V.K.Helfrich III, B. Moore III, and C. J. Vörösmarty, 1998: Effect of interannual climate variability on carbon storage in Amazonian ecosystems, *Nature*, **396**, 664-667

Torrence, C. and P. J. Webster, 1998: The Predictability Barrier in El Nino-Southern Oscillation Statistics and Coupled Models. *Q. J. Roy. Met. Soc.*, **124**, 1985-2004.

Trenberth, K. E., D. P. Stepaniak, and J. M. Caron, 2000: The Global Monsoon as Seen through the Divergent Atmospheric Circulation, *J. Clim.* **13**, 3969–3993

Vera, C. S., and P. K. Vigliarolo, 2000: A Diagnostic Study of Cold-Air Outbreaks over South America, *Mon. Wea. Rew.*, **128**, 3–24

Vera, C. S., P. K. Vigliarolo, and E. H. Berbery, 2002: Cold Season Synoptic-Scale Waves over Subtropical South America, *Mon. Wea. Rev.*, **130**, 684–699

Virji, H., 1981: A preliminary study of summertime tropospheric circulation patterns over South America estimated from cloud winds. *Mon. Wea. Rev.*, **109**, 599–610.

Vourlitis, G.L., N. Priante, M.M.S. Hayashi, J. D. Nogueira, F. T. Caseiro, J. H. Campelo,2001: Seasonal variations in the net ecosystem CO2 exchange of a mature Amazonian transitional tropical forest (cerradao), *Funct. Ecol.*, **15**, 388-395

Wang, H., and R. Fu, 2002: Cross-equatorial flow and seasonal cycle of precipitation over South America. *J. Climate*, **15**,1591–1608.

Williams, E., and N. Renno, 1993: An analysis of the conditional instability of the tropical atmosphere. *Mon. Wea. Rev.*, **121**, 21–36.

Webster, P. J., 1987: The variable and interactive monsoon, in *Monsoon*, edited by J. S. Fein and P. L. Stephens, John Wiley, New York, 269-328

Webster, P. J., V. O. Magana, T. N. Palmer, J. Shukla, R.A. Tomas, M. Yanai, and T. Yasunari, 1998: Monsoon; process, predictability, and the prospects for prediction, *J. Geophys. Res.*, **103**, 14451-14510

WWF Profile, 2001: Amazon River and Flooded Forests, National Geographic Society

Xie, S. P., and N. Saiki 1999: Abrupt onset and slow seasonal evolution of summer monsoon in an idealized GCM simulation, *J. Meteor. Soc. Jpn*, **77**, 949-968

Xue, Y., and J. Shukla, 1993: The influence of land processes on Sahel climate, Part I: Desertification, *J. Clim.* **6**, 2232-2245

Yanai, M. C. Li, and Z. Song, 1992: Seasonal heating of the Tibetan Plateau and its effects on the evolution of the Asian summer monsoon, *J. Meteor. Soc. Jpn*, **70**, 319-351

Yang, S. and K. M., Lau, 1998: Influence of sea surface temperature and ground wetness on Asian summer monsoon, *J Clim.*, **11**, 3230-3246

Yasunari, T., A. Kitoh and T. Tokioka, 1991: Local and remote response to excessive snow mass over Eurasia appearing in the northern spring and summer climate-A study with the MRI-GCM, *J. Meteor. Soc. Jpn*, **69**, 473-487

Ye, D., T.C. Yeh, and Y.X. Gao, 979: *The meteorology of the Qinghai-Xizang (Tibet) Plateau*, Sci. Press, Beijing, 278pp

Zhou, J. Y., and K.-M. Lau 1998: Does a monsoon climate exist over South America? *J. Climate,* **11,** 1020–1040